



ARCHITECTURE & ENGINEERING

Volume 2

Issue 4

December, 2017



By Architects. For Architects.
By Engineers. For Engineers.

Architecture
Civil and Structural Engineering
Mechanics of Materials
Building and Construction
Business and Management in Construction
Urban Planning and Development
Transportation Issues in Construction
Geotechnical Engineering and Engineering Geology
Designing, Operation and Service
of Construction Cite Engines

Architecture and Engineering

Volume 2 Issue 4

Editorial Board:

Prof. A. Akaev (Kyrgyzstan)
Prof. Emeritus D. Angelides (Greece)
Prof. A. Asaul (Russia)
Prof. S. Bertocci (Italy)
Prof. T. Dadayan (Armenia)
Prof. M. Demosthenous (Cyprus)
T. C. Devezas (Portugal) Associate Professor with Habilitation
Prof. J. Eberhardsteiner (Austria)
V. Edoyan (Armenia) Associate Professor
Prof. G. Esaulov (Russia)
Prof. S. Evtiukov (Russia)
Prof. A. Gale (UK)
Prof. G. Galstyan (Armenia)
Prof. Th. Hatzigogos (Greece)
Y. Iwasaki (Japan), Ph.D., Doctor of Engineering
Prof. Jilin Qi (China)
K. Katakalos (Greece) Dr. Engineering
Prof. N. Kazhar (Poland)
Prof. G. Kipiani (Georgia)
Prof. D. Kubečková (Czech Republic)
Prof. H. I. Ling (USA)
E. Loukogeorgaki (Greece) Assistant Professor
Prof. S. Mecca (Italy)
Prof. Menghong Wang (China)
S. A. Mitoulis (UK) Lecturer
Prof. V. Morozov (Russia)
Prof. A. Naniopoulos (Greece)
S. Parrinello (Italy) Architect, Associate Professor
Prof. P. Puma (Italy)
Prof. Qi Chengzhi (China)
Prof. J. Rajczyk (Poland)
Prof. M. Rajczyk (Poland)
Prof. Yu. Safaryan (Armenia)
Prof. S. Sementsov (Russia)
A. Sextos (Greece) Associate Professor
E. Shesterov (Russia) Associate Professor
Prof. A. Shkarovskiy (Poland)
Prof. E. Smirnov (Russia)
Prof. Emeritus T. Tanaka (Japan)
Prof. S. Tepnadze (Georgia)
M. Theofanous (UK) Lecturer
G. Thermou (Greece) Assistant Professor
Prof. R. Tskhevadze (Georgia)
Prof. L. Ungváry (Germany)
I. Wakai (Japan) Dr. Eng, Lecturer
Prof. A. Zhusupbekov (Kazakhstan)



Editor in Chief:

Prof. Emeritus G. C. Manos (Greece)

Associate editor:

Viktoriya Rapgof (Russia) Executive Editor



CONTENTS

- 3 **Jungmann Choi**
Case Studies of the Design, Construction and Certification of Energy-efficient Houses in the Republic of Korea
- 9 **Konstantin Dmitriev, Victor Zverev**
Innovative construction material based on aerated ceramics
- 14 **Jurij Kotikov**
Transport Energy Efficiency Assessment on the Basis of the Life Cycle with the Attraction of the Bartini *Transfer* Essence
- 20 **Elena Kurakina, Sergey Evtyukov, Anna Shimanova**
Improvement of the Technology of Earthworks in Megacities
- 26 **Victor Kuzmichev, Vladimir Verstov**
Gravity Mixers with Vibration Activator in Construction Engineering
- 34 **Leonid Lavrov, Fedor Perov, Raffaele Gambassi**
Future of the Obvodny Canal — the Main Line of the Saint Petersburg Grey Belt
- 42 **Viktor Pukhkal, Vadim Bulgakov**
Generation of Natural Convective Air Flows in Rooms with the Use of In-Floor Convectors with Natural Circulation
- 48 **Marlena Rajczyk, Paweł Rajczyk**
Multilayer Concrete Industrial Flooring Solutions Analysis
- 56 **Ravil Safiullin, Mukhtar Kerimov, Alexander Afanasyev**
Study of the Influence of the Energoinformational Field on Quality of the Fuel Applied in Internal Combustion Engines of Road-Building Machinery
- 65 In memory of Professor Ray W. Clough of the California University at Berkeley, who died on October 8, 2016

CASE STUDIES OF THE DESIGN, CONSTRUCTION AND CERTIFICATION OF ENERGY-EFFICIENT HOUSES IN THE REPUBLIC OF KOREA

Jungmann Choi

Soongsil University, 577 Olympic-ro, Songpa-gu, Seoul, Korea

jungmann.choi@gmail.com

Abstract

Passive houses with three principles of comfort, low energy and economic efficiency started from Germany in 2009. Passive houses must have a heating energy demand of less than 15 kWh/(m²a) per year, and there are currently about 4,000 passive houses certified in Europe. Currently, Korea has begun experimental construction of passive houses from 2005, and it started to introduce it in construction market from 2009. To date, 160 units have been certified, which differs from Europe in that Korea is certified as a passive house up to 50 kWh/(m²a). In order to establish this standard, Passive House Institute Korea (PHIKO) collected and analyzed the data of the completed buildings over the years.

As a result, Korea Passive House standard was newly defined considering the climatic condition (humidity and solar radiation) of Korea and the lifestyle of floor-heating and sitting on that. Of course, these standards are not definitive, and they are still underway, and if more data is accumulated, the standards can change.

Keywords

Passive house, climate of Korea, standard, life style.

Passive House Certification Criteria

Passive house definition in Europe is "a building with a heating energy demand of 15kWh or less per year." Of course, there are additional requirements such as primary energy requirements and air tightness standards (Feist, 1993). And the five principles for this goal are well known (<https://passipedia.org/basics>).

The passive house is designed to raise the air coming in through the ventilation system a little bit or get off to get a comfortable temperature, so of course, 15kWh is calculated based on air heating. This value is then calculated using PHPP based on the local climate data.

Status of Passive House in Korea

Experimental passive houses have been constructed in Korea since 2005, and about 175 passive houses have been certified to date. Housing is the most common, and offices and schools are also being built. In addition, many products that are essential for passive houses such as thermal bridge blockers have been developed, and passive houses in Korea are helping to make them more economical (https://passipedia.org/basics/building_physics_-_basics/heating_load). As a result, construction costs, which have risen by nearly 20% compared to exist-

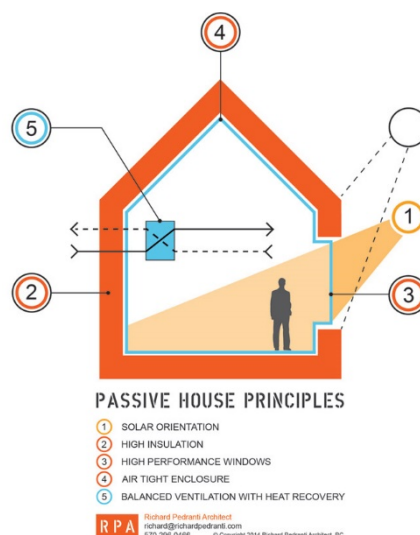


Figure 1. The five principles of Passive House (<https://richardpedranti.com/passivehouse/>)

ing buildings, are now stabilizing at around 10~15%. Window's frame has been dependent on German products so far, but this part is expected to be available as Korean products. If it does, the cost of construction will be lower.

Passive house technician training is held four times a year, and about 20 students graduate each time. About 300 people have been educated to date, and about 40% of graduates are architects (Bradshaw, 2006).

Recently, several passive Single-family housing complex are in the process of being designed and will start construction in 2018. One complex consists of 30 to 60 households, and five housing projects will be built nationwide (Bansal et al., 1994). These projects are meaningful because if the passive house was a market for a small construction company, it would be a chance that a middle-sized construction company will become interested in a passive house through this project.



Figure 2. Community centre at Asan City



Figure 3. Lamda house, Desing by Doyoung Hong

Characteristics of Passive House in Korea

PHIKO has been monitoring the energy use and indoor environment of passive houses built in Korea over the years. And based on these results, we found that passive houses in Korea differ from those in Europe (Pèrez-Lombard et al., 2008).

This is a correlation between the exterior wall performance and the energy demand of the house. In Europe, the predicted value of energy performance is in agreement with the actual usage. In Korea, however, the actual usage is more than the calculated value is. That is, actual energy usage did not fall to European level.

The cause was the difference in lifestyle. Indoor temperature of a passive house is very comfortable. However, the floor temperature of the passive house in Korea, which

is used to heating the floor, was low for Koreans to feel comfortable. (Temperature of floor heating: about 30°C) Even though the temperature of the air was good enough, most Koreans had to operate the boiler to adjust the floor temperature. In addition, the climatic conditions are different (Feist, 1993).

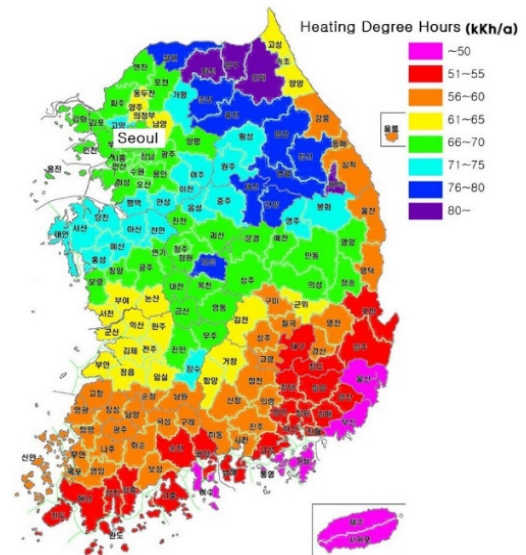


Figure 4. Heat Degree Hours in South Korea

In Korea, there is a tendency to be smaller than the heating degree hours mentioned in European passive house standards, but the difference in that between provinces is quite large. Also, summer is very humid in Korea. This high humidity will inevitably affect the design of the passive house. To understand this more precisely, we compared the average of passive houses built in Korea and European standard passive houses by several factors (Künzel and Holm, 2009). Based on these results, it is concluded that it is difficult to match the performance of the outer wall to the European level.

In addition to this, an important factor in Korea is that the humidity of summer is very high.

This part is very different from Europe, most of which is over 80% of summer humidity.



Figure 5. Standard Passive House by PHIKO

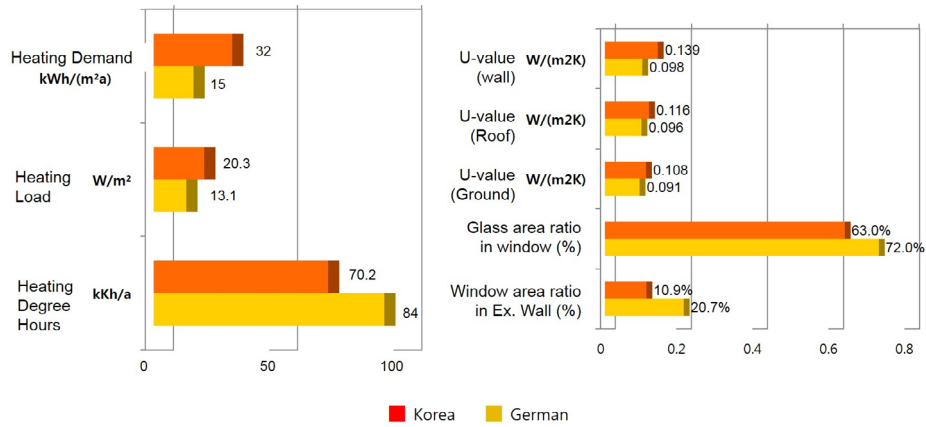


Figure 6. Performance comparison

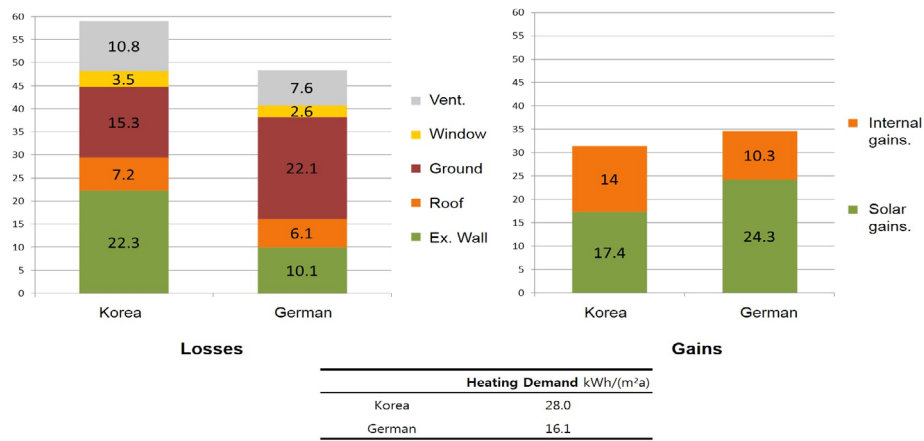


Figure 7. Energy balance comparison

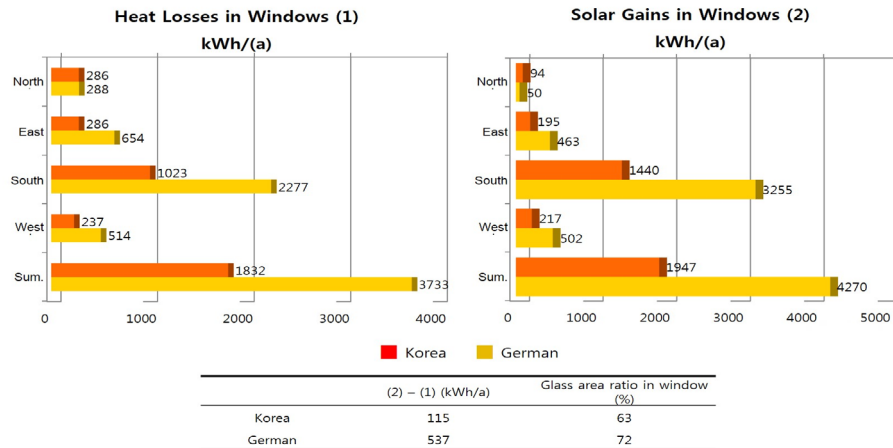


Figure 8. Solar Energy Gain comparison

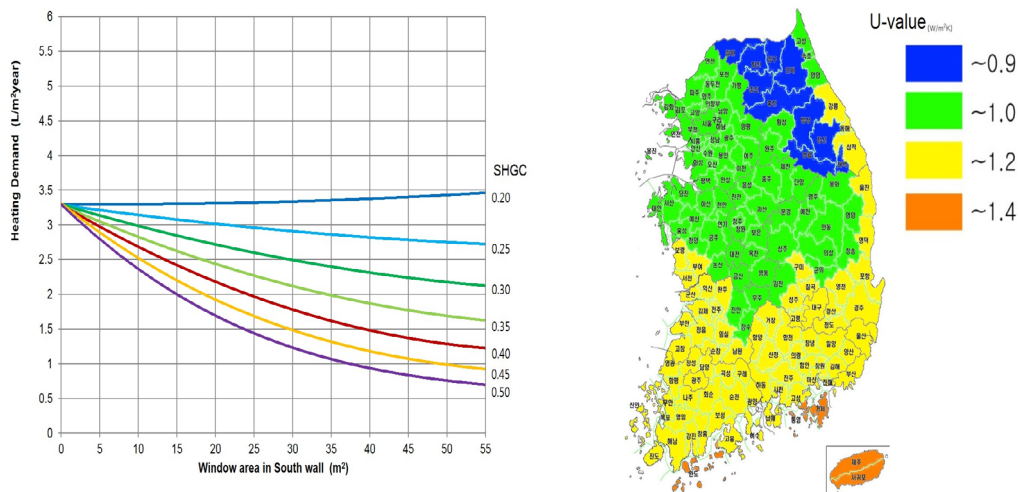


Figure 9. Windows performance standard of passive house in Korea

Field test site in Holzkirchen (alt.: 680 m, lat.: 48° N)
 Seoul (alt.: 20 m, lat.: 37° N)

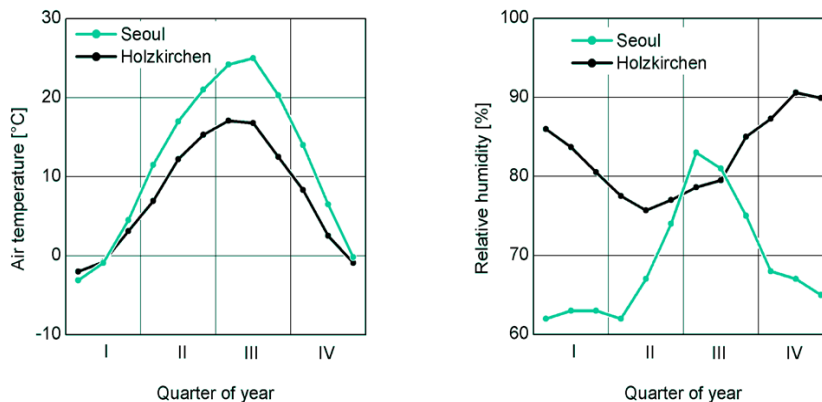


Figure 10. Differences in temperature and humidity between Germany and Korea by Fraunhofer

Table 1. Low Energy House and Passive House standard in Korea

		German (by PHI)	Korea (by PHIKO)
U-value	Ex. Wall	0.15 W/m ² · K	0.15 ~ 0.18 W/m ² · K
	roof	0.15 W/m ² · K	0.12 ~ 0.15 W/m ² · K
	U-glass	0.8 W/m ² · K	0.9 ~ 1.4 W/m ² · K
	U-frame	0.8 W/m ² · K	0.8 ~ 1.4 W/m ² · K
	U-window	0.85 W/m ² · K	0.9 ~ 1.5 W/m ² · K
	glass g-value (SHGC)	0.5	0.4
	door	0.8 W/m ² · K	1.2 W/m ² · K
Heat Exchanger	Efficiency	75%	75%
	Power Consumption	0.45 W/m ³ · h	0.50 W/m ³ · h
Performance	Air tightness	0.6 / h @ 50Pa	0.6 ~ 1.5 / h @ 50Pa
	Heating Demand	15 kWh/ m ² · a	50 kWh/ m ² · a
	Primary energy consumption	120 kWh/ m ² · a	150 kWh/ m ² · a

So passive houses in Korea have more days of dehumidification load than cooling loads, and they are not considered in passive houses in Europe (Sadineni et al., 2011).

In particular, as the ventilation system was operated for 24 hours, the high humidity of the summer entered the room, causing the problem to be more serious. Passive houses in Korea will be an important goal to solve this summer moisture problem (Yongsang, 2014).

Passive house and Low energy house certification standard in Korea

Based on the data, PHIKO summarized the certification standards of passive houses certified in Korea as

shown in the table 1. This criterion is not yet finalized and may change as more measurements are accumulated (Sangtae, 2016). This data is still in progress, and in addition to these criteria, there will be added a mandatory requirement to address the above-mentioned summer humidity.

For this purpose, PHIKO has developed "Standard Passive House" for two years ago and has supplied about 16 houses with the same performance nationwide.

Since all houses with the same performance and design are located in different climates in Korea, the data from this house will have a great significance in determining Korea's passive house standards in the future.

References

- Bansal, N.K., Hauser, G., Minke, G. (1994). *Passive Building Design: a handbook of Natural Climatic Control*. Amsterdam: Elsevier Science B.V.
- Bradshaw, V. (2006). *The Building Environment: Active and Passive Control Systems*. New Jersey: Wiley.
- Feist, W. (1993). *Passive Houses in Central Europe*. Dissertation. Kassel: Comprehensive University of Kassel.
- Künzel, H.M., Holm, A.H. (2009). *Moisture control and problem analysis of heritage constructions*. PATORREB: Encontro sobre Patologia e Rehabilitação de Edifícios.
- Parker, J., Hardy, A., Glew, D., Gorse, C. (2017). A methodology for creating building energy model occupancy schedules using personal location metadata. *Energy and Buildings*, 150, pp. 211–223. DOI: 10.1016/j.enbuild.2017.06.014
- Pérez-Lombard, L., Ortiz, J., Pout, C. (2008). A review on buildings energy consumption information. *Energy and Buildings*, 40(3), pp. 394–398. DOI: 10.1016/j.enbuild.2007.03.007
- Sadineni, S.B., Madala, S., Boehm, R.F. (2011). Passive Building energy savings: are view of building envelope components. *Renewable and Sustainable Energy Reviews*, 15, pp. 3617–3631. DOI: 10.1016/j.rser.2011.07.014
- Sangtae, R. (2016). *A Comparison of Insulation Performance between Domestic and International Passive House*. Architectural Institute of Korea.
- Wanga, Z., Wanga, Y., Srinivasan, R.S. (2017). A novel ensemble learning approach to support building energy use prediction. *Energy and Buildings*, 159, pp. 109–122. DOI: 10.1016/j.enbuild.2017.10.085
- Yongsang, Y. (2014). *A Study on the Correlation of Domestic Local Climate and Annual Heating Energy Demand - Focused on passive house performance buildings*. Architectural Institute of Korea.

INNOVATIVE CONSTRUCTION MATERIAL BASED ON AERATED CERAMICS

Konstantin Dmitriev ¹, Victor Zverev ²

¹INFOSMIT Co. Ltd,
Finlyandskaja ul. 16, k. 1, Kolpino, St. Petersburg, Russia

²Saint Petersburg State University of Architecture and Civil Engineering
Vtoraja Krasnoarmejskaja ul. 4, St. Petersburg, Russia

¹dm-konstantin@mail.ru, ²centeririna@spbgasu.ru

Abstract

The study looks at the production of effective construction materials based on clay rocks of various mineral and chemical compositions. A method for the manufacturing of aerated ceramic materials and products with the specified average density is described; results of their structure analysis, as well as physical and mechanical characteristics of aerated ceramic samples are presented.

The main production stages for the creation of a cellular structure of a ceramic shard are presented, and the prospects of aeration technology for clay masses for the production of a non-combustible material that allows the construction of wall enveloping structures with high strength and thermophysical parameters is proved.

Keywords

Clay, aeration, cellular ceramics, ceramic slurry, structure.

Introduction

Ceramic bricks and stones are basic wall materials widely used in private residential and multi-storey construction. Baked clay products are characterized with durability, fire resistance, environmental friendliness, architectural expression and certain physical and mechanical properties required for the construction of high reliability buildings and structures with optimum microclimate in premises (Zavadskiy et al., 2004).

The technology for the manufacturing of dense lightweight ceramic products has been known for a long time, but to ensure particular thermal and physical parameters of modern buildings, it is necessary to use effective heat insulating materials. Mineral wool and foamed polystyrene are the most popular among them. Both materials have certain advantages and disadvantages. Mineral wool is preferably used as heat insulation for building walls. Since this material shall not be exposed to direct atmospheric influences, construction engineers have to use various facade finishing systems.

However, their use leads to inevitable complications of construction compared to walls made of ceramic bricks or stones only. To ensure the homogeneity of wall heat and moisture transfer parameters, it is preferably to build walls with related construction materials, i.e. use dense ceramic

bricks and highly porous ceramics simultaneously (Dmitryev, 2015).

Methods for the production of cellular ceramics

As for traditional wall ceramics, there are two basic ways to reduce the average density of products: removal of foaming agents and cavitation. Porous ceramic stones widely used in the construction practice can be obtained by the combination of several methods: generation of through cracks and introduction of pore-forming agents into the initial ceramic mass. This method allows for the reduction of fuel consumption, efficient product density decrease, use of industrial by-products, etc. Sawdust, coal, ash, foamed polystyrene, by-products of paper and coal industries, etc. are used as pore-forming agents (Rogovoy, 1974).

In foreign countries, the Poroton technology for manufacturing porous-hollow products, developed in Germany and Sweden more than 25 years ago (Rekitar, 1981; Boldyrev et al., 1980), has become widespread. The patent for manufacturing these products was purchased by 32 countries. Poroton products are manufactured by plastic molding and introduction of foamed polystyrene beads as burning addition.

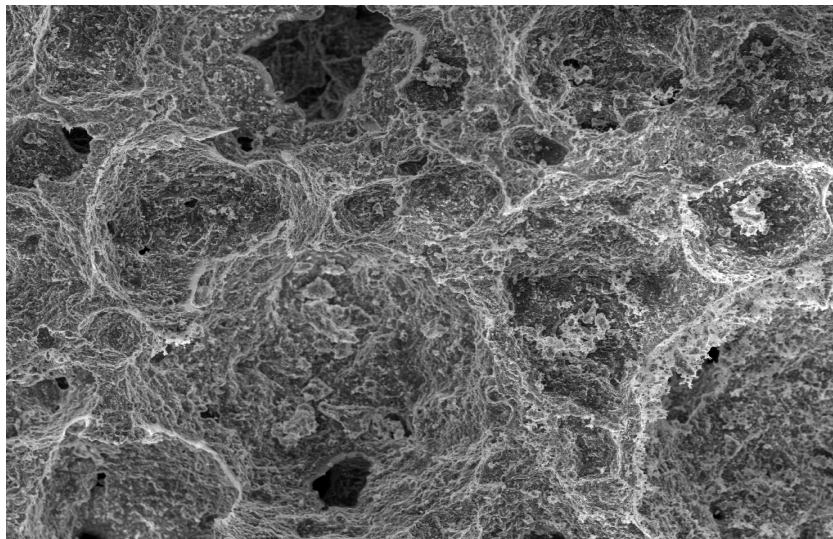


Figure 1. Fragment of the micro-porous structure of an aerated ceramic product made of Mix 1, division value — 20 μm

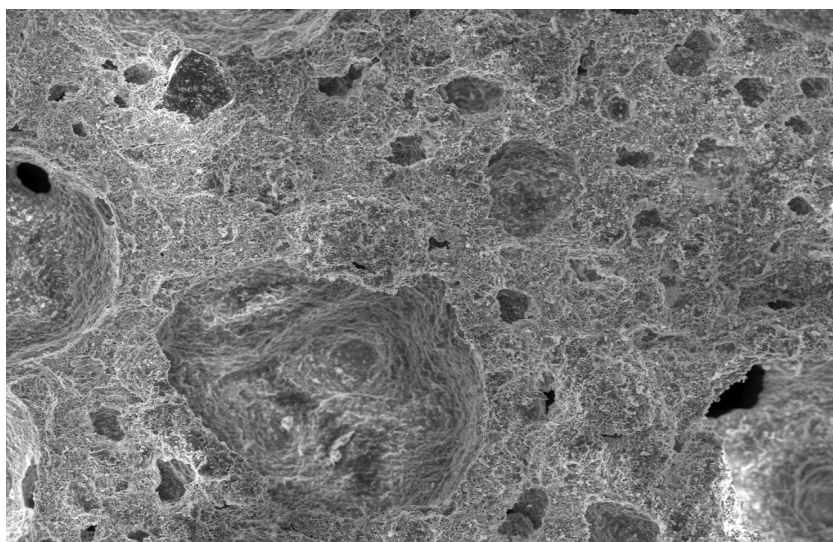


Figure 2. Fragment of the micro-porous structure of an aerated ceramic product made of Mix 2, division value — 20 μm

Besides, the method of gas generation with aluminum powder, as well as the method of foam formation using individually manufactured commercial foam as a foaming agent (Selivanov et al., 2013; Krutov and Gavrilyuk, 2012), are actively used and developed to obtain cellular structures. However, these methods have not come into common industrial use due to insufficient theoretical substantiation and practical background.

Analysis of literature and research data shows prospects for the development of the porous structure of a ceramic piece by the aeration of clay ceramic slurry in a high-speed mixer, based on modern advances in the ceramic industry and production of cellular concrete.

Experimental setup

Due to effective cooperation of the INFOSMIT testing laboratory and the Department of Technology of Building Materials and Metrology (Saint Petersburg State University of Architecture and Civil Engineering), practical and

theoretical regulations in the field of clay slurry aeration and production of highly porous ceramic materials possessing high strength and thermal-physical properties were established.

The main features of the technology for the development of the cellular structure in a ceramic piece are the following:

- preparation of the following raw components: clay raw materials, electrolytes, thinning agents, reinforcing agents, pore-forming agents, and water.
- preparation of a raw mix in the form of slurry with a certain viscosity;
- pore formation (aeration) in slurry until the achievement of the required density by the clay mass;
- molding of the aerated clay mass into rigid molds using vibrating devices, if necessary;
- drying of the aerated mass until the achievement of the residual moisture content of less than 15%, followed by cutting into work pieces;

- heat treatment of prepared raw products;
- cooling, surface treatment, packaging and dispatch to the finished goods warehouse.

Slurry aeration is performed with forced air entrainment and its retention in the mass in the form of bubbles. Retaining of the cellular structure during drying is based on clay slurry coagulation. One of the main difficulties in the preparation of raw mixes and a production line is the variety of clay deposits establishing various approaches to the development of the composition, its rheological properties and basic production conditions.

The experiment is based on the use of clays from different deposits to produce aerated ceramic bricks with dimensions of 250 × 120 × 65 mm.

The chemical composition of the used clays is shown in Table 1. The raw mix consists of the following components: sodium silicate (electrolyte), finely crushed aerated ceramic bricks (thinning agent), basalt fiber (reinforcing agent), synthetic foaming agent (pore forming agent), and process water. The clay component and thinning agent are pre-dried to 5% moisture content and grinded to powder with the maximum particle size of 0.16 mm.

The ratio of components is given in Table 2.

The above-mentioned mixes were selected to produce defect-free aerated ceramic bricks with the average density of 600 kg/m³ and compression strength of at least 5.0 MPa.



Figure 3. Appearance of the aerated clay mass made of Mix 1 during drying

Slurry preparation and aeration are carried out in a high-speed mixer with the propeller stirrer rotation frequency of 2 100 rpm to obtain the porous clay mass of the required density. The aeration time is 4 minutes.

The obtained aerated clay mass is portioned into rigid molds with sides, coated with an agent reducing adhesion of the laid aerated clay mass to the inner walls of the mold. The molded aerated clay mass is dried in drying chambers with the maximum heat-transfer medium temperature of 65°C until shrinkage completion and the moisture level of 7%. Then products are heat treated at the max-

Table 1. Chemical composition of clays

No.	Clay type	Content of basic oxides						
		SiO ₂	Al ₂ O ₃ +TiO ₂	Fe ₂ O ₃	CaO	MgO	Na ₂ O+K ₂ O	LOI
1	Brick clay from the Novgorod Region	56.45	18.23	6.92	4.71	2.22	4.14	7.33
2	Brick clay from the Leningrad Region	62.19	16.56	6.14	1.53	4.05	4.94	4.59
3	Brick loam from the Udmurt Republic	65.17	14.07	5.17	1.84	2.74	5.25	5.76

Table 2. Composition of the raw mix

No.	Component	Contents		
		Mix 1	Mix 2	Mix 3
1	Brick clay from the Novgorod Region	45.54	–	–
2	Brick clay from the Leningrad Region	–	55.05	–
3	Brick loam from the Udmurt Republic	–	–	60.17
4	Sodium silicate	0.48	0.45	0.41
5	Crushed aerated ceramic bricks	20.46	10.58	9.45
6	Basalt fiber	0.32	0.28	0.30
7	Synthetic foaming agent	0.67	0.73	0.65
8	Process water	32.53	32.91	29.02

imum temperature of 980°C during 240 minutes. In this case, the time of temperature rise to the maximum level is 180 minutes; the cooling time is 360 minutes.

One of the engineering advantages of aerated ceramics production is an accelerated baking mode in comparison with solid ceramic products (the total baking time is less than 15 hours). Such acceleration is due to the high gas permeability of the dried raw material, allowing it to warm up to the maximum temperature faster, as well as due to the cellular structure with thin pore walls which do not require long-term heating at the maximum temperature (Morris et al., 2008; Gonzenbach et al., 2007).

Table 3. Main parameters of clay slurry and finished products

No.	Parameter	Mix 1	Mix 2	Mix 3
1	Prepared slurry density, kg/m ³	1,684	1,726	1,703
2	Aerated slurry density, kg/m ³	679	667	659
3	Air shrinkage, %	9.769	10.85	8.97
4	Baking shrinkage, %	1.84	2.45	2.18
5	Average density, kg/m ³	606	598	595
6	Compression strength, MPa	5.84	6.38	6.49

Photos of the micro-porous structure of aerated ceramic bricks made of Mix 1 and Mix 2 were made using a

Tescan VEGA 3 SBH scanning electron microscope and are shown in Figures 1 and 2.

Main physical and mechanical parameters of clay slurry and corresponding aerated ceramic bricks are presented in Table 3.

Appearance of the molded aerated clay mass made of Mix 1 in the mold with dimensions of 287 x 138 x 75 mm is shown in Figure 3.

The described above method for the production of aerated ceramic products is implemented based on the closed cycle principle, where by-products are excluded: defective products are returned back to the production in the form of a thinning agent. The very principle of the development of the cellular structure in products is a new solution; it does not use standard binders as stabilizing additives, but reveals the natural properties of clays to the fullest extent possible.

Conclusion

The presented method of clay mass aeration makes it possible to regulate the density and strength of finished products in wide range; however, it is necessary to perform experiments on raw mix development, as well as on the selection of optimum drying and baking modes for each particular clay deposit.

In general, it is worth noting the high potential for the application of the technology for the production of aerated ceramics with high strength and thermal-physical parameters in production lines of existing ceramic plants with the aim to expand the range of products, as well as in the design of new manufacturing plants based on widely used clay raw materials without expensive components and complex production operations.

References

- Boldyrev, A.S., Dobuzhinskiy, V.I., Rekitar, Ya.A. (1980). *Tekhnicheskii progress v promyshlennosti stroitelnykh materialov [Technological advances in the construction materials industry]*. Moscow: Stroyizdat, p. 399. (in Russian)
- Dmitryev, K.S. (2015). Peptizatsiia glinistykh suspenzii v tekhnologii penokeramiki [Peptization of clay suspensions in the foam ceramics technology]. *Fundamental Research*, 10 (2), pp. 249–253. (in Russian)
- Gonzenbach, U.T., Studart, A.R., Tervoort, E., Gauckler, L.J. (2007). Macroporous ceramics from particle-stabilized wet foams. *Journal of the American Ceramic Society*, 90 (1), pp. 19–22. DOI: 10.1111/j.1551-2916.2006.01328.x
- Krutov, Yu.M., Gavrilyuk, A.Yu. (2012). *Sposob polucheniia penokeramiki i izdelii iz nee [Method for the preparation of foam ceramics and foam ceramics products]*. Patent No. 2469979 of the RF, MPK S 04 V 33/13, S 04 V 28/26, S 04 V 38/00, S 04 V 40/00 [МПК C 04 B 33/13, C 04 B 28/26, C 04 B 38/00, C 04 B 40/00]. No. 2010130850/03, Application dd. 22.07.2010. Bulletin, 35, p.9. (in Russian)
- Morris, G., Pursell, M. R., Neethling, S. J., Cilliers, J. J. (2008). The effect of particle hydrophobicity, separation distance and packing patterns on the stability of a thin film. *Journal of Colloid and Interface Science*, 327, pp. 138–144. DOI: 10.1016/j.jcis.2008.08.007
- Rekitar, Ya. A. (1981). *Tendentsii razvitiia stroitelstva v vedushchikh kapitalisticheskikh stranakh [Trends in the development of construction in leading capitalist countries]*. Moscow: Nauka, p. 336. (in Russian)
- Rogovoy, M.I. (1974). *Tekhnologiya iskusstvennykh poristykh zapolnitelei i keramiki [Technology of artificial porous fillers and ceramics]*. Moscow: Stroyizdat, p.315. (in Russian)
- Selivanov, Yu.V., Shiltsyna, A.D., Loginova, Ye.V., Selivanov, V.M. (2013). *Syrevaia smes dlia izgotovleniia keramicheskikh teploizolatsionnykh stroitelnykh materialov [Raw mix for the production of ceramic heat-insulating construction materials]*. Patent No. 2484063 of the Russian Federation: MPK S 04 V 38/02, S 04 V 33/00 [МПК C 04 B 38/02, C 04 B 33/00]. Siberian Federal University. Application dd. 06.02.2012, No. 2012104036/03. Bulletin, 16. p. 6. (in Russian)
- Zavadsky, V.F., Putro, N.B., Maksimova, Yu.S. (2004). Porizovannaia stroitelnaia keramika [Porous construction ceramics]. *Stroitelniye Materialy [Construction Materials]*, 2, pp. 50–51. (in Russian)

TRANSPORT ENERGY EFFICIENCY ASSESSMENT ON THE BASIS OF THE LIFE CYCLE WITH THE ATTRACTION OF THE BARTINI TRANSFER ENTITY

Jurij Kotikov

Saint Petersburg State University of Architecture and Civil Engineering
Vtoraja Krasnoarmejskaja ul. 4, St. Petersburg, Russia

cotikov@mail.com

Abstract

A technique for assessing the transport energy efficiency on the basis of the life cycle is developed with the use of the Bartini *Transfer* entity.

Main elements of the technique are the following: 1) assertion of the necessity to correlate (compare) the amount of energy to the absolutized transfer of a transport object with the life-cycle Cumulative Energy Demand (CED); 2) selection of the Bartini *Transfer* entity (and the corresponding cell of the Bartini table) for the mentioned correlation; 3) use of the Tiguntsev model for calculations of the kinetic and potential energy for the motion of an absolutized transport object in the gravitational field; 4) construction of a diagram with axes Speed V and Specific CED; 5) carrying out of the analysis in the field of the V -CED diagram for the comparison of the amount of energy to the transfer of an absolutized transport object with the transport system CED for such transportation. A number of examples are given.

Keywords

Transport, squared speed, Bartini, Transfer, *Tran*, energy efficiency, life cycle.

Introduction

Let us make several statements which hold for the energy, economy and transport industries on the threshold of a historically new technological paradigm.

1. The transportation customer is keenly interested in the express delivery of the freight itself, but pays less attention to the means of transportation.

2. All resistances (air resistance, road resistance, etc.) depend on the squared speed of a vehicle.

3. It is the squared speed which determines the energy of object transfer and even processes of manufacturing transport system elements.

4. With the approach of a new technological paradigm, it becomes more and more important to take into account the speed of process implementation (or, more specifically, the squared speed).

5. Since the early days, manufacturing of all items has been carried out due to the solar energy.

6. The following question is relevant: what is the efficiency of the initial solar energy utilization in the industry, e.g., by a transport system?

7. To answer this question, it is reasonable to correlate the energy to the absolutized transfer of a target transport object in the Earth's gravitational field, in vacuum, under levitation conditions and in the absence of mechanical environmental resistances, on the one hand, with the fossil CED through the production chain up to and including the freight delivery to the consignee, on the other hand.

8. The correlation (comparison) of the amount of energy to the mentioned absolutized transfer of a transport object with the CED (according to the terminology of ISO 14040: 2006 and ISO 14044: 2006 standards for Life Cycle Assessment (LCA)) will allow establishing an indicator (index) for the energy efficiency of the transport system, the transport mode, the fleet of vehicles, an individual vehicle.

9. The amount of energy to the mentioned absolutized transfer of an object will play the role of the minimum minimum idealized estimate. Technically, it is unattainable, but being abstract and unrelated to the specific transport mode, it can serve as the basis for obtaining comparative

assessments of energy efficiency for operational groups of vehicles within transport modes and between them.

Problems and methods

The energy efficiency of the A system is the ratio of the value of A useful services to the energy consumption of this A system. Usually both the output and the energy consumption are related to a period of time, which obviously leads to the elimination of time and yields the dimension "services per energy" such as km/kJ for a vehicle, kg/kWh for a waste disposal process, or kByte/Ws for an internet service (Hilty, 2009).

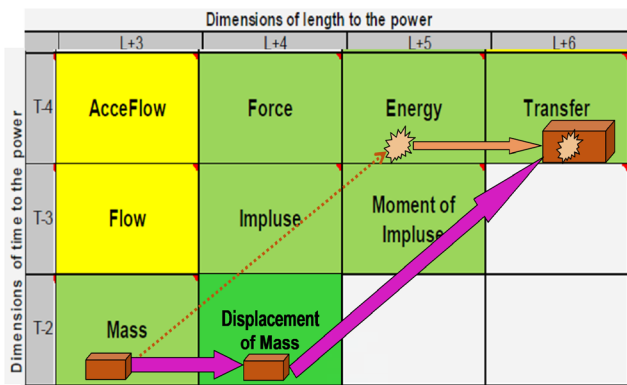


Figure 1. Part of matrix of physical laws as a canvas for analysis

Let S be the service estimate at the system output, and E — the system energy consumption. Then, the energy efficiency can be determined as $\mu = S/E$.

Let us note that according to this definition the energy efficiency differs from the efficiency (sometimes called the energy efficiency as well) defined in physics as $\eta = E_{out}/E_{in}$, where E_{out} is the useful output energy of the system, and E_{in} is the input energy (where these essences are of the same kind). Obviously, the η efficiency is a special case of the μ energy efficiency. For computer systems, it is possible to assume $\eta = 0$, as all energy is converted to heat in the end, while the purpose of these systems is not heat supply.

As for the transport sector, it shall be noted that the operation of a transport system (by analogy with a computer system) results in object transfer or, more precisely, rendering of services for the transfer of a target object to a certain customer. Thus, the energy efficiency of a transport system shall be determined by the following equation:

$$\mu = \frac{S}{E} \quad (1)$$

The objective of the author's studies (Kotikov, 2001, 2005a, 2005b, 2006, 2017a, 2017b) and the present study is to develop a new methodological approach to the assessment of the energy efficiency of transport and provided transport services considering the squared speed of the transport object delivery. This approach is related to the development of Robert Bartini's ideas on LT -systema-

tization of physics laws on the basis of a pair of coordinate parameters Length (L) – Time (T) (Bartini, 1965, 1974). The core of this approach is to form the ratio between the transferred transport output to the destination point (considering the squared speed of the freight transfer — transfer service S) and the specific embodied energy consumption of the transport system for this freight transfer. Convergence of dimensionalities of two mentioned ratio variables is provided at the *Transfer* entity level with the dimensionality **L6T-4** (Aleinikov, 2007) of Bartini LT -table.

Case studies considered in works (Kotikov, 2005b, 2017a and 2017b) by instances of freight delivery by a single-unit KamAZ-5320 vehicle with speeds of 40 km/h and 60 km/h, and by a high-speed train with a speed of 120 km/h showed low energy efficiency (in terms of the utilization of the total borrowed solar energy) of modern freight transportation: $\mu = 0.05–0.16$.

In the present article, an attempt is made to strengthen the methodological approach in terms of terminology as well as through visual analysis tools. An important feature of the approach is the active use of the Life Cycle Assessment (LCA) concept for the transport system and carrying out of a design study covering energy consumption of the main functional constituent elements of the system: creation, technical support, working process (ISO 14040-2006 and 14044-2007).

A fragment of R. Bartini LT -table (Bartini, 1965) in the interpretation of A. Aleinikov (Aleinikov, 2007) serves as a methodological canvas for the study (Kotikov, 2017a, 2017b) and is given in Figure 1.

The upper branch in Figure 1 (Mass – Energy – Transfer) reflects the freight mass M_{net} transfer to the composition of the transport carrier, thus, forming the mass $M_{gross} = M_{net} + M_{carr}$. Here M_{carr} is a specific part of the transport carrier mass, associated with the freight mass M_{net} . Hereinafter, the mass M_{gross} with the energy consumption E_{Σ} is transferred over distance L to the destination point, thus, forming real value for *Transfer* S_{gross} index.

Here $E_{\Sigma} = E_{Emb} + E_{Supp} + E_{Input}$, where E_{Emb} , E_{Supp} and E_{Input} — utilization of specific parts of energy, respectively:

- embodied in the transport carrier and infrastructure;
- designed for technical support;
- input and directly consumed for transportation.

All three components are in shares associated with the mass M_{gross} and transportation distance L .

The dashed line from Mass to Energy means a relation between the Demand (object mass transfer) and Supply (availability of transfer means and infrastructure with preliminary embodied energy, as well energy for support and input).

The lower branch in Figure 1 (Mass – Displacement of Mass – Transfer) represents a process of the formation of the ideal, illusory assessment of transport service *Transfer* S_{net} (net-process) for abstract transfer of net-mass of the freight M_{net} over distance L at speed V . Strictly speaking, the Customer is interested in the implementation of these factors (it is almost not interested in the transfer of

gross-mass M_{gross} , realized by an energy-intensive carrier under the conditions of the real transport system).

Transfer of the transport object itself is absolutized. The object is transferred from the initial to the final point with conditional consideration of energy consumption for overcoming of the Earth's gravitational field (proportional to the squared speed of the transfer). Everything connected with energy consumption for the manufacture of the transport carrier structure, erection of the traveling construct, overcoming of the carrier motion resistances, motion control, technical operation, etc. is put to the "upper branch" (with introduction of the above into the Energy cell).

This provides a possibility of numerical assessment of the correlation between the transport object transfer by means of real transport under real conditions and the conditional absolutized transfer of a transport object which is the utmost effective to the Earth's gravitational field.

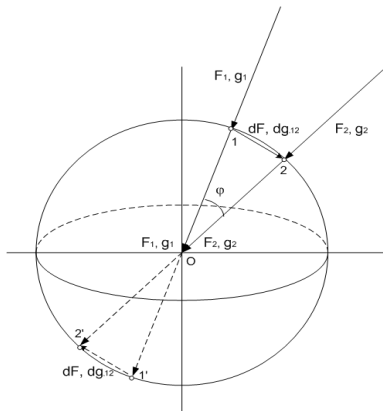


Figure 2. Model for the formation of the force required for the uniform motion of a body along the equipotential surface of the Earth's force field (Tiguntsev, 2014, 2015)

The ratio $\mu = S_{net} / S_{gross}$ characterizes the level of excellence of the carrier type in the existing technological paradigm within the scales of the development of solar energy by mankind.

A distinctive feature of the calculation for the specific embodied energy of the transport system using the author's method is the reduction of energy consumption for the life cycle of all system components to the life cycle of the transport carrier. Under consideration of the total mileage of the transport carrier within its life cycle, this provides a direct possibility to calculate energy consumption for the performance of a particular transportation.

To present and calculate the mentioned absolutized transfer of a transport object, let us use the model of S.G. Tiguntsev for the formation of a force required for the uniform motion of a body along the equipotential surface of the Earth's force field (Tiguntsev, 2014, 2015). For small areas of transfer and low-speed vehicles, the model represents the "horizontal movement". For high speeds and large areas (aviation, Hyperloop (http://www.spacex.com/sites/spacex/files/hyperloop_alpha-20130812.pdf), space

transport), the model is able to represent the motion along the equipotential surface. Such model flexibility is useful for a "seamless" analysis of the operation of the entire range of vehicles on a single canvas. Let us represent the model briefly.

The body with the mass m experiences the gravity force F equal to the product of the mass m by the gravity acceleration vector g (the boldface characters are vectors). In two separated points 1 and 2 of the Earth's surface, the body with the mass m experiences gravity forces F_1 and F_2 equal to the product of the mass m by the gravity acceleration vectors g_1 and g_2 , respectively, equal in magnitude (see Figure 2). The vectors g_1 and g_2 converge in the center of the Earth (point O) at an angle φ to each other. The vectors of forces F_1 and F_2 are also equal in magnitude and converge in the center of the Earth at an angle φ to each other. For illustrative purposes, the vectors are shown in the figure at a sufficiently large angle to each other, although this angle can be arbitrarily small.

Let us assume that, after the application of the force impulse, the body is in a state of the uniform motion along the "horizontal" surface of the Earth from point 1 to point 2 in the absence of braking effects of the surface and the air. The path between these points 1 and 2 is curvilinear (even in the smallest section) with a curvature radius equal to the radius of the Earth.

When the body moves uniformly from point 1 to point 2, it permanently experiences the force equal to the difference of the F_2 and F_1 forces (after the transfer of the origin of the F_2 and F_1 vectors to the point O, for the transferred vectors F_1 and F_2 having the common point O, the rule of subtraction of vectors can be applied). The vector dF equal to the difference of the vectors F_2 and F_1 , represents a force, which being external relative to the body, acts from point 1 to point 2 and ensures the uniform motion of the body along the equipotential surface, in the absence of inhibiting factors, as long as desired. Thus, the force acting on a body with the mass m is determined by the following equation:

$$dF = m \cdot (g_2 - g_1) \tag{2}$$

In equation (2), the difference of vectors $dg = (g_2 - g_1)$ represents the acceleration, which is constantly provided by the force dF . The mentioned acceleration is related to the gravity acceleration, the only difference being that the gravity acceleration acts always, and the mentioned acceleration acts only from the moment when, after the force application, the body falls in a state of the uniform motion. Experiencing the force dF , the body is in a state of the uniform motion with the following speed:

$$V = |g_2 - g_1| \cdot \frac{R}{g} \cdot \Delta t \tag{3}$$

Based on equation (3) at $\Delta t = 1$ unit of time, it is possible to obtain the following equation:

$$\left| \frac{dg}{\Delta t} \right| = g \cdot \frac{V}{R} \quad (4)$$

In the Tiguntsev model, a part of the potential energy of gravity is constantly converted into the kinetic energy of the body motion K_{ig} , which is determined as the product of the force dF by the covered distance (L):

$$K_{ig} = dF \cdot L \quad (5)$$

After transformations of traditional theoretical mechanics, working equations are obtained. For the potential energy:

$$E_p = A = m \cdot g \cdot L = m \cdot g \cdot V \cdot \Delta t \quad (6)$$

where A is gravitational work.

The kinetic energy of the body moving uniformly with a speed V is equal to the energy which the body received when speeding from zero to the speed of the uniform motion V :

$$E_k = \frac{m \cdot V^2}{2} \quad (7)$$

Case Study

Let us consider graphs of types of the required energy vs. the speed of the uniform absolutized motion, plotted according to equations (6) and (7).

As for our idealized object, the kinetic energy accumulates (blue curve in Figure 3) in the course of its acceleration as a result of the propulsive force impulse from the side of the leading element, with the transformation of the impulse into the object momentum. At the stage of deceleration, the kinetic energy returns to the leading element (with the full recovery for our idealized minimum minimorum scheme). Thus, the dependence of the potential energy on the speed of motion (red curve in Figure 3) remains as an estimate of the lower field boundary required for the energy transfer.

Because of the wide range of speeds V of the transport modes under study and high values of energy consumption E , which are expected during the analysis, axes of the graph on a logarithmic scale are used (Figure 4).

Depending on the transport object (freight or passengers), the corresponding ordinate axis of the specific energy consumption shall be referred to: MJ/tkm for freight traffic (the left axis), kWh/pkm for passenger traffic.

The selection of such dimensions is determined by the convenience of their recalculation and alignment with the mentioned axes, namely: with the assumption that 1 ton corresponds to a weight of 14 persons (71.43 kg/person), 1 kWhr/pkm \approx 50 MJ/tkm.

The following vehicles are shown in Figure 4, for which information on the life-cycle CED is available:

- 1) KamAZ-5320 truck, speed 40 km/h (Kotikov, 2006);
- 2) KamAZ-5320 truck, speed 60 km/h (Kotikov, 2017a);

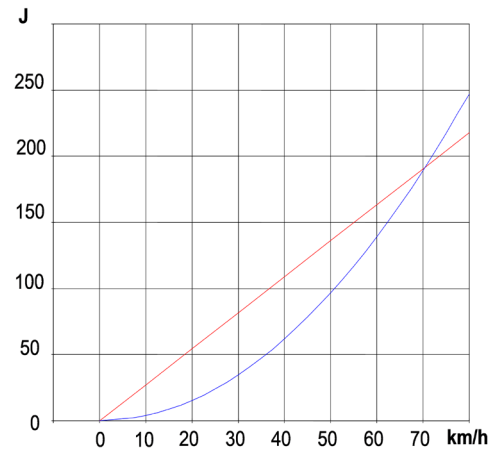


Figure 3. Graphs of energy vs. the rate of the uniform motion (vertical axis — energy, $\text{kg} \cdot \text{m}^2/\text{s}^2$, horizontal axis — the speed of the uniform motion, km/h)

- 3) Freight train (Rail diesel/electric), speed 75 km/h (Mithraratne, 2011);
- 4) 15–30 t trucks, speed 75 km/h (Mithraratne, 2011);
- 5) 7.5–15 t trucks, speed 75 km/h (Mithraratne, 2011);
- 6) 5–7.5 t trucks, speed 75 km/h (Mithraratne, 2011);
- 7) Passenger car, speed 75 km/h (Mithraratne, 2011);
- 8) Passenger train (Heavy Rail Transit (HRT)), capacity 35–350 passengers, speed 75 km/h (Chester, 2010);
- 9) Bothnia Line freight train, speed 120 km/h (Kotikov, 2017b);
- 10) Mercedes-Benz A passenger car (diesel), speed 120 km/h (Life Cycle, 2015);
- 11) Mercedes-Benz A passenger car (petrol), speed 120 km/h (Life Cycle, 2015);
- 12) Mercedes-Benz S400 Hybrid passenger car, speed 120 km/h (Life Cycle, 2015);
- 13) Passenger car, capacity 1–5 passengers, speed 120 km/h (Chester, 2010);
- 14) CRH2 passenger train, speed 250 km/h (Zhou, 2014);
- 15) CRH3 passenger train, speed 350 km/h (Zhou, 2014);
- 16) HS2 passenger train, speed 360 km/h (Zhou, 2014);
- 17) TGV duplex passenger train, speed 330 km/h (Zhou, 2014);
- 18) Passenger train (California High Speed Rail (CASHR)), capacity 120–1,200 passengers, 354 km/h (Chester, 2010);
- 19) Maglev UK Ultraspeed train, speed 500 km/h (Zhou, 2014);
- 20) B757-200 aircraft, speed 880 km/h (Zhou, 2014);
- 21) B737-300 aircraft, speed 820 km/h (Zhou, 2014);
- 22) B747-400 aircraft, speed 940 km/h (Zhou, 2014);

23) Aircraft, capacity 24–120 passengers, 820 km/h (Chester, 2010).

Discussion

In Figure 4, two indicative lines are seen, which originated in Figure 3 and transitioned to Figure 4 with significant expansion of the speed range up to 1,000 km/h.

The blue parabola of the kinetic energy from Figure 3 transformed in logarithmic coordinates of Figure 4 into a straight line. Upon the transition, the red straight line of the potential energy slightly bent (typical for low speeds of less than 40 km/h, where both curves tend to zero).

The blue curve shows the level of energy required for the acceleration of the unit mass of a target object (1 t of freight — on the left axis of ordinates, or 1 passenger — on the right axis of ordinates). As we know, all kinetic energy received by a target object from a vehicle is returned to such vehicle at the stage of deceleration.

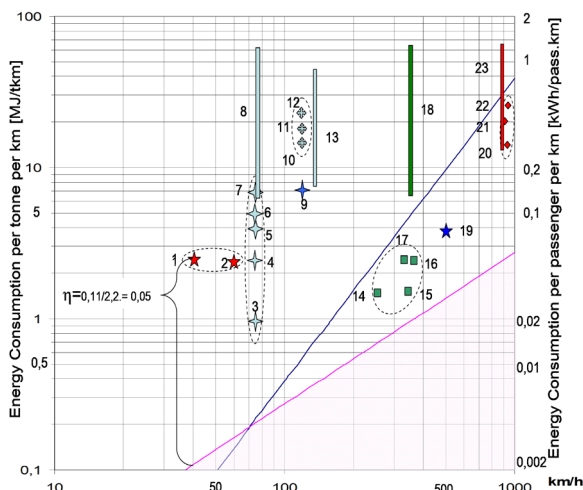


Figure 4. Location of vehicles in the V–E graph

The potential energy does not return to the source of energy supply, i.e. our vehicle. Its level increases with the speed increase, according to the red curve, but this energy is continuously spent on the work of forces of the interaction with the gravitational field. When the vehicle stops, it is reset to zero.

Since the work of a vehicle has, as a rule, unsteady and/or cyclic nature of motion speed change, at the first stage of approximation (anyway, within the framework of the article), let us replace the non-stationary process with

the steady uniform process with a representative average motion speed. This also corresponds to the Life Cycle Assessment (LCA) technology at first stages of the formation of the corresponding assessments.

The diagram in Figure 4 allows carrying out the corresponding analysis of the energy efficiency, since average values for average motion speeds within life cycles are plotted on two axes of ordinates.

On top of that, the red line represents the limit for the feasibility of transportation and the ability to provide transportation services; any points below the line mean that the energy set in the transport system is not enough even for the motion of one absolutized transport object, not to mention the energy consumption for transfer of transport containers, i.e. a vehicle.

This is the absolute lower limit, independent on the transport mode and corresponding to the transportation service *S* in equation (1). Even a quick overview of the diagram canvas in Figure 4 allows noting several factors. With the transition to high speeds of motion, the energy efficiency of transport modes increases (cars: 0.05–0.20, railway trains: 0.15–0.30, aircrafts: 0.40–0.60).

At the same time, too high energy efficiency of high-speed trains (points 14–17) gives pause on reflection on shallow coverage (by the observer) of energy processes and products in the chain of the creation of these vehicles.

Conclusion

The sequence of research activities of the author allowed forming a technique for transport energy efficiency assessment on the basis of the life cycle with the attraction of the Bartini *Transfer* entity.

Main elements of the technique are the following: 1) assertion of the necessity to correlate (compare) the amount of energy to the absolutized transfer of a transport object with the life-cycle Cumulative Energy Demand (CED); 2) selection of the Bartini *Transfer* entity (and the corresponding cell of the Bartini table) for the mentioned correlation; 3) use of the Tiguntsev model for calculations of the kinetic and potential energy for the motion of an absolutized transport object in the gravitational field; 4) construction of a diagram with axes Speed *V* and Specific CED; 5) carrying out of the analysis in the field of the V–CED diagram for the comparison of the amount of energy to the transfer of an absolutized transport object with the transport system CED for such transportation.

It shall be noted that the technique requires further development both in terms of more accurate determination and interrelation of its main functionalities, and in terms of the particularization of analytical activities.

References

- Aleinikov, A. (2007). Nine new laws of conservation: future science horizons. In: *Proceedings of the Allied Academies International Conference*, 6(2), pp. 5–10.
- Aseev, A.G. (2012). *Glamour and Emptiness of our world*. Available at: http://noocosmology.com/article/glamour_and_emptiness_of_our_world.html (accessed on: 30.09.2017)
- Bartini R.O., Kuznetsov P.G. (1974). Multiplicity in geometries and physics. In: *Proceedings of the seminar “Cybernetics of electric power systems”*, p.11. Available at: <http://www.metodolog.ru/01380/01380.html> (accessed on: 30.09.2017)
- Bartini, R.O. (1965). Some relations between physical constants. *Reports of the Academy of Sciences of the USSR*, 163 (4), pp.861–864.
- Chester, M., Horvath, A. (2010). Life-cycle assessment of high-speed rail: the case of California. *Environmental Research Letters*, 5(1), paper ID 014003. DOI:10.1088/1748-9326/5/1/014003
- Daimler AG, Mercedes-Benz Cars (2015). *Life Cycle. Environmental Certificate Mercedes-Benz S-Class*. Stuttgart. Available at: <https://www.daimler.com/images/sustainability/produkt/new-environmentalcertificates/daimler-umweltzertifikat-mb-s-klasse.pdf> (accessed on: 30.10.2017)
- Hilty, L.M., Coroama, V., Eicker, M., Ruddy, T., Müller, E. (2009). *The Role of ICT in Energy Consumption and Energy Efficiency*. Available at: <http://s3.amazonaws.com/publicationslist.org/data/lorenz.hilty/ref-42/2009-08%20Hilty%20Coroama%20et%20al%20EU%20ENSURE%20ICT%20Energy.pdf> (accessed on: 30.10.2017)
- Kotikov, Ju.G. (2001). *Osnovy sistemnogo analiza transportnykh sistem [Fundamentals of system analysis for transport systems]*. Saint Petersburg: Saint Petersburg State University of Architecture and Civil Engineering, p.264. (in Russian)
- Kotikov, Ju.G. (2005a). Analiz energoeffektivnosti transporta s pomoshchiu izmeritel'ia Tran [Analysis of transport energy effectiveness using the Tran unit]. *Integrated logistics*, 3, pp. 15–20. (in Russian)
- Kotikov, Ju.G. (2005b). Energeticheskaia effektivnost avtotransportnogo kompleksa [Energy effectiveness of the automotive transportation system]. *Bulletin of Transport*, 4, pp. 37–39. (in Russian)
- Kotikov, Ju.G. (2017a). Estimation of Transportation Energy Efficiency by Bartini Criterion L6T-4. *Architecture and Engineering*, 2 (2), pp.15–19. DOI: 10.23968/2500-0055-2017-2-2-15-19.
- Kotikov, Ju.G. (2017b). Calculation of Freight Rail Transport Energy Efficiency by Bartini Criterion L6T-4. *Architecture and Engineering*, 2 (3), pp. 21–25. DOI: 10.23968/2500-0055-2017-2-3-21-25.
- Kotikov, Ju.G., Lozhkin, V.N. (2006). *Transportnaya energetika [Transport power energy]*. Moscow: Publishing Center “Academia”, p.272. (in Russian)
- Mithraratne, N. (2011). *Lifetime liabilities of land transport using road and rail infrastructure*. <http://www.nzta.govt.nz/assets/resources/research/reports/462/docs/462.pdf> (accessed on: 30.10.2017).
- Oak Ridge National Laboratory (2016). *Transportation Energy Data Book*, Edition 35. Available at: http://cta.ornl.gov/data/tebd35/Edition35_Chapter01.pdf (accessed on: 07.09.2017)
- Obraztsova, R.I., Kuznetsov, P.G., Pshenichnikov, S.B. (1997). *Inzhenerno-ekonomicheskii analiz transportnykhsistem [Engineering and economic analysis of transport systems]*. Novosibirsk, p.156. Available at: http://lib.uni-dubna.ru/search/files/ur_enjekan/~ur_enj-ek-an.htm (accessed on: 30.09.2017). (in Russian)
- Stripple, H., Uppenberg, S. (2010). *Life Cycle Assessment of Railways and Rail Transports*. Available at: <http://www.ivl.se/download/18.343dc99d14e8bb0f58b75d4/1445517456715/B1943.pdf> (accessed on: 30.06.2017)
- Technical Committee ISO/TC 207 (2006) *ISO 14040:2006: Environmental management — Life cycle assessment — Principles and frame-work*. Available at: http://www.pqm-online.com/assets/files/lib/std/iso_14040-2006.pdf (accessed on: 12.10.2017)
- Tiguntsev, S.G. (2014). *Potencialnaia i kineticheskaia energija pri ravnomernom gorizontalnem dvizhenii tel [Potential and kinetic energy upon the uniform horizontal motion of bodies]*. Nauchno-entciklopedicheskii portal [Scientific encyclopedic portal]. Available at: http://www.russika.ru/userfiles/adm_1404275497.pdf (accessed on: 30.10.2017). (in Russian)
- Tiguntsev, S.G. (2015). *Ob inertcii i printcipe otnositelnosti [On inertia and principle of relativity]*. Available at: <http://www.bourabai.kz/tiguntzev/index.htm> (accessed on: 30.10.2017). (in Russian)
- U.S. Energy Information Administration. (2016). *International Energy Outlook*. Available at: [https://www.eia.gov/outlooks/ieo/pdf/0484\(2016\).pdf](https://www.eia.gov/outlooks/ieo/pdf/0484(2016).pdf) (accessed on: 30.09.2017)
- Zhou, J., (2014). *Improving the energy efficiency of high speed rail and life cycle comparison with other modes of transport*. London: Imperial College London. Available at: https://www.google.ru/url?sa=t&rct=j&q=&esrc=s&source=web&cd=1&ved=0a-hUKewjvMLYarWAhUBDJoKHxNaAc0QFggnMAA&url=https%3A%2F%2Fspiral.imperial.ac.uk%3A8443%2Fbitstream%2F10044%2F1%2F25066%2F3%2FZhou-J-2014-PhD-Thesis.pdf&usq=AFQjCNHMI73iTD9wyjJevIVpeOs_1H9CgA (accessed on: 30.10.2017)

IMPROVEMENT OF THE TECHNOLOGY OF EARTHWORKS IN MEGACITIES

Elena Kurakina ¹, Sergey Evtuykov ², Anna Shimanova ³

^{1,2,3} Saint Petersburg State University of Architecture and Civil Engineering
Vtoraja Krasnoarmejskaja ul. 4, St. Petersburg, Russia

¹elvl_86@mail.ru

Abstract

The study substantiates the need to improve the existing technology of earthworks in megacities. The use of alternative types of over-ground transport technological machines would change the management and process control algorithm, increase performance efficiency and quality of operations, reduce costs for procedure implementation. Shortcomings of the existing technology of earthworks in the space-limited urban environment are analyzed. An implementation procedure for the existing technology to carry out operations with the use of transport technological machines and auxiliary equipment is presented.

The study also substantiates the need for practical application of such alternative type of over-ground transport technological machines as the vacuum excavator during earthworks. A set of transport technological machines for earthworks based on the improved technology with the use of the vacuum excavator was formed; space-limited conditions of megacities were taken into account.

Keywords

Construction machinery, vacuum excavator, construction machinery operation, earthworks and road works, megacity.

Introduction

The relevance of the issue is determined, firstly, by technological advances and the need to improve the machinery and equipment used in the road construction industry, in particular, in earthworks during utilities construction. Earthworks include reconstruction, maintenance, current and major repair of underground utilities (gas and water pipelines, laying of power cables, etc.). Secondly, all process operations can be improved with the available modern mobile machinery and equipment designed for earthworks during utilities construction. Thirdly, the existing process technologies imply the risk of utilities damaging with heavy machinery, e.g. excavators. To avoid such damaging, all works are performed manually, reducing mechanization. All these aspects are “included” in works performed in the space-limited urban environment, which is due to inaccessibility of actual working areas. Practical work requires operation quality improvement, risk reduction with regard to utilities damaging caused by the introduction of a universal transport technological machine — the vacuum excavator — into earthworks. This sphere was partially investigated by Volkov S. A. (Volkov and Evtuykov, 2008) and Beletskiy B. F. (Beletskiy and Bulgakova, 2012); however, taking into account the recent

application of the vacuum excavator in the North-Western region, we can state that the issue has not been studied in full and is not considered in researches performed by leading experts and scientists of the industry. Therefore, studies on the improvement of earthworks technologies are necessary and relevant.

The relevance of the study is determined by the need to develop a flow chart to perform earthworks with the vacuum excavator on different types of road surfacing, taking into account the space-limited megacity environment and various temperatures.

Subject, objectives and methods

The subject of the study is the technology of earthworks in the space-limited megacity environment.

The study objectives are the following:

- analysis of shortcomings related to the existing technology of earthworks in the space-limited urban environment;
- substantiation of the need for practical application of an alternative type of over-ground transport technological machines (OTTMs) during earthworks;
- formation of a set of OTTMs for earthworks in various megacity conditions.

Table 1. Set of mechanized OTTMs for earthworks based on the existing technology used in megacities

3	2		1		Set of mechanized OTTMs, option	
	concrete	1–1.5	Dirt surfacing — lawn	Type of surfacing in the working area	Working area parameters	Activity
1.5 and more			–	Working area, m ²		
Trench digger machine based on MITZ-92. JCB 4CX Super II excavator with a bucket capacity of 0.65 m ³ and attachments (hydrohammer)	Pavement cutter for asphalt-concrete surfacing. JCB 4CX Super II excavator with a bucket capacity of 0.65 m ³ and attachments (hydrohammer)		–	1	Asphalt-concrete surfacing demolition	
KAMAZ 5511 dump truck, JCB 4CX Super excavator, size category: II, bucket capacity: 0.65 m ³	KAMAZ 5511 dump truck, JCB 4CX Super excavator, size category: II, bucket capacity: 0.65 m ³		–	2	Loading of the demolished asphalt-concrete surfacing into a vehicle for transportation	
JCB 4CX Super excavator, size category: II, bucket capacity: 0.65 m ³	JCB 4CX Super excavator, size category: II, bucket capacity: 0.65 m ³		Top-soil stripping for its subsequent reclamation	3	Soil excavation	
Manual operation at a depth of 30 cm to utilities	Manual operation at a depth of 30 cm to utilities		JCB 4CX Super II excavator with a bucket capacity of 0.65 m ³ and attachments	4	Manual soil excavation in areas inaccessible for OTTMs	
JCB 4CX Super excavator, size category: II, bucket capacity: 0.65 m ³	JCB 4CX Super excavator, size category: II, bucket capacity: 0.65 m ³		Manual operation at a depth of 30 cm to utilities	5	Loading of the excavated soil into a vehicle for transportation	
KAMAZ 5511 dump truck	KAMAZ 5511 dump truck		Water pump with a mechanical drive; light wellpoint systems. Sewage suction truck	6	Pumping-out of underground water, removal of gravel, etc.	
Water pump with a mechanical drive; light wellpoint systems. Sewage suction truck	Water pump with a mechanical drive; light wellpoint systems. Sewage suction truck		KAMAZ 5511 dump truck	7	Transportation of soil/surfacing, other substances	
JCB 4CX Super excavator, size category: II, bucket capacity: 0.65 m ³ . Front and clamshell loaders. Soil spreading: Komatsu D37EX-22 dozer	JCB 4CX Super excavator, size category: II, bucket capacity: 0.65 m ³ . Front and clamshell loaders. Soil spreading: Komatsu D37EX-22 dozer		JCB 4CX Super excavator, size category: II, bucket capacity: 0.65 m ³ . Front and clamshell loaders. Soil spreading: Komatsu D37EX-22 dozer	8	Soil backfilling and spreading at the working area	
Pneumatic and electric compactors, self-propelled plate compactors and jackhammers with special attachments, self-propelled rollers	Pneumatic and electric compactors, self-propelled plate compactors and jackhammers with special attachments, self-propelled rollers		Backfilling of utilities: TR-04 hand-held compactors. Protective layer (at least 25–40 cm); Champion plate compactors. Top layer: self-propelled rollers	9	Soil compacting at the working area	
Asphalt-spreader Caterpillar AP255E (for operation in space-limited conditions, laying width range — 150–3400 mm)	Asphalt-spreader Caterpillar AP255E (for operation in space-limited conditions, laying width range — 150–3400 mm)		Arrangement of lawn on the prepared and leveled soil with the base slope equal to 0.5–0.6%. Vegetable soil thickness — 15–20 cm.	10	Laying of surfacing after completion of works	

Table 2. Set of mechanized OTTMs for earthworks based on the improved technology used in megacities

Set of mechanized OTTMs, option		Working area parameters	
3	2	1	Activity
1.5 and more	concrete	Dirt surfacing — lawn	Type of surfacing in the working area
Digging milling machine.	1–1.5	–	Working area, m ²
JCB 4CX Super II excavator with a bucket capacity of 0.65 m ³ and attachments (hydrohammer)	Pavement cutter for asphalt-concrete surfacing. JCB 4CX Super II excavator with a bucket capacity of 0.65 m ³ and attachments (hydrohammer)	–	1 Asphalt-concrete surfacing demolition
Vacuum excavator	Vacuum excavator	–	2 Loading of the demolished asphalt-concrete surfacing into a vehicle for transportation
			3 Soil excavation
			4 Manual soil excavation in areas inaccessible for OTTMs
			5 Loading of the excavated soil into a vehicle for transportation
			6 Pumping-out of underground water, removal of gravel, etc.
			7 Transportation of soil/surfacing, other substances
JCB 4CX Super excavator, size category: II, bucket capacity: 0.65 m ³ . Front and clamshell loaders. Soil spreading: Komatsu D37EX-22 dozer	JCB 4CX Super excavator, size category: II, bucket capacity: 0.65 m ³ . Front and clamshell loaders. Soil spreading: Komatsu D37EX-22 dozer		8 Soil backfilling and spreading at the working area
Pneumatic and electric compactors, self-propelled plate compactors and jackhammers with special attachments, self-propelled rollers	Pneumatic and electric compactors, self-propelled plate compactors and jackhammers with special attachments, self-propelled rollers	Backfilling of utilities: TR-04 hand-held compactors. Protective layer (at least 25–40 cm): Champion plate compactors.	9 Soil compacting at the working area
Asphalt-spreader	Asphalt-spreader	Top layer: self-propelled rollers	
Caterpillar AP255E (for operation in space-limited conditions, laying width range — 150–3400 mm)	Caterpillar AP255E (for operation in space-limited conditions, laying width range — 150–3400 mm)	Arrangement of lawn on the prepared and leveled soil with the base slope equal to 0.5–0.6%. Vegetable soil thickness — 15–20 cm.	10 Laying of surfacing after completion of works

Methods to accomplish the set objectives include methods to analyze solutions to problems of large-scale construction mechanization, processes of practical management and actual performance of works, technical and operating characteristics and properties of OTTMs.

Results and discussion

Technological advances contribute to the continuous improvement of design properties of OTTMs and their mechanisms to perform a wide range of activities in various fields, in particular, the road construction industry which includes not only the construction of facilities, buildings and structures, but also earthworks. The main types of earthworks and road works are the following: soil excavation, soil filling, soil transportation and movement, excavation of frozen soils, demolition and resurfacing of asphalt-concrete pavement, opening-up and repair of underground utilities, preparation of road mixtures, bitumen transportation and distribution, laying, distribution and compaction of the asphalt-concrete mixture.

The earthworks technology is based on the developed and approved design documentation and a set of mechanized OTTMs. Taking into account the specifics of the labor-intensive operations performed, an analysis of the technical and economic parameters that determine the most efficient combination of machines with regard to cost and labor input is made (Kurakina, 2016a, 2016b; Evtuyukov et al., 2016; 2017). Reconstruction, repair and improvement of the utility network are considered to be in demand among other types of earthworks. This process is rather labor-intensive in the space-limited urban environment and requires a specific approach to the improvement of its implementation technology. The shortcomings of the existing technology of earthworks in megacities are the following (Evtuyukov et al., 2017; Kurakina, 2017):

- risk of utilities damaging (heat and gas pipelines, power transmission lines);
- manual soil excavation in areas inaccessible for OTTMs;
- increase in the number of OTTMs in the set, increase in the working area for the performance of works involving asphalt-concrete surfacing;
- increase in the area of lawn damage during OTTM operation;
- reduction of lanes (or temporary lane closure) during works on the driveway;
- complexity of processes during the performance of works at freezing temperatures;
- decrease in environmental safety.

Practical implementation of activities limits operation of OTTMs during the reconstruction, repair and improvement of the utility network. Safety requirements to gas supply systems do not allow for the operation of percussive mechanisms for soil loosening at a distance less than 3 m from a gas pipeline. Driving of piles shall not be carried out at a distance less than 30 m from a gas pipeline (in case of compliance with additional safety measures, such distance can be reduced to 10 m).

Earthworks at a distance less than 3 m and at a depth of 30 cm to utilities imply manual soil excavation. Winter operations are characterized by complicated processes, e.g. excavation of frozen soil due to the impossibility to use certain types of OTTMs, which leads to the decrease in their performance rate and accelerated deterioration of working parts and equipment, and possible compacting of frozen soil.

The increase in the number of OTTM units leads to the increase in the occupied working area, as well as to the increase in the number of maintenance specialists. All these factors contribute to the decrease in the efficiency of earthworks and labor management, increase in costs for the implementation of the earthworks technology and OTTM operation (Kurakina, 2017; Kurakina et al., 2017; Kurakina and Tsymbal, 2017; Kurakina et al., 2017).

The application of an alternative type of OTTMs — the vacuum excavator — for earthworks is conditioned by the need to eliminate all existing shortcomings. The rules of earthworks and urban landscaping are regulated by individual legal documents of the Ministry of Regional Construction. Options for the performance of earthworks at various stages according to the existing technology are presented in Table 1.

Subsequent measures on the reconstruction, repair and improvement of the utility network are specified for cases when underground water, silt, gravel or other substances are present at positive temperatures or have been removed.

set of mechanized OTTMs with a vacuum excavator was specified to improve the technology of earthworks in megacities (Table 2).

The improvement of the technology of earthworks in megacities is determined by the following factors:

- formation of a set of OTTMs and auxiliary equipment for earthworks;
- changing of the process algorithm.

Firstly, the formation of the necessary number of units of transport technological machines and auxiliary equipment contributes to obtaining higher performance and reliability rates, as well as values of environmental and engineering aspects. The introduction of a modern multi-functional OTTM — the vacuum excavator — would eliminate shortcomings in the arrangement and performance of earthworks, and improve their quality and performance rate.

Technical capabilities of the vacuum excavator include removal of dirt, sand, clay, gravel, damp soil, dust, water, crushed stones, debris and stones, as well as liquids and gases, large and heavy objects with a weight of up to 40 kg and a diameter of up to 250 mm. Secondly, the changing of the process algorithm is aimed at the replacement of several OTTMs (the excavator, the sewage suction truck and the dump truck), as well as complete elimination of manual operations.

According to the overall assessment of over-ground transport technological machines (Volkov and Evtuyukov, 2008; Repin and Chmil, 2012), their efficiency involves

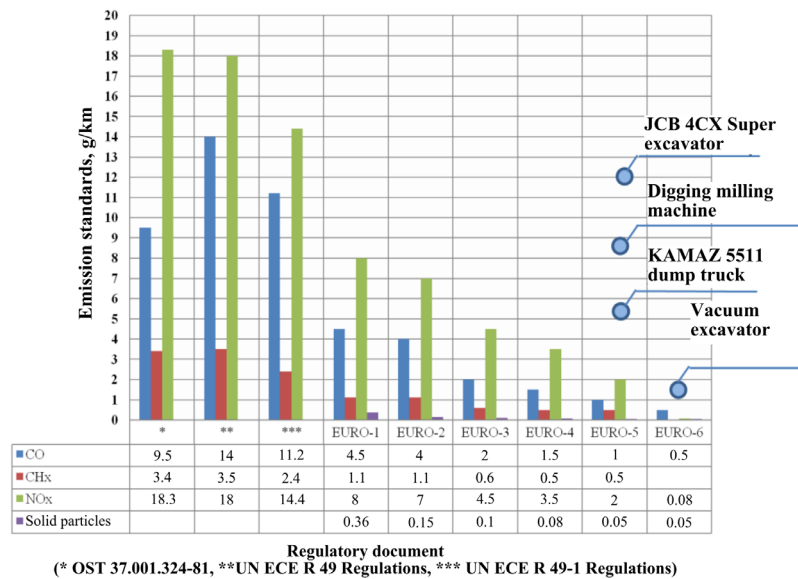


Figure 1. Histogram of emissions of harmful substances in accordance with the international standards upon OTTM operation

the reduction of fuel consumption and period of work performance, increase in the performance rate, reduction of the lane closure area in the urban environment, elimination of manual operations and risks of damage to utilities (Erokhov, 2013). An important condition for selection of OTTMs for the fleet of vehicles to be used in a megacity is compliance with the international standards for environmental safety.

Figure 1 shows a histogram of emissions of harmful substances in accordance with the international standards and compliance of the OTTMs most often used during earthworks with those standards.

An important factor for the technology improvement is to avoid downtimes and lost time during a shift, reduce costs as well as the number of OTTM units in the mechanized set and the number of maintenance specialists. When comparing the existing earthworks technology with the alternative technology, it is important to compare fuel consumption in operating OTTMs. For example, when performing operation 7 (Tables 1, 2) taking into account the type of excavated material (soil or asphalt-concrete surfacing) and other substances (if any), the fuel consumption during operation of the vacuum excavator is less by 1/3 than the fuel consumption of the dump truck and the sewage suction truck (Table 3). During operations from 3 (2) to 6, the fuel consumption of the vacuum excavator is almost the same as the fuel consumption of the excavator with the sewage suction truck (Table 3). With account for the basic specifications of OTTMs for fuel consumption, operational parameters for the stated types of OTTMs were obtained with regard to the consumption rates for fuels and lubricants in motor vehicles (Ministry of Transport of the RF, 2015).

Table 3. Operational parameters with regard to OTTM fuel consumption

OTTM	Fuel consumption	
	l/h	l/100 km
Vacuum excavator	31	59.6
JCB excavator with attachments	14.3	–
KAMAZ 5511 dump truck	–	43.4
Sewage suction truck	14.0	41.4

An advantage of the vacuum excavator over three OTTMs used during earthworks is in overall dimensions; its application allows reducing the area of damage to lawns and the lane closure area.

Conclusion

The improvement of the earthworks technology with the application of the vacuum excavator is relevant and necessary to improve the quality of the management and process control procedure, especially in space-limited conditions of megacities, as well as to increase the performance rate. The alternative technology compared to the existing one (or alternative to the existing technology) allows reducing the number of OTTM units in the mechanized set and the number of maintenance specialists, eliminating manual operations, improving quality and reducing the period of work performance, reducing risks of damage to utilities due to the knuckle boom of the vacuum excavator, and reducing fuel consumption by almost 30% of the total volume.

References

- Beletskiy, B.F., Bulgakova I.G. (2012). *Stroitelnaia tekhnika i oborudovanie [Construction machinery and equipment]*, 3rd edition. Saint Petersburg: Lan Publishing House, p.608. (in Russian)
- Erokhov, V.I. (2013). *Toksichnost sovremennykh avtomobilei (metody i sredstva snizheniia vrednykh vybrosov v atmosferu) [Toxicity of modern vehicles (methods and means of reducing harmful emissions into the atmosphere)]*. Moscow: Infra-M, p.448. (in Russian)
- Evtyukov, S.A., Evtyukov, S.S., Chudakov, A.V., Kurakina, E.V. (2017). Over-ground transport technological machines and complexes // Textbook for higher educational institutions. Saint Petersburg: Petropolis Publishing House, p.644. (in Russian)
- Evtyukov, S.S., Chudakov, A.V., Kurakina E.V. (2016). *Nazemnye transportno-tekhnologicheskie mashiny [Over-ground transport technological machines]*. Saint Petersburg: LLC Petropolis Publishing House, p.504. (in Russian)
- Kurakina, E.V. (2016a). Effektivnost ispolzovaniia nazemnykh transportno-tekhnologicheskikh mashin [Efficiency of use of over-ground transport technological machines]. *Vestnik grazhdanskikh inzhenerov [Bulletin of Civil Engineers]*, 3 (56), pp. 203–208. (in Russian)
- Kurakina, E.V. (2016b). Tekhnicheskaiia ekspluatatsiia nazemnykh transportno-tekhnologicheskikh mashin [Operation and maintenance of over-ground transport technological machines]. In: *Proceedings of the 69th Scientific and Practical Conference of Students, PhD Students and Young Scientists "Challenging Issues of Modern Construction"*. Saint Petersburg: (in Russian)
- Kurakina, E.V. (2017). Povyshenie effektivnosti nazemnykh transportno-tekhnologicheskikh mashin v zimnikh usloviakh [Improving the efficiency of land transport and technological machines in winter conditions]. *Vestnik grazhdanskikh inzhenerov [Bulletin of Civil Engineers]*, 2 (61), pp. 205–213. DOI: 10.23968/1999-5571-2017-14-2-205-212. (in Russian)
- Kurakina, E.V., Shimanova, A.A., Lyalinov, A.N. (2017). Sovershenstvovanie metodiki proektirovaniia vibroshnekovykh smesitelei [Improving the design technique of vibro-auger mixers]. *Vestnik grazhdanskikh inzhenerov [Bulletin of Civil Engineers]*, 3 (62), pp. 200–206. DOI: 10.23968/1999-5571-2017-14-3-194-199. (in Russian)
- Kurakina, E.V., Stepina, P.A., Druzhinin, V.M. (2017). Kompleksnaia mekhanizatitsiia zemlianykh rabot v usloviakh otritsatelnykh temperatur [Complex mechanization of earthwork operations in conditions of subzero temperatures]. *Vestnik grazhdanskikh inzhenerov [Bulletin of Civil Engineers]*, 4 (63), pp.182–187. DOI: 10.23968/1999-5571-2017-14-4-182-187. (in Russian)
- Kurakina, E.V., Tsybal L.V. (2017). Osobennosti ekspluatatsii vakuumno-vsasyvaiushchego ekskavatora pri proizvodstve rabot v usloviakh nizkikh temperatur [Features of vacuum suction excavator operation at low temperatures]. In: *Proceedings of the 70th All-Russian Scientific and Practical Conference of Students, PhD Students and Young Scientists "Challenging Issues of Modern Construction"*.
- Ministry of Transport of the RF (2015). No. AM-23-r dd. 14.03.2008 (revision: 14.07.2015) "On implementation of guidelines "Consumption rates for fuels and lubricants in motor vehicles".
- Repin, S.V., Chmil, V.P. (2012). *Raschetnye modeli obespecheniia rabotosposobnosti i effektivnosti transportno-tekhnologicheskikh mashin v ekspluatatsii [Calculation models to ensure the operating capability and efficiency of transport technological machines]*. Saint Petersburg: Saint Petersburg State University of Architecture and Civil Engineering, p.89. (in Russian)
- Volkov, S.A., Evtyukov, S.A. (2008). *Stroitelnye mashiny [Construction machinery]*. Saint Petersburg: Publishing House DNK, p.704. (in Russian)

GRAVITY MIXERS WITH VIBRATION ACTIVATOR IN CONSTRUCTION ENGINEERING

Victor Kuzmichev ¹, Vladimir Verstov ²

¹ Peter the Great Saint Petersburg Polytechnic University, Polytechnicheskaya st. 29, St. Petersburg, Russia

² Saint Petersburg State University of Architecture and Civil Engineering Vtoraja Krasnoarmejskaja ul. 4, St. Petersburg, Russia

¹ kuzmichev_va@mail.ru, ² 5750195@mail.ru

Abstract

Vibration processes and corresponding machinery and equipment are widely used in construction, production of construction materials and other industries. Compaction, crushing, separation, piling, dosing and transportation of bulk materials are just several processes where it is expedient to use vibration.

The article presents original designs of gravity (drum) mixers with vibration activators placed inside the mixing chamber. A vibration activator is installed in "dead" zones located along the geometrical axis of the mixing chamber where intensity of convective mixing is low.

Methods of design of balanced eccentric vibration activators of precessing type are considered. Results of production tests with regard to the industrial design of the gravity vibration mixer are presented. Considerable attention is paid to measurement of the vibration level reflecting the quality of dynamic balancing of the vibration activator. Vibrational impact on the environment and maintenance personnel amounts to $\sim 5 \text{ m/s}^2$, corresponding to standard values for processing equipment as per GOST 22061-76.

Keywords

Gravity mixer, vibration activator, design methods, dynamic balancing.

Introduction

The history of mankind is inextricably associated with inventions, discoveries, development and improvement of various technical facilities and engineering processes. At present, their diversity even within the framework of the same industry has reached the level when further improvement of technical facilities and engineering processes is impossible without modern methods for searching innovative technologies.

It is obvious that it is worthwhile to consider the social and economic expediency of the development and application of new-generation machinery and equipment only given the necessary scientific and technical potential ensuring the fundamental possibility of their design, manufacturing and practical use. At the same time, the social and economic expediency indicates that, firstly, their manufacturing and practical use to meet particular needs is economically possible and advantageous, and that, secondly, anthropogenic criteria of progressive development do not deteriorate.

Important principles of the laws of historical technology development are the following:

- the principle of limit transition: technical systems (TS) with constant functions stabilize and cease further constructive evolution, if their technical solution is approaching the global extremum based on the principle of operation (PO) and design, unless **new physical effects**, providing improved PO, arise;

- the principle of preference: when moving to new PO in TS using particular physical effects, preference is given to **newer principles**, which were discovered later.

In 1930s, H. Freundlich discovered the effect of thixotropy, i.e. viscosity reduction in disperse systems under mechanical impacts, followed by restoration of the structure after impact elimination. Vibration holds a prominent place among various mechanical impacts.

Mixing of materials is a mechanical process resulting in uniform distribution of mineral constituents' particles and a binder in a mixed volume, which, in their turn, form a uniform mix.

Based on the developed ideas, the following types of mixing are distinguished: convective and diffusing. Convective mixing is classified as a macromixing process while diffusive mixing is classified as a micromixing process.

Along with mixing, separation takes place in a mixer (separation of constituents' particles and their concentration in certain areas of the mixer body under the action of gravitational and centrifugal forces). Actual mix formation usually represents superposition of mixing and separation.

Upon mixing in mixers of various types, the mix structure changes continuously and, therefore, its structural and rheological properties change. Control over structural and rheological properties is the main direction of intensification of the diffusion component with regard to mixing processes. At the present time, the following methods are used: pseudo-liquefaction, use of surface active agents (SAA) ensuring mix viscosity reduction; binder feeding by means of nozzles, etc.

Vibration is one of the widely applied types of mechanical impact on environments in the field of construction and production of construction materials, considerably affecting changes in rheological properties of mixes (Bauman, Bykhovsky, 1977; Blekhman, 1994; Verstov et al., 20013; Chelomey, 1981; Efremov, Lobanov, 2008, 2009).

Gravity mixers have a number of advantages in comparison with mixers of forced action: gravity mixers have simple design and low energy intensity. Their disadvan-

tage is in low intensity of the mixing process. Such mixers are mainly used in flow concrete mixing.

To intensify the mixing process, it is reasonable to apply vibration.

Description of designs

The accumulated experience in the design of various vibration mixers presented in the literature (Kuzmichev, 2013, 2014) made it possible to develop production drawings and manufacture a gravity vibration mixer with the prepared batch volume of 0.5 m³ by improvement of the commercial model SB-91B at the Tyumen Construction Machinery Plant.

The improvement implied installation of a balanced precessing eccentric vibration activator of the cone shape along the geometrical axis of the drum. A fragment of the production drawing and photos are shown in Figures 1 and 2.

The mixing process is as follows. When the motor is turned on, the drum and the vibration exciter start performing working motions. Under the influence of vibration, the mix is diluted and mixed with blades in the rotating drum.

In order to confirm that an integrated vibration activator enhances the capabilities of the mixer regarding the mix composition, analysis of the mixing process was carried out.

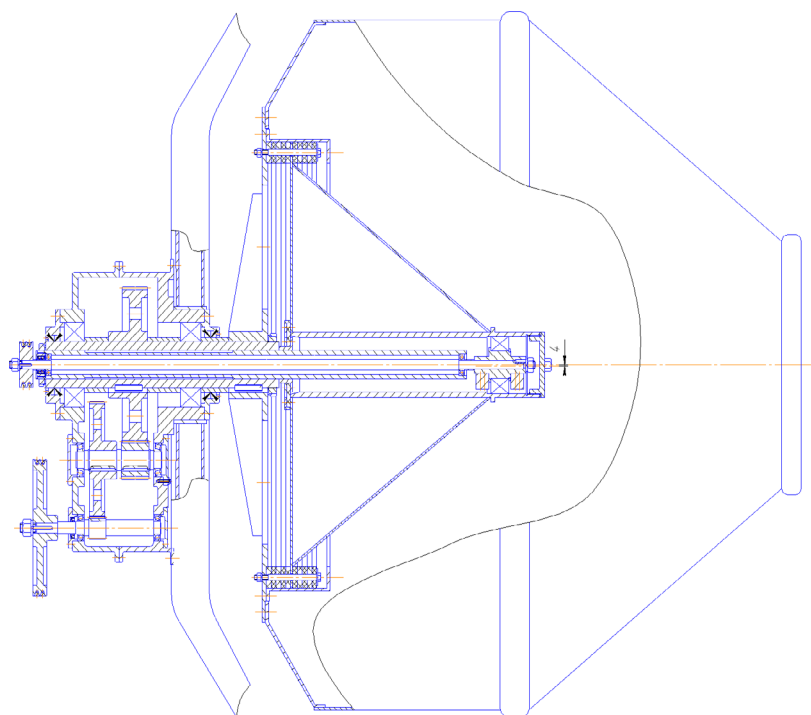


Figure 1. Fragment of the production drawing



Figure 2. Gravity vibration mixer:
 a) fragment showing the vibration level at the mixer frame during mixing; b) fragment of the mixing process

The following concrete grades were selected as test objects: M300, a mix with the cone slump of 0 cm and the stiffness index of 10 s; M200, a mix with the cone slump of 0 cm and the stiffness index of 30 s.

Table 1. Technical characteristics of vibration mixers

Prepared batch volume, m ³	0.5
Rotation frequency of the mixing drum, rad/s	2.0
Parameters of the vibration exciter: - oscillation amplitude, mm; - oscillation frequency, rad/s; - maximum acceleration of oscillations, m/s ² ; - vibrating surface, m ² ; - type of oscillations	3.5 220 170 0.2 precessing
Installed power of the drive: - for rotation of the drum and vibration exciter, kW - for drum tilting, kW	4.0 1.1
Dimensions, mm	1,850 × 2,000 × 1,800 1,850 × 2,000 × 1,800
Mass, kg	1,100

Compositions of concrete mixes were accepted in accordance with the standards of material consumption established at the Tyumen Reinforced Concrete Products Plant. The obtained control samples were tested in accordance with GOST 10180-90. After 28 days of hard-

ening, the strength of the samples corresponded to the standards, the coefficient of strength uniformity (coefficient of variation) was 10%; the mixing time was 90 s.

Technique of balancing of vibration activators

A console precessing three-point vibration exciter is shown in Figure 3. It consists of carrying drive shaft 1, main bearings 2, a body designed to extend the active vibration surface by connecting pipe 3 and cone shell 7, rod bearing 4 installed on the eccentric bushing with mechanically set eccentricity *e*, counterbalances 5, and coupling 6 located concentrically in relation to the carrying drive shaft.

Upon rotation of the carrying drive shaft, the vibration activator body executes a precessing motion with the shaft rotation frequency and nutation angle:

$$\beta = \frac{\arctg e}{L}$$

Design models are presented in Figure 3.

In accordance with the calculation procedure described in detail in (Kuzmichev, 2013, 2014, 2017), upon application of the superposition method (the principle of independence of forces), the resultant of centrifugal forces *Q* and its application point (distance *L*) are determined taking into account the following equations:

1. for the cylindrical part (Figure 3a):

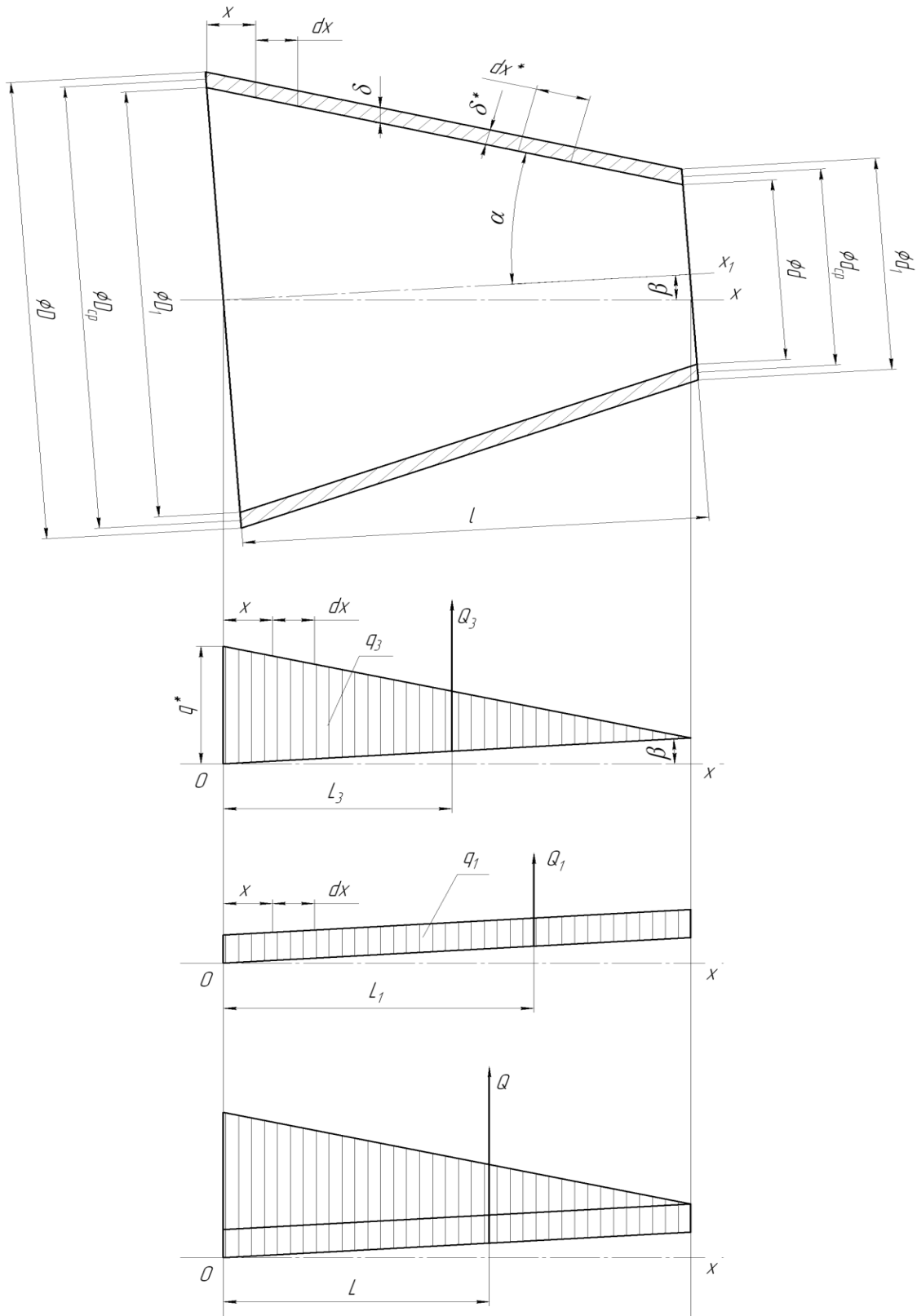


Figure 4. Design model of the cone shell

$$\begin{aligned} \Sigma Q &= Q_1 + Q_2 + Q_5 + Q_6 = \\ &= \omega^2 \operatorname{tg} \beta \left(\frac{1}{2} q_1 l_1^2 + \frac{1}{2} q_2 \left[(l_1 + l_2)^2 - l_1^2 \right] + \right. \\ &\left. + M_5 l_5 + M_6 l_6 \right) \end{aligned} \quad (1)$$

$$\begin{aligned} L &= \frac{Q_1 l_1 + Q_2 l_2 + Q_5 l_5 + Q_6 l_6}{\Sigma Q} = \\ &= \frac{\omega^2 \operatorname{tg} \beta \left(\frac{1}{3} q_1 l_1^3 + \frac{1}{3} q_2 \left[(l_1 + l_2)^3 - l_1^3 \right] + M_5 l_5^2 + M_6 l_6^2 \right)}{\Sigma Q} \end{aligned} \quad (2)$$

Let us consider the procedure for the development of the cone shell design model in more detail (Figure 4).

The design wall thickness is determined based on the condition of equality of the mass per unit length:

$$dx \cdot \delta \cdot \rho = dx^* \cdot \delta^* \cdot \rho; \delta = \frac{dx^* \cdot \delta^*}{dx};$$

$$\delta = \frac{dx^* \cdot \delta^*}{dx^* \cdot \cos \alpha};$$

$$\delta = \frac{\delta^*}{\cos \alpha}$$

Here δ is the sheet thickness.

$$q_1 = \pi d_{ave} \delta \rho; \quad (3)$$

$$Q_1^1 = \frac{1}{2} \omega^2 q_1 l^2 \operatorname{tg} \beta; L_1^1 = \frac{2}{3} l.$$

$$q_3 = q^* \left(1 - \frac{x}{l} \right);$$

$$Q_3^1 = \frac{1}{6} \omega^2 q^* l^2 \operatorname{tg} \beta; \quad (4)$$

$$q^* = \pi (D_{ave} - d_{ave}) \delta;$$

$$L_3^1 = \frac{l}{2}$$

$$\Sigma Q^1 = Q_1^1 + Q_3^1 = \omega^2 \operatorname{tg} \beta \left(\frac{1}{2} q_1 l^2 + \frac{1}{6} q^* l^2 \right) \quad (5)$$

$$L^1 = \frac{Q_1^1 L_1^1 + Q_3^1 L_3^1}{\Sigma Q^1} = \frac{\omega^2 \operatorname{tg} \beta}{\Sigma Q^1} \left(\frac{1}{3} q_1 l^3 + \frac{1}{12} q^* l^3 \right). \quad (6)$$

(Note: in Figure 4 $L_1 \rightarrow L_1^1; L_3 \rightarrow L_3^1$).

The total centrifugal force and its application point are determined based on the following equations:

$$\Sigma Q^{**} = \Sigma Q + \Sigma Q^1; \Sigma L^{**} = \frac{L \Sigma Q + L^1 \Sigma Q^1}{\Sigma Q^{**}} \quad (7)$$

The rod bearing assembly is designed and its mass m_{bear} and center-of-gravity position are determined. The vibration exciter construction is made with one rod bearing center-of-gravity of which is determined at the point of application of the resultant of centrifugal forces.

The mass of the bearing assembly includes the bearing, eccentric part of the bushing and cover. The centrifugal force from the mass of the rod bearing assembly is determined according to the following equation:

$$R = m_{bear} \cdot e \cdot \omega^2$$

Dynamic balancing is carried out in accordance with the design model presented in Figure 5.

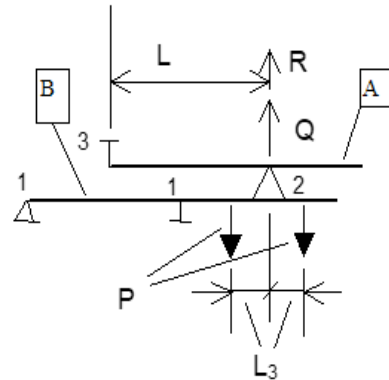


Figure 5. Design model

Balancing condition:

$$P = 1/2 (\Sigma Q^{**} + R) \quad (8)$$

(here $\Sigma Q^{**} = Q; \Sigma L^{**} = L$)

The counterbalances are located symmetrically and designed in accordance with (Kuzmichev, 2013, 2014, 2017).

Vibration monitoring on a mixer reflecting the quality of dynamic balancing was performed using the following devices: noise and vibration meter VShV-003-M2 (BШВ-003-M2), logarithmic noise-and-vibration integrator ShVIL-01 (ШВИЛ-01), air humidity and temperature meter Testo-15. Sensors were mounted on the traverse. Measurements were carried out in three modes: test No. 1 (the

Table 1. Vibration level on the mixer body

Measurement mode	Acceleration of vibration exciter oscillations V , m/s^2	Acceleration along X , m/s^2	Acceleration along Y , m/s^2	Acceleration along Z , m/s^2	Root-mean-square value $U = \sqrt{x^2 + y^2 + z^2}$, m/s^2	$\frac{V}{U}$
1	170	2.1	2.8	2.5	4.3	40
2	170	2.8	3.4	3.2	5.45	31

vibrator is turned on, the drum does not rotate); test No. 2 (both drives (for vibration and rotation of the drum (mixing process)) are turned on). The results of vibration acceleration measurements are presented in Table 2.

The analysis of the measurement results shows that application of balanced eccentric vibration activators ensures reduction of vibration affecting the environment (drive, frame, etc.) by ~ 30 times. The measured peak values of acceleration amount to $\sim 5 m/s^2$, corresponding to standard values for processing equipment as per GOST 22061-76.

Conclusions

The presented materials confirm legitimacy of the balancing technique for vibration activators which is presented in detail in (Kuzmichev and Verstov, 2017a, 2017b), and expediency of their application in mixing equipment for production of construction mixes.

It should be noted that numerous researches in the field of intensification of technological processes with vibration application, conducted by Russian researchers, have shown that the main principles of physical and chemical mechanics of disperse systems can also be successfully used in mixing.

Control over structural and rheological properties of mixes at the stage of mixing, in particular, destruction of the structure of mixed materials and, therefore, viscosity reduction, allows increasing uniformity of mixed materials, production quality, affecting molding processes, etc.

It is expedient to use gravity mixers with vibration activators for mixing of plastic and dry concrete mixes, as well as other highly concentrated disperse systems, e.g. dry mixes, powders, etc.

References

- Bauman, V.A., Bykhovsky, I.I. (1977). *Vibratsionnye mashiny i protsessy v stroitelstve [Vibration machines and processes in construction]*. Moscow: Vysshaya Shkola, p.256. (in Russian)
- Blekhman, I.I. (1994). *Vibratsionnaya mekhanika [Vibration mechanics]*. Moscow: Fizmatlit, p.400. (in Russian)
- Chelomey, V.N. (1981). *Vibratsiya v tekhnike. Spravochnik v 6 tomakh [Machinery vibrations. Reference book in 6 volumes]*. Moscow: Mashinostroenie Publishing House, vol.6, p.509. (in Russian)
- Efremov, I.M., Lobanov, D.V. (2008). Novye rotornye smesiteli s razlichnymi sistemami vibrozvuzhdeniya [New rotary mixing devices with various systems of vibration activation]. *Stroitel'nye i dorozhnye mashiny [Construction and road machinery]*, 9, pp. 7–9. (in Russian)
- Efremov, I.M., Lobanov, D.V. (2009). Vibrobetonosmesiteli: put' dlinoy v 70 let [Vibration concrete finishers: 70 years old experience]. *Stroitel'nye i dorozhnye mashiny [Construction and road machinery]*, 10, pp. 15–19. (in Russian)
- Kuzmichev, V.A. (2013). *Osnovy proektirovaniya vibromikserov [Basics of designing of vibration mixers]*. LAP LAMBERT Academic Publishing, p.136. (in Russian)
- Kuzmichev, V. A. (2014). *Osnovy proektirovaniia vibratsionnogo oborudovaniia [Fundamentals of vibration equipment design]*. Saint Petersburg: Lan, p.208. (in Russian)
- Kuzmichev, V., Verstov, V. (2017a). Vibration activators in the construction production technology. *Architecture and Engineering*, 2 (1), pp. 24–32. DOI: 10.23968/2500-0055-2017-2-1-41-50
- Kuzmichev, V., Verstov, V. (2017b). Vessel mixers with vibration activator in construction engineering. *Architecture and Engineering*, 2 (2), pp.20–26. DOI: 10.23968/2500-0055-2017-2-2-20-26
- Verstov, V.V., Tishkin, D.D., Romanovsky, V.N. (2013). Sovershenstvovanie tekhnologii bespodkladochnogo montazha promyshlennogo oborudovaniia [Improvement of the technology of installation of industrial equipment without backing plates]. *Installation and special works in construction*, 7, pp. 27–31. (in Russian)

FUTURE OF THE OBVODNY CANAL — THE MAIN LINE OF THE SAINT PETERSBURG GREY BELT

Leonid Lavrov ¹, Fedor Perov ², Raffaele Gambassi ³

^{1,2} Saint Petersburg State University of Architecture and Civil Engineering
Vtoraja Krasnoarmejskaja ul. 4, St. Petersburg, Russia

³ Via Salceto 87, Poggibonsi, Siena, Italy

¹ leonid.lavrov@gmail.com, ² f.perov@gmail.com

Abstract

The study looks at the issues of the development of territories in the Obvodny Canal area. These issues, which are of great interest as related to the planned transformation of the Grey Belt, become more aggravated due to the increase in traffic load after the Western High-Speed Diameter (WHSD) opening.

A significant decrease in the housing quality and cost of apartments facing embankments is observed, which can be explained by an extremely high level of noise and contamination with exhaust gases.

Options for the improvement of environmental conditions, based on the conversion of territories allocated for the canal water area, are proposed. It is being noted that the Obvodny Canal has lost its functional purpose and can be converted as dozens of (nowadays former) canals in the historic center of Saint Petersburg.

Keywords

Grey Belt, Saint Petersburg transport infrastructure, Obvodny Canal, ecology of living environment.

Introduction

The Obvodny Canal was constructed in 1803–1835. In 1766, a drainage ditch was dug from the Ligovsky Canal to the Ekateringofka River; the western part of the Obvodny Canal was developed along this ditch. The canal length is 8.08 km, its width is 21.3 m (in the eastern part — up to 42.6 m). The canal was designed to drain water from the Neva River in case of flooding, but mainly for transport needs of enterprises located along its banks. The canal was developed along the border of the city as of the first half of the 19th century and "enclosed" it from the south. From the second half of the 19th century till the mid-20th century, the Obvodny Canal was actually an open waste water sewers for wastes of industrial enterprises. In 1835, the first ship navigated the canal, but at the beginning of the 20th century the shipping traffic through the canal was closed.

The canal was abandoned and for a long time it served as a waste canal for local enterprises and residential blocks. In the 1960s, a proposal to fill up the canal was debated. Nowadays, its banks are one of the most significant transport routes distributing traffic flows in the central part of the city. Currently, the possibilities of canal conversion to ensure its use in modern conditions, solving urgent transport, environmental, architectural and planning issues facing the studied area of Saint Petersburg, are considered.

Materials and methods

The following research methods are used in the article: a historical analysis of the development of the Saint Petersburg system of waterways and canals, a comparative analysis of the experience in laying and operating of canals, and design modeling.

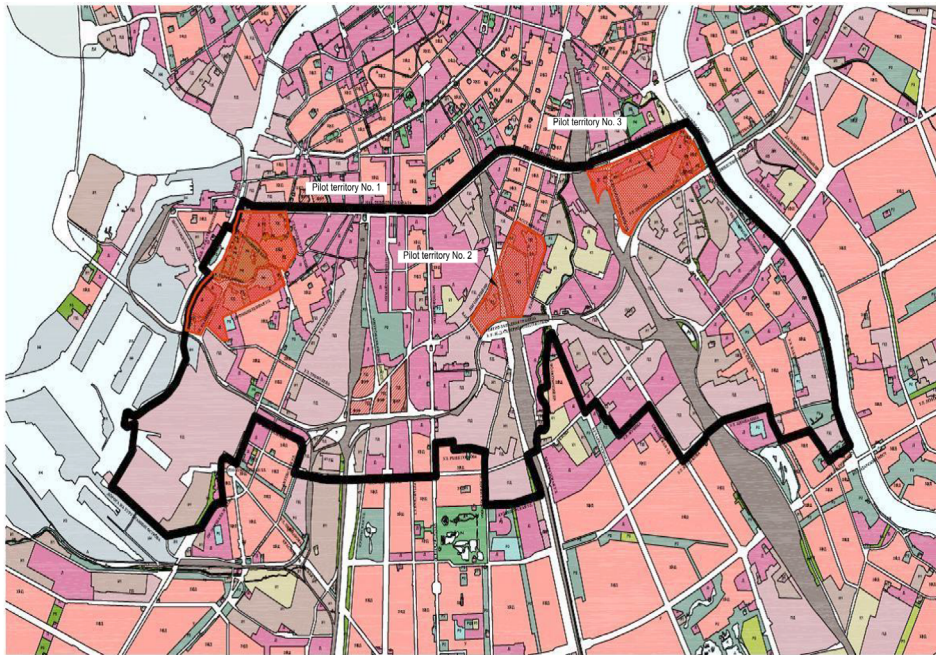


Figure 1. Territories along the southern bank of the canal, allocated for pilot designing

Results

When Saint Petersburg is compared to Venice, it is often pointed out that our city is located on 42 islands, crossed by approximately 90 rivers and canals with more than 500 bridges (Frolov, 2005). The historic part of Venice includes 118 islands, 398 bridges and 175 canals.

Such correlation does not take into account fundamental differences in architectural and planning designs of canals:

- in Venice, a lot of canals lack embankments, houses rise directly from the water, and only several areas have narrow passages for pedestrians;

- in Saint Petersburg, roads for urban transport are laid along the banks of all waterways. In the 18th–19th centuries, all main cargoes (food, firewood, hay for horses, raw materials for industrial use) were delivered by barges navigating in the water area of rivers and canals. Nowadays, embankments play the key role: the main routes of passenger and freight transport are laid along the Neva River and other waterways of the Neva Delta;

- only one Venetian canal — the Grand Canal — follows a natural channel, preserving its meanderings. In Saint Petersburg, rivers of the Neva Delta form the system of waterways. Their natural routing was fixed at the end of the 18th century, when the banks of the Moyka River, Fontanka River and Catherine Canal (the former Krivusha River) were stabilized with granite embankments and fenced with highly-artistic cast-iron grilles.

Local landscapes give the city a peculiar charm: granite embankments, green trees, water shine, gently sloping bridges, and austere facades of buildings merge together. This picture set an image of Saint Petersburg as the Northern Venice, although such comfortable promenades

are not typical for Venice. The embankments became the favorite places of townspeople for walking and nowadays they attract lots of tourists.

The Obvodny Canal plays a special part in the system of large waterways of the Neva Delta. It has become a water main that can determine the appearance of new urban blocks which are planned to be constructed in the Grey Belt of the city (see <http://spb-projects.ruzsdsch2.jpg>). In particular, the territories along the southern bank of the canal are allocated for their pilot designing (Figure 1).

It is the longest waterway of the Neva Delta (its length is 8 km), unlike the Fontanka River, Griboyedov and Moyka Canals which were formed as a result of the sewage collection system development at the place of the existing rivers (see <http://spb300.osis.ru/vek20/F20/1971-1980/1978.shtml>). The Obvodny Canal is a 100% engineering structure, its routing and design were determined following pragmatic considerations. It was laid along the border of the city of those days and partially outside it.

At the first stage of development it was constructed as a part of the military fortification system on the southern approaches to the city. In 1769–1780, a sheet of water stretched from the Ekateringofka River to the Ligovsky Canal, and embankment protection was installed along the banks. To the north of the canal, the Izmaylovsky Guards Regiment compound was situated; and at the beginning of the 19th century, the Nikolai Cavalry School campus was built in the neighborhood. At the time the canal was extended to the Neva River, and in its eastern part near the Nevsky Monastery, the Alexander Military Parade Ground and barracks were built, where the Cossack and Ataman regiments, Don and Black Sea battalions were located. It was decided to use the waterway for the procurement

to these military units, and, therefore, to start cargo traffic through the canal (Sementsov, 2012). In 1819–1821, supply warehouses were built by outstanding architect V. P. Stasov on the northern bank (Administration of Saint Petersburg, 2003).

The second stage of the Obvodny Canal development is related to Saint Petersburg industrialization in the 19th century. At the time, shipbuilding in the center slowed down, the Particular Shipyard was closed, the Admiralty was transformed into a military chancellery. Canals that provided industrial communications and a protective canal around the Admiralty were filled up (see http://www.spb-guide.ru/page_465.htm).

The Obvodny Canal lost its value as a fortification, but it was not filled up at the time unlike numerous canals in the center of the city which became useless. It took on new significance as it was expected to be able to reduce the risk of flooding and become a new way for the transportation of bulky cargo round about the central part of the city. In 1835, shipping traffic was opened throughout the entire canal; barges with cargoes were transported to the internal elements of the city waterways along the Tarakanovka River and the Vvedensky Canal.

The established communication promoted the fast development of the entire southern part of Saint Petersburg of the time. In contrast to the central part of the city where residential areas prevailed, the landscape of the Obvodny Canal was determined by the housing and utilities infrastructure and industrial structures. Warehouses and factory buildings appeared on its banks. In some places they alternated with workers' barracks and manufacturers' mansions. In the eastern part of the canal, a terminal

with the French boat basin for transfer of goods was constructed. Three railway stations were constructed along the route (Lisovskiy, 2004). According to the European urban-planning terminology, territories with such use of plots are defined as "areas of mixed-use development" (Mischgebiet), while in the modern domestic professional language they are designated as the Grey Belt.

At the beginning of the 20th century, the Obvodny Canal became narrow for vessels with increased draft, and navigation through the canal basically ceased. The canal changed its function; it became an open waste water sewers for wastes of industrial enterprises located in the neighborhood. Its unattractive banks were formed by earth slopes with wooden reinforcements at the water edge (see <http://polypipe.info/history/93-drainagehistory-ofstpetersburg.html>).

The 1937 master plan of Leningrad was meant to reverse the situation. It was offered to convert the Obvodny Canal following the example of canals and rivers of the historic center (Kamenskiy, Naumov, 1973). However, those great plans were not fulfilled. The plan was implemented only partially. Permanent embankments and several new bridges were constructed, and old bridges were reconstructed in two stages (in 1930s and after World War II).

The current stage of situation development along the Obvodny Canal route is characterized by the deindustrialization of the area. All former industrial enterprises located along the banks stopped their production. Their buildings are being spontaneously converted into shopping and office centers. The area development becomes chaotic, causing understandable concerns raised by specialists and the city administration.

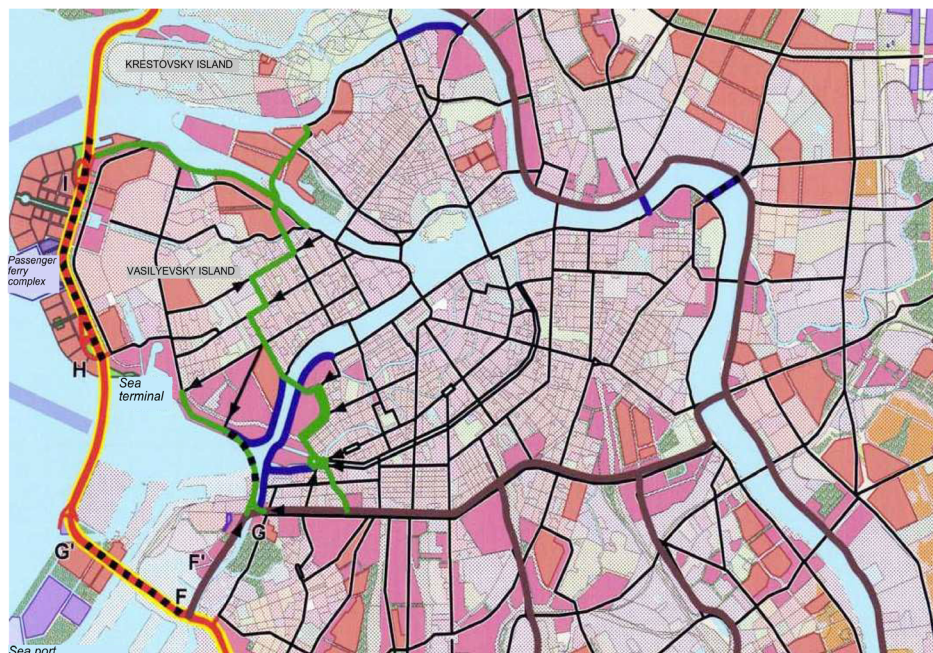


Figure 2. Saint Petersburg traffic diagram with the Obvodny Canal highlighted as a latitudinal link between the Western High-Speed Diameter, the city center and the embankments of the Neva River in the Okhta River area

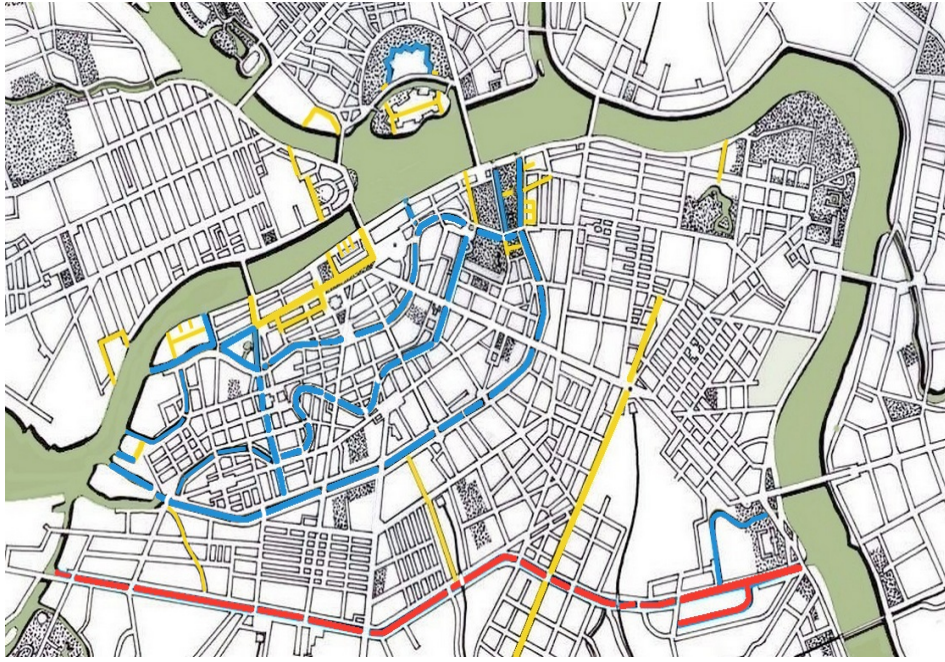


Figure 3. Urban-planning layout of former canals

CONDUCTED COMPETITION

The future of the Grey Belt territories, their use for housing are increasingly debated. These areas are attractive as they are located directly at the border of the historic center. The conducted contest revealed the ways of using the potential of the areas located to the south of the Obvodny Canal, but the future of the buildings stretching along this city main was not discussed. The issue becomes more aggravated due to the planned increase in Obvodny Canal traffic load. According to the strategy of the Saint Petersburg transport infrastructure development, this route has an outstanding value. It should become the main and the only latitudinal link between the Western High-Speed Diameter, the city center and the embankments of the Neva River in the Okhta River area (Figure 2).

It is well known that the ecological state of the Obvodny Canal area is of great concern. The noise level in this area reaches 70–75 dB; the level of contamination with exhaust gases is very high. These negative factors directly affect the area development. It is indicative that authors of the article with the dramatic headline "Apartment buyers are least of all concerned with the district ecology" acknowledge that "the apartments facing the Obvodny Canal are 30% cheaper than the similar apartments at a distance from the embankment" (see https://www.dp.ru/a/2010/06/10/Pokupatelej_kvartir_mensh).

It is obvious that the further planned increase in transport load along the Obvodny Canal will have negative consequences for the ecology of the local development. However, this aspect goes entirely unnoticed. It is indicative that this issue was only touched upon in 2011, when fundamental problems of the Obvodny Canal future were

discussed. During that meeting, the focus was on the possibility to fill up the canal and construct additional lanes in the obtained area. B.M. Murashov, the Chairman of the Saint Petersburg Committee on Transport Infrastructure Development viewed this idea negatively and noted possible consequences: "We should understand that we develop not a traffic environment, but a living environment. Indeed, Obvodny Canal filling-up would be efficient in terms of traffic capacity. But in terms of the city center value this cannot be done, of course." Newspapers carried the following report: "The reconstruction of the Obvodny Canal will not affect its water function. The filling-up of one of the Saint Petersburg waterways is not anticipated (see <http://www.ntv.ru/novosti/245219/>).

However, it is not clear which "water function" of the Obvodny Canal was meant. Cargo shipping stopped long ago, tourist and water sport boats prefer not to enter local waters. Obviously, the transport function is prevalent: large-tonnage trucks and thousands of cars move on the embankments day and night.

A fundamental decision is required to ensure the compliance with the environmental requirements to residential areas near the Obvodny Canal. The canal has ceased to perform its function as an engineering structure, and the issue regarding its future shall be resolved taking into account urban-planning considerations. There are three possible ways of the situation development:

- minimization of the vehicle traffic on the embankments. This option can be considered unrealistic in the nearest future;
- transformation of the Obvodny Canal into a landscaped waterway similar to those that give a particular charm to our city, to attract tourists;

- development of the Obvodny Canal as a modern traffic artery.

To implement the second option, it is necessary to minimize traffic flows along the banks and transform the development along the embankments fundamentally, find places for green areas and pedestrian alleys. Otherwise, local reconstruction will be meaningless: the embankment lining with beautiful stones or metal lattices of exquisite design will remain unnoticed. However, the attempts to reduce the vehicle traffic on all city embankments (including the Obvodny Canal embankments) have been unsuccessful so far.

The third option is aimed to ensure the functioning of the Obvodny Canal as one of the most important elements of the city transport system, as well as improve environmental conditions and protect adjacent buildings from noise and exhausts. To begin with, it shall be admitted that the waterway has lost its functional significance and therefore can be liquidated. Hundreds of examples when unnecessary canals ceased to exist can be found in the world practice of urban development.

In the eastern part of Venice (Castello district), straight-line Via Garibaldi stands out among numerous narrow streets due to its width. For several centuries, waters of a large canal had splashed here; timber was delivered to the shipyards of the Arsenal and new large galleys rode over it. However, in the beginning of the 19th century, when the construction of large ships started, this shallow canal became useless. It was filled up and converted into a boulevard. Venice also has other streets laid along former canals. In the Venetian dialect, they are usually called Rio tera, which can be translated as an "earth canal" or a "canal filled with earth" (e.g. a large segment of Via Garibaldi is called Rio Santa Anna).

Industrial canals of the Admiralty and Particular Shipyard are analogous to the canals of the Venetian Arsenal. They were developed in the beginning of the 18th century, and for about a century they were used as a part of the shipbuilding production chain. When production conditions changed, they were abandoned in the early 19th century. The principle of engineering expediency contributed to the disappearance of the defensive canal of the Admiralty Fortress, the running Ligovsky Canal in the late 19th and early 20th centuries, the transport routes of the Tarakanovka River and the Vvedensky Canal in the middle of the 20th century (Lindley, 1884).

The history of Saint Petersburg also reminds of a system of similar transformations: if a canal ceased to perform its main function, and its very existence created problems for urban life, the canal was filled up, while its territory was repurposed (Enakiyev, 1912). The Vvedensky Canal was dug in 1807–1810 following the project developed by engineer F. I. Gerard in 1804. It flowed out of the Obvodny Canal, passed between the former barracks of the Jaeger Regiment on the left bank and the Vitebsk Railway on the right bank, then crossed the Zagorodny Prospect near the Vitebsk Railway Station and flowed into the Fontanka River near the Obukhov Bridge. It was used

for the needs of navigation, water intake, and then as a waste water sewers (see <http://opeterburge.ru/history/per-vyj-vodoprovod-v-peterburge.html>).

The Vvedensky Canal was arched over by four bridges. Since 1836, the embankment along the canal had been called the Embankment of the Vvedensky Canal and was renamed the Embankment of the Vitebsk Canal on September 10, 1935 after the canal renaming.

In 1967, after the canal filling-up, the street which replaced it was called the Street of the Vitebsk Canal. Since December 29, 1980 it has been called the Vvedensky canal (alternatively, the Street of the Vvedensky Canal) (Sementsov, Margolis, 2004).

The list of the most famous former canals of Saint Petersburg is quite broad (Nikitenko, Sobol, 2002, Nikitenko, Privalov, 2009) (Table 1).

Table 1. List of the most famous former canals

Main function of the canal	Name, location	Period of existence
Water draining, drying	Lines of Vasilyevsky Island	1720–1760
	Canal in front of the Twelve Colleges building	18th century
	Krasny Canal of the Field of Mars	1711–1770s
	Poperechny Canal of the Summer Garden	1719–1777
Water feeding	Ligovsky Canal	1721–1892, 1926
Industrial transportation	Admiralty Shipyard complex	1706–1840s
	New Holland complex	1717–1842
	Particular Shipyard Complex	1726–1780s
	Kosoy Dementiev Canal and "Gavanets" of the Sytniy (Zapasnoy) Courtyard	1719–1790
Protective dykes	Admiralty Fortress	1704–1817
	Peter and Paul Fortress	1703–1900s
	Engineers' Castle	1800–1819
	Salnobuyansky Canal	1804–1915
	Maslobuyansky Canal	1870s, 1930s
In-city transportation	Canal by the Stary Gostiny Dvor at the Birzhevaya line of Vasilyevsky Island	1720–1760s
	Vvedensky Canal	1807–1971
Municipal domestic services	Canal in the Peter and Paul Fortress courtyard	1706–1800s
	Canals of the Pracheshny Courtyard	18th century

The urban-planning layout of former canals represents their location within the structure of Saint Petersburg (Figure 3).



Figure 4. Development at the Griboyedov Canal embankment in Saint Petersburg

Yellow lines on the layout represent routes of canals which were liquidated when they became useless, the red line is the Obvodny Canal. Waterways of the Fontanka River, Griboyedov and Moyka Canals, and some other canals in the center were preserved and granted a second chance due to their unique landscape characteristics. They became symbols of the city image, representing the city spirit (Figure 4).

Their unique landscapes attract landscape painters, and serve as a model for modern architects. The great emotional and artistic potential helped to resist proposals on the filling-up of the Kryukov Canal and a part of the Catherine Canal, which were submitted in the second half of the 19th and early 20th centuries. Unfortunately, the Obvodny Canal has too few chances to fit into this attractive picture.

Local landscapes are not marked by artistic merits. During White Nights, when citizens and tourists gather on the banks of the Moyka or Griboyedov Canals, and holiday cruisers ride on water, the Obvodny Canal em-

bankments are filled with flows of heavy-duty container vehicles (Figure 5).

To make room for intense traffic flows, starting from the 1960s it has been proposed to fill up the canal and convert it into a street. The analysis of the project proposals makes it possible to determine advantages and disadvantages of several possible options for the Obvodny Canal conversion (Figure 6).

The proposed options for the conversion of the Obvodny Canal embankment have their advantages and disadvantages.

Option a. This option implies the filling-up of the canal (and soil compaction), translocation of transport routes to the center of the main road and installation of protective walls that would reduce the effect of noise and exhaust gases (Mangushev, Osokin, 2010). Unfortunately, it would not be easy to achieve the desired architectural and artistic quality in this case;

Option b. This option resembles the project of Konnogvardeyskiy boulevard which appeared on the site of the



Figure 5. Transport flows on the Obvodny Canal embankments



Figure 7. Translucent roofing in the Petuel Tunnel (Munich)

Admiralty Canal filled up in 1842. Tall trees in the center of the main road can give it an attractive look, but local residents will hardly reach them. The ecological potential of the green area is used only to a small extent;

Option c. It would be practical to use the canal bed as a main road below the ground level. This option involves water draining. In this case, it would be possible to allow main-line traffic along the bottom of the former canal. Its walls will provide protection from noise and exhaust gases contamination, and the upper section will provide places for local access and green areas;

Option d. The option implies that the canal flow will be stopped and the canal will be converted into a transport tunnel with a pedestrian zone on its roof. In some areas, it will be possible to use translucent roofs. The main road can be isolated from the residential area if required (Figure 7). This option opens unique prospects for the joint conversion of the development on the former northern and southern banks of the canal.

Conclusions

1. Throughout its history, the Obvodny canal played a critical role in the system of large waterways of the Neva

Delta and was a water traffic artery of the industrial belt of the city. Nowadays, it can determine characteristics of architecture and appearance of new urban blocks, which will be developed in the Grey Belt of Saint Petersburg, to a large extent.

2. The Obvodny Canal has few opportunities to become an attractive urban landscape and architectural landmark for citizens and tourists. Local landscapes are not marked by artistic merits. The Obvodny Canal is a traffic artery. The Obvodny Canal embankments are permanently occupied with freight and public transport.

3. The analysis of the project proposals makes it possible to determine advantages and disadvantages of several possible options for the Obvodny Canal conversion.

The most preferable are the option with the canal bed used as a main road below the ground level (in this case, it would be possible to allow main-line traffic along the bottom of the former canal) and the option to stop the canal flow and convert the canal into a transport tunnel with a pedestrian zone on its roof. These options open unique prospects for the joint conversion of the development on the former northern and southern banks of the canal.

References

- Administration of Saint Petersburg (2003). *Pamiatniki istorii i kultury Sankt-Peterburga, sostoiashchie pod gosudarstvennoi okhranoi: spravochnik [State-protected historical and cultural monuments of Saint Petersburg: reference book]*. Saint Petersburg, Russian Federation. (in Russian)
- Enakiyev, F. (2013). *Zadachi preobrazovaniia S.-Peterburga [Saint Petersburg transformation challenges]*. Moscow: Nobel Press, p.120. (in Russian)
- Frolov, A. (2005). *Sankt-Peterburg ot A do Ia. Reki, kanaly, ostrova, mosty, naberezhnye [Saint Petersburg from A to Z. Rivers, canals, islands, bridges, and embankments]*. Saint Petersburg: Glagol. (in Russian)
- Kamenskiy, V., Naumov, A. (1973). *Leningrad. Gradostroitelnye problemy razvitiia [Leningrad. Urban development issues]*. Leningrad: Stroyizdat. (in Russian)
- Lindley, W. (1884). *Vodostoki stolichnogo g. Sankt-Peterburga sera Viliama Lindleia. Proekt na ustroistvo vodostokov na prostranstve mezhdur. B. Nevoiu i Obvodnym kanalom. Poiasnitelnaia zapiska [Water drainage in the capital city of Saint Petersburg by Sir William Lindley. Project for the arrangement of a drainage system between the Bolshaya Neva River and the Obvodny Canal. Explanatory note]*. Saint Petersburg. (in Russian)
- Lisovskiy, V. (2004). *Arkhitektura Peterburga. Tri veka istorii [Architecture of Petersburg. Three centuries of history]*. Saint Petersburg: Slavia. (in Russian)
- Mangushev, R., Osokin, A. (2010). *Geotekhnika Sankt-Peterburga [Geotechnics of Saint Petersburg]*. Saint Petersburg: ASV. (in Russian)
- Nikitenko, G., Privalov, V. (2009). *Petrogradskaia storona. Bolshoi prospekt [Petrograd Side. Bolshoy prospect]*. Moscow: Tsentrpoligraph. (in Russian)
- Nikitenko, G., Sobol, V. (2002). *Vasileostrovskii raion (Entsiklopediia ulits Sankt-Peterburga) [Vasileostrovsky District (Encyclopedia of Saint Petersburg streets)]*. Saint Petersburg: Beloye i Chernoye [White and Black]. (in Russian)
- Sementsov, S. (2012). *Sankt-Peterburg v planakh i kartakh. XX vek. Istoriko-kulturnoe nauchno-populiarnoe izdanie [Saint Petersburg in plans and maps. XX century. Historical and cultural popular scientific publication]*. Saint Petersburg: North-Western Mapping Center. (in Russian)
- Sementsov, S., Margolis, A. (2004). *Sankt-Peterburg. Plany i karty [Saint Petersburg. Plans and maps]*. Saint Petersburg: Karta LTD. (in Russian)
- Sementsov S.V., Akhmedova E.A., Volkov V.I. (2017). Rivers and canals as the main public spaces of town-planning compositions and functional systems of the largest cities. *Water and Ecology*, 4, pp. 88–95. DOI:10.23968/2305–3488.2017.22.4.88–95

GENERATION OF NATURAL CONVECTIVE AIR FLOWS IN ROOMS WITH THE USE OF IN-FLOOR CONVECTORS WITH NATURAL CIRCULATION

Viktor Pukhkal¹, Vadim Bulgakov²

^{1,2} Saint Petersburg State University of Architecture and Civil Engineering
Vtoraja Krasnoarmejskaja ul. 4, St. Petersburg, Russia

¹ pva1111@rambler.ru

Abstract

To prevent the intake of downward cold air flow from translucent structures into the room serving area, convectors with natural convection, embedded in floor construction, are used.

Convector operation was simulated at various distances from the glazing to the convector with ANSYS Fluent 14.5 program. Temperature and velocity fields inside the room were determined.

Natural convective flows in the room (downward cold air flow at the glazing and upward warm air from the convector) were described. Application conditions of in-floor convectors with natural air circulation were determined.

Keywords

Heating, residential and public buildings, in-floor convector, natural convection.

Introduction

Glazed window openings represent a source of discomfort for people inside the building due to the generation of downward cold air flows at the glazing and their intake into the room serving area. Use of heating units in the form of convectors with natural or forced air circulation, embedded in floor construction (in-floor convectors), is one of the solutions preventing cold air intake (Krupnov and Krupnov, 2010; Mayorov, 2014; Makhov, 2014; composite author, 2012; "VITATERM", 2008; Babiak et al., 2013). The convector is located directly at the glazing or at a distance of 80–350 mm from it.

To develop a procedure for engineering of water heating systems with in-floor convectors, it is necessary to get an overview of interaction between two air flows: the downward cold air flow at the glazing and the upward warm air flow from the heating unit.

Figure 1 presents the data of experimental studies of the glazing temperature influence on the generation of

flows coming from the fan convector embedded in floor construction (convector with forced air circulation), and a qualitative picture of the air flows movement at the convector inlet and outlet (Muller M. et al., 2013).

A conclusion of the insignificant influence of glazing cooling in the measured area on the movement of the adhering air flow from the convector fan was made. However, it does not mean that this effect cannot occur at a higher vertical position.

The heat flow from the convector was experimentally determined and the pattern of air flows and temperature fields was simulated for the room with a convector with natural convection (Bašta and Legner, 2017).

It was established that the radiation component of the heat flow was less than 1%. The mathematical simulation of temperature and velocity fields for the room with the area of 4 x 4 x 2.6 m and window dimensions of 2 x 2.4 m was performed (Figure 2).

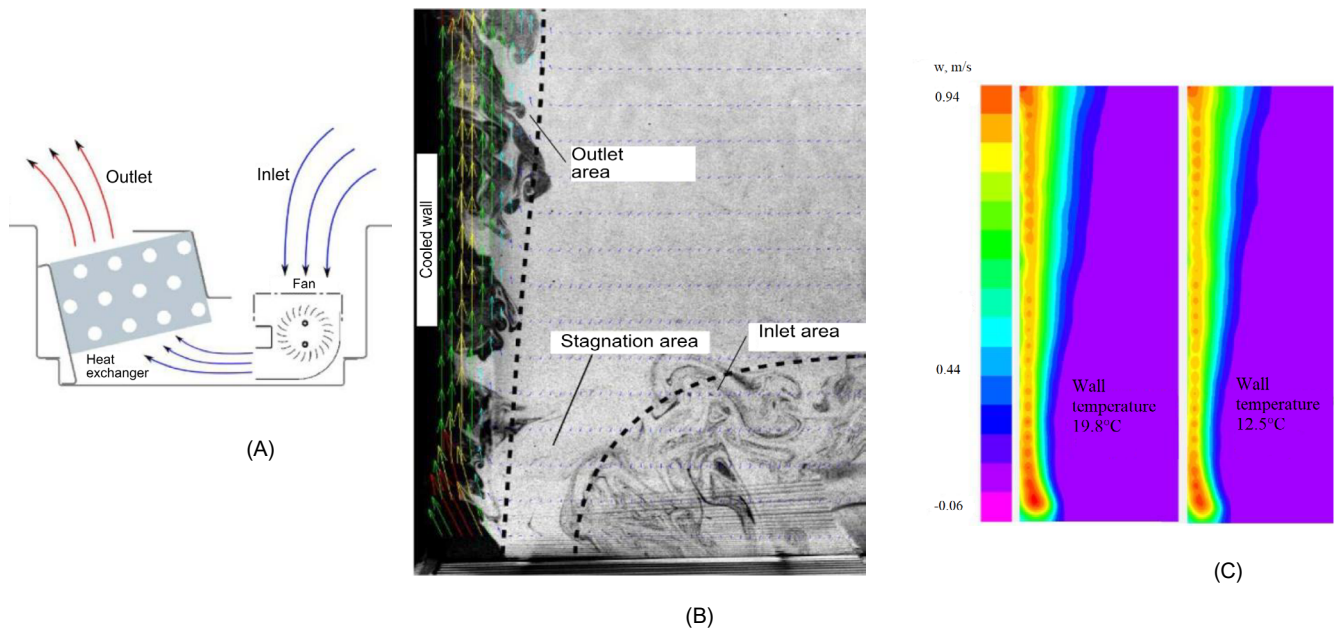


Figure 1. Air flow patterns during fan convector operation: A – fan convector principle; B – air flow patterns; C – comparison of vertical velocity components for temperatures

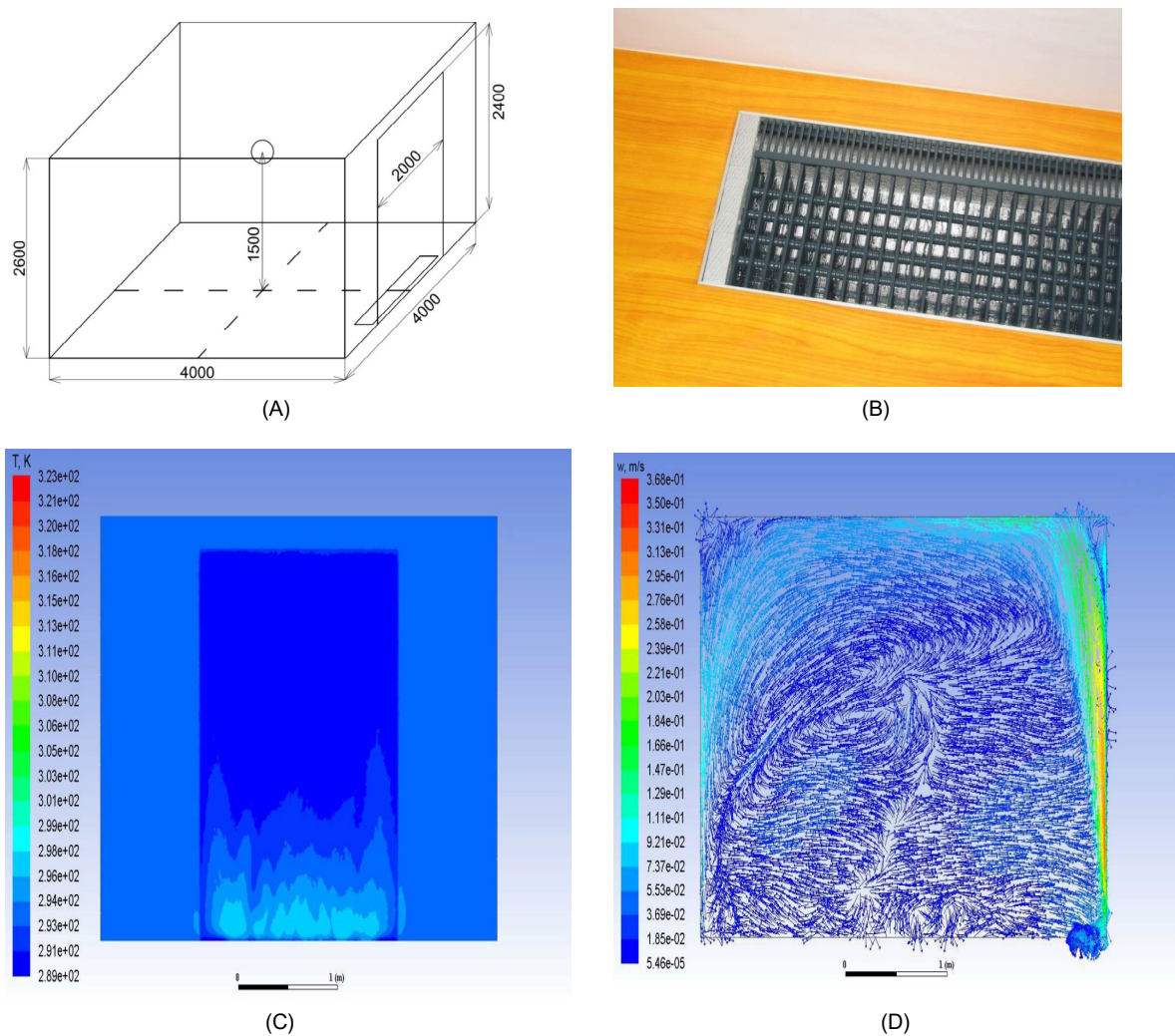


Figure 2. Design model of the room and results of temperature and velocity field studies: A, B – design model of the room and the studied convector; C – temperature field of the internal surface of the external wall and glazing; D – velocity field at section along the convector axis in a plane perpendicular to the window

A BITHERM Floor convector with natural convection (dimension: 2000 x 245 x 55 mm) was installed at a distance of 70 mm from the glazing. The specific heat flow on the glazing surface is equal to 38.4 W/m^2 , and on the surface of the external wall it is equal to 8 W/m^2 . The temperature at the surface of the heating element was assumed to be 50°C .

Taking into account simulation conditions, it was established that the heated air flow from the convector was adhering to the glazing surface (Figure 2). In the upper part of the room, an enclosed circulation area with the downward cooled air flow is generated upon air flow turning and adhering to the ceiling (Smirnov et al., 2017).

This study allows concluding that the convective flow from the convector, progressing at the vertical cooled barrier (glazing), shows a tendency to adhering. The adhering of convective flows has been understudied. Therefore, the study objective is to obtain qualitative characteristics related to the progressing of convective flows depending on the distance between the glazing surface and the convector (Vasiliev, 2017).

Methods

To account the actual operating conditions of the convector embedded in floor construction and for a detailed study of distribution of velocity and temperature fields inside the room, convector operation was simulated with ANSYS Fluent 14.5 program.

A room with the dimensions typical for residential and public buildings was adopted as a model: width — 3 m; depth — 6 m; height — 3 m (Figure 3). The window dimensions — 3 x 3 m. A KRKP-1.058-128 convector (OJSC "Izoterm", Russia) was simulated (VITATERM, 2008). The

convector is located at a distance of 100 mm from the glazing.

In simulation, the following conditions were preset:

- temperatures on the internal surfaces (side walls, floor, ceiling) — plus 18°C ;
- outside air temperature — minus 24°C ;
- heat transfer coefficient of the external surface of the glazing — $23 \text{ W/(m}^2 \text{ K)}$;
- heat transfer coefficient of the internal surface of the glazing — $8 \text{ W/(m}^2 \text{ K)}$;
- average thermal resistance of the glazing — $0.685 \text{ (m}^2 \text{ K)/W}$;
- temperature on the surface of the heating element — 64.5°C ;
- location of the heating element of the convector — in the center of the box.

Results

The calculation results for velocity and temperature fields in the room, obtained at various distances from the glazing to the convector (l , mm), are presented in Figures 4 and 5. Based on these calculations, it is possible to evaluate the nature of the interaction between the downward flow at the glazing and the upward flow coming from the convector provided the heat flow from the convector is equal to heat losses through the glazing.

If the distance between the glazing and the convector is less than 400 mm, the warm air flow adheres to the glazing throughout its height. At a distance of 400 mm, three areas are generated at the internal surface of the window: a downward cold flow of natural convection (a cold air jet), a vortex area and a semi-restricted gravitational (warm) jet from the convector (Figure 4).

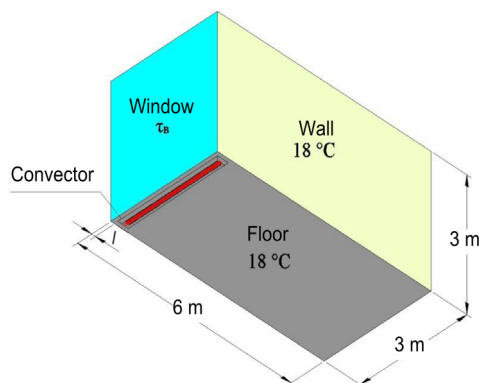


Figure 3. Design model of the room and the convector

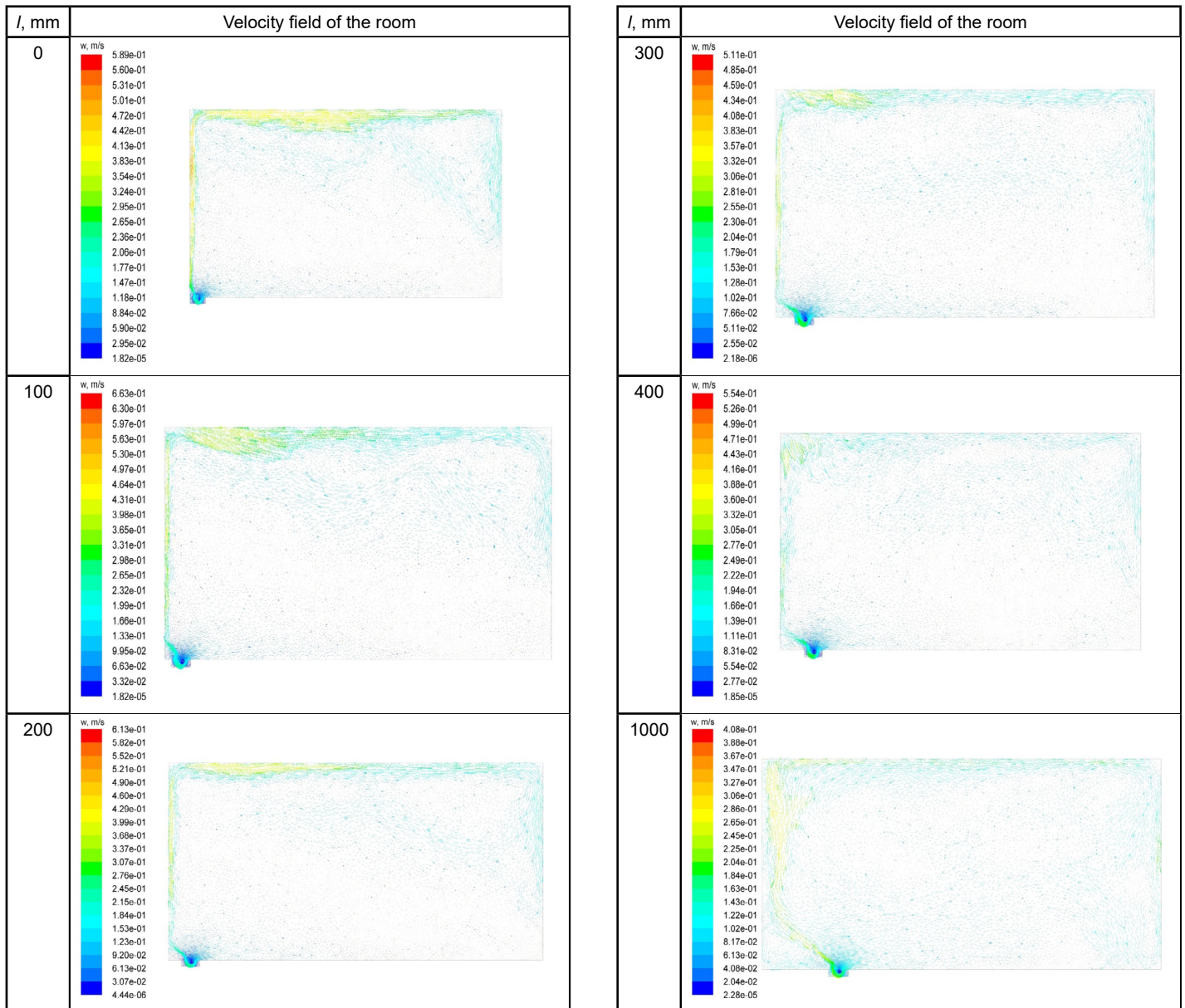


Figure 4. Simulation results for velocity fields of the room (section along the room axis; a plane perpendicular to the window)

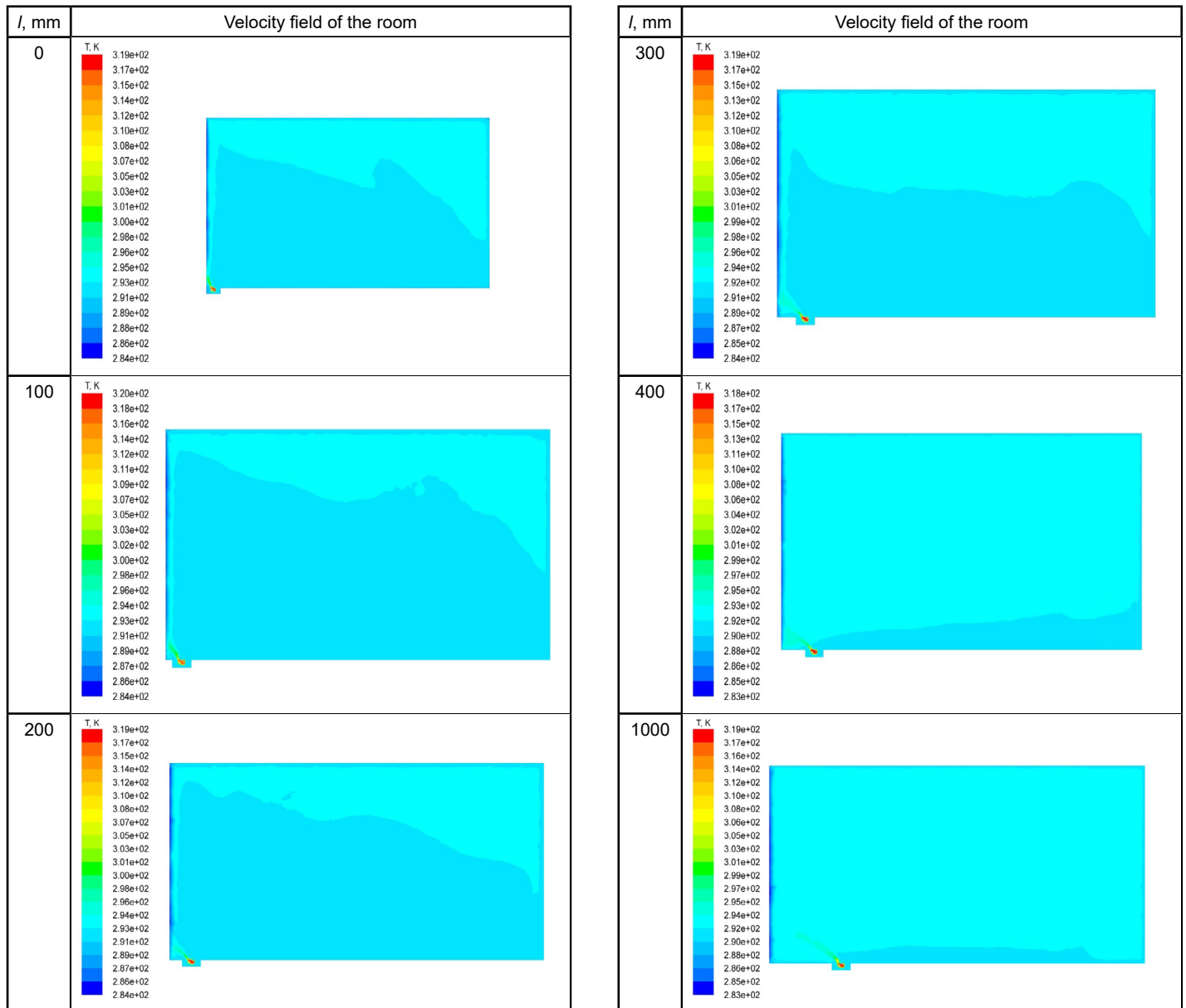


Figure 5. Simulation results for temperature fields of the room (section along the room axis; a plane perpendicular to the window)

In the vortex area, where the warm and cold jets merge, the direction of a newly formed jet changes sharply. The jet is deflected deep into the room. The merging area is located at ~ 2.4 m from the floor.

The increase in the distance from the glazing to the convector to 1,000 mm results in the generation of two flows: a downward cold air flow throughout the entire glazing height, which is partially mixed with an upward heated air flow from the convector and enters the convector for heating, and an upward warm flow from the convector, which deflects towards the glazing.

The calculation data presented in Figures 4 and 5 show that the adhering convective jet from the convector ascends to the upper part of the room and an area of elevated temperatures develops, if the distance between the convector and the glazing is less than 400 mm. Several enclosed circulation areas are formed instead of a single

circulating air flow. The increase in the distance to 1,000 mm allows adjusting the temperature field in the room.

Conclusions

1. Convectors with natural circulation, embedded in floor construction, with a heat flow equal to heat losses through the glazing and located at a distance less than 400 mm from the glazing, form a convective jet adhering to the glazing and protecting the room from the downward cold flow at the glazing.
2. To eliminate the nonuniform heating of the glazing, the distance from the in-floor convector to the glazing should be at least 100 mm.
3. It is recommended to place the heating element of the in-floor heater with natural air circulation close to the box wall on the glazing side or in the center of the box.

References

- Babiak, J. (2013). *Low temperature heating and high temperature cooling: embedded water based surface heating and cooling systems*. Brussels: REHVA.
- Basta, J., Legner, T. (2017). *In-floor convector analysis*. Prague: Czech Technical University in Prague.
- Krupnov, B., Krupnov, D. (2010). *Otopitel'nye pribory, proizvodimye v Rossii i blizhnem zarubezh'e [Heating devices made in Russia and neighboring countries]*. Moscow: ASV. (in Russian)
- Makhov, L. (2014). *Otoplenie [Heating]*. Moscow: ASV. (in Russian)
- Mayorov, V. (2014). *Peredacha teploty cherez okna [Heat transfer through windows]*. Moscow: Izdatel'stvo ASV. (in Russian)
- Muller, M., Frana, K., Kotek, M., Dancova, P. (2013). The influence of the wall temperature on the flow from the floor convector (experimental results). *EPJ Web of Conferences*, 45. DOI: 10.1051/epjconf/20134501130.
- Otopitel'nye pribory i poverkhnosti [Heating devices and surfaces] (2012). Moscow: Akva-Term (in Russian)
- Smirnov, E.B., Datciuk, T.A., Taurit, V.R. (2017). Estimation of ecological safety of the designed buildings. *Water and Ecology*, 3, pp. 82–99. DOI: 10.23968/2305–3488.2017.21.3.83–99
- Vasiliev V. F. (2017). Ecological influence of industrial buildings with aeraty on the quality of city air. *Water and Ecology*, 4, pp. 70–75. DOI:10.23968/2305–3488.2017.22.4.70–75
- VITATERM (2008). *Rekomendatsii po primeneniyu konvektorov "Gol'fstrim" ("Izoterm-TD"), vstraivaemykh v konstruktsiyu pola [Recommendations for use of "Gol'fstrim" ("Izoterm-TD") convectors which are built into the floor construction]*. Moscow: VI-TATERM. (in Russian)

MULTILAYER CONCRETE INDUSTRIAL FLOORING SOLUTIONS ANALYSIS

Marlena Rajczyk ¹, Paweł Rajczyk ²

^{1,2} Faculty of Civil Engineering Technical University of Czestochowa,
Akademicka 3, 42-200 Czestochowa

¹ mrajczyk@bud.pcz.czest.pl

Abstract

The subject of the article is the presentation of European experience in the field of construction of industrial concrete floors. For the construction of the concrete slab floor to be prepared subsoil. Land stabilization can include mechanical stabilization, physical stabilization, and chemical stabilization.

The most commonly used stabilization is mechanical stabilization. In order to determine the efficiency and effectiveness of the process, the treatment depends on the soil moisture for the soil type, so attention is paid to this material feature. Accordingly, the recipes from the French experience for the concrete stabilization layer are presented.

For such prepared substrate the choice of material parameters and properties of concrete mixtures for concrete slabs for the concrete class in the strength of 10 to 35 MPa was presented.

Keywords

Industrial flooring, concrete floors, stabilization, concrete mixes, material properties.

Introduction

The paper analyzes the ways to determine industrial properties and technologies in floor construction. The requirements for the preparation of soil under the floor are discussed. The requirements to be met in the production, development and configuration of the concrete equipment are listed.

The industrial flooring needs to provide a surface ready to withstand loads and forces generated by vehicles. At the same time, the floor should provide safety and comfort. There are two typical structural concepts in industrial floorings: (a) concrete flooring and (b) resin flooring. They are shown in Figure 1.

Exposure of flooring material to the traffic generated load requires optimization of engineering features, thickness and mechanical properties of individual flooring layers. Industrial floorings shall be designed with consideration of soil properties and assumed loads. This brings

about the following aspects to be explored during design of industrial floorings:

- specification of mechanical qualities of materials used to make individual layers and their thickness;
- selection of soil that does not deform as deformations can cause flooring damage.

The properly made industrial flooring should include the following layers:

- soil — homogeneous and densified,
- undercoat — bearing layer,
- processed concrete plate.

Proper and long-term functioning of flooring requires making three interacting layers. For low traffic, making a single layer coating is sufficient. In this case, the concrete surface is laid directly on the soil. Higher resistance floorings require using proper materials having elevated standards of undercoat layer bending resistance. In this case, it is necessary to make an undercoat layer of reinforced

concrete having steel rods (OD 3–8 mm) with 20–30 cm spacing of rebars or mesh.

The industrial flooring type depends on the intended use of the facility designed or on the processing technology. The flooring thickness needs to be determined in the same manner as the road surface (Potrzebowski, 1998; Rajczyk, 2013; Rajczyk and Kosin, 2011; Wolski, 1996).

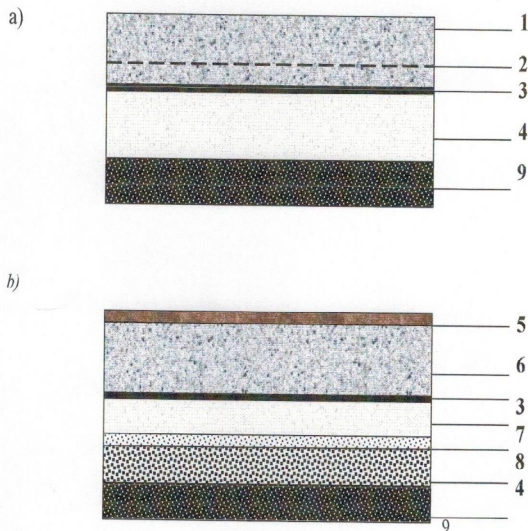


Figure 1. Typical structural concepts in industrial flooring: (a) concrete flooring, (b) resin flooring (Czarnecki and Rydz, 1995, 1998)

Structural concrete solutions in industrial floorings require considering several basic factors which influence resistivity, durability and safety. They include the following:

- the type and magnitude of load,
- the soil load bearing capacity,
- the properties of material to develop individual layers,
- the process chosen and its quality (Rajczyk, 2013; Rajczyk and Kosin, 2011; Rajczyk et al., 2016).

The thickness of the bearing layer can be calculated. The requirements depend on the actual load and the calculations are made using theoretical recommendations and equations of Hetenyi, Westergaard and Eisenmann. The recommendations on selecting concrete flooring are listed in Table 1.

Modern industrial, storing and transporting technologies requirements (supermarket, production shop, warehouse) indicate that the potential flooring needs to meet the requirements depending on resistance to traffic, abrasion and impact. It also shall have high water-proof qualities, evenness and be easily cleaned. The modern surface needs to provide faultless performance without repairs and renovations within decades.

Undercoat and soil layer

The industrial surface structure, which needs to bear extremely high loads (forklifts of several dozens of tons of lifting capacity and similar concentrated loads) requires the undercoat and foundation.

Soil layer

The soil foundation consists of the original soil under the bearing structure. It can have both natural and improved surface; it can be located directly under the concrete surface, or underpin the undercoat. The soil layer needs to be properly densified.

Table 1. Recommendations on selecting concrete flooring regarding operational conditions (based on ACI — 302/89) (Rolla, 1983)

Operational conditions	Facility type	Concrete class	Flooring type	Flooring category
Low pedestrian traffic	Residential buildings	B20	Troweling	I
Intense pedestrian traffic	Public buildings	B22,5	Troweling + possible slip resistant layer	II
Intense pedestrian traffic + rubber wheel vehicles	Internal warehouses, access roads	B25	Superficial hardening (troweling)	III
Intense pedestrian traffic + rubber wheel vehicles + light vehicles	Internal warehouses, access roads	B28	Superficial hardening (troweling)	IV
Vehicles traffic including steel wheel vehicles	Industrial facilities, warehouses	B30	Superficial hardening, hard metallic or mineral fillings in the superficial layer	V
Vehicles traffic including steel wheel vehicles + impact load	Industrial facilities	B35 (undercoat B25)	According to the special project	VI
Pedestrian traffic + rubber wheel vehicles + light vehicles + vehicles including steel wheel vehicles	Cooling chambers/freezers, or flooring laid on the old undercoat	B35	According to the special project + min. thickness of 75 mm	VII

It is considered that the surface should rest on strong underlying soil. Only in this situation proper durability can be guaranteed. The soil needs to be protected against ingress of excessive humidity and from negative impact of frost.

General methods of soil stabilization can be divided into the following:

- mechanical stabilization involving application of optimized mixtures featuring no stabilizers, which is obtained through the following: densification (decreasing internal soil porosity), dehydration and maintenance of stable humidity, and mixing of several types of soil together,
- physical stabilization using stabilizers, such as: portland cement or cement emulsions,
- chemical stabilization involving ionization, polymerization or oxidation.

Designing heavily loaded industrial floorings needs to be preceded with geotechnical research in order to confirm the soil load bearing capacity. Unstable soils may need reinforcement. Basic soil parameters are determined under laboratory conditions. The Table below lists the values of *E* modules, internal angles friction ϕ and consistency *c* as functions of the soil humidity expressed in percentage of liquidity limit.

Prior to the development of an undercoat layer, it is important to ensure that the soil has proper stabilization. Most often the soil is stabilized through mechanical densification. Among the methods used, the most popular involve rolling, compacting and vibrating.

Under normal conditions, soil particles are loose featuring empty spaces filled with air or water. Densifica-

tion involves compressing solid particles and maximum elimination of free space. The method chosen depends on the type of soil, its humidity and thicknesses of design layers. Each method (rolling, vibrating, compacting) requires specific equipment and machinery. Cohesive soils need to be vibrated and compacted, or vibrated and rolled. Loose soils (sand and gravel) require using the vibrating technique as the most efficient. Densification should be performed with vibrating plates (regular and/or trailing) and vibratory rollers.

Concrete bearing plate

The undercoat has a task to create a hard layer underneath the surface. The undercoat needs to form homogeneous support for the concrete plate. The undercoat thickness is defined accounting for the following factors:

- soil type,
- traffic intensity,
- material used.

The undercoat is required to:

- provide strong support under the concrete plate,
- improve soil bearing capacity,
- decrease plates cracking rate.

The undercoat can be composed of a mechanically stabilized aggregate, soil stabilized using cement or applying a lean concrete layer.

The 10-cm thick undercoat can be made of a mechanically stabilized aggregate, or soil stabilized with cement. In case operations involve applying extremely high loads it is recommended to develop a lean concrete undercoat.

Table 2. Properties of soil as a function of its humidity (Rolla, 1985)

Soil type	Soil properties	Relative humidity (w/w1)						
		0.6	0.65	0.7	0.75	0.8	0.85	0.9
Thick sand, sand and gravel mix	<i>E</i> [MPa]	130	130	130	130	130	130	130
	ϕ [degrees]	43	43	43	43	43	43	43
Medium-thick sand	<i>E</i> [MPa]	120	120	120	120	120	120	120
	ϕ [degrees]	40	40	40	40	40	40	40
Fine sand	<i>E</i> [MPa]	100	100	100	100	100	100	100
	ϕ [degrees]	38	38	38	38	38	38	38
Dusty sand	<i>E</i> [MPa]	50	50	50	50	50	50	50
	ϕ [degrees]	36	36	36	36	36	36	36
Clay and thick sand	<i>E</i> [MPa]	60	60	60	60	60	60	60
	ϕ [degrees]	40	40	40	40	40	40	40
Clay sand	<i>E</i> [MPa]	45	42	39	37	35	-	-
	ϕ [degrees]	35	35	34	34	33	-	-
	<i>C</i> [kPa]	12	11	10	9	8	-	-
Dust, clay, loam	<i>E</i> [MPa]	60	42	34	28	24	21	20
	ϕ [degrees]	24	21	18	15	13	11	10
	<i>C</i> [kPa]	32	26	19	15	10	7	5

Table 3. Examples of lean concrete types used at French construction sites (Rolla, 1983)

Ingredient	Unit	Construction site		
		I	II	III
Aggregate				
0–2.5 mm	kg	-	305	-
0–5 mm	kg	786	545	770
0–20 mm	kg	632	655	640
0–40 mm	kg	632	505	640
Cement 325 or 400	kg	160	160	160
Fly-ash	kg	70	50	70
Water	l	160	165	190
Plasticizer (% cement)	%	0.5	0.5	0.5
Aerator (% cement)	%	0.075	0.15	0.075

Lean concrete composition should be selected with regard to high resistance standards and low shrinkage. The disadvantage of such solution is that undercoat cracks can propagate to the main plate. In order to prevent developing these defects, it is necessary to extend the time of response of the undercoat and plate to mechanical deformation paying major attention to make the undercoat smooth and levelled promptly responding to shrinkage joints of the plate.

Examples of lean concrete used at French construction sites are shown in Table 3.

Shrinkage joints do not appear when the undercoat is made upon the sand surface stabilized with cement or an aggregate with cement. The cement content in the aggregate undercoat is 3.5% and the aggregate content is dependent on the surface load; low content is used in natural gravel and sand mixes; high content is used in the full aggregate.

The influence of cement on stabilized sand resistance is shown in Figure 2.

Concrete, as a main ingredient, is an artificial stone having the resistance depending on numerous factors. The quality and composition of ingredients (cement, aggregate, water) are the most vital ones that influence performance and processing quality. The concrete resistance also depends on humidity and temperature, as well as on chemically invasive factors.

The mix composition involves cement, aggregate, water and additives in order to obtain design properties. The criteria for industrial concrete floorings are as follows:

- resistance — to comply with project assumptions,
- consistency — to ensure suitability of the selected application method,
- durability — depends on conditions of use.

The concrete composition should be established accounting for its functions. It involves aggregate granulation, selecting cement and individual ingredients in the required quantity, ensuring workability and consistence.

According to PN-88/B-06256, the minimum class of abrasion resistivity of concrete should be B25; the Boehme disc abrasiveness evaluated using electrolytically produced corundum powder B80 should not exceed the following values:

- 0.40 cm for the concrete grade selected for intense traffic,
- 0.50 cm for the concrete grade selected for abrasive movements.

The thickness of layers exposed to direct abrasion should be at least:

- 4 cm when laid on a concrete mix before hardening,
- 6 cm when laid on hardened concrete.

It is known that above thickness values can be decreased by 1.0...1.5 cm through adding steel fibers in the amount of 0.8...1.2 %.

The maximum amount of water allowed penetrating the abrasion resistant concrete is as follows:

- 5% of weight for the concrete exposed to constant or periodical humidity and intense traffic,

Cement influence on stabilized sand resistance

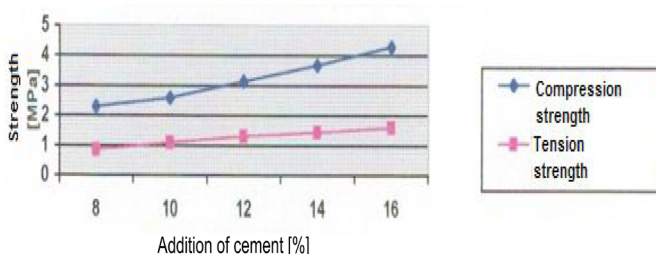


Figure 2. Cement influence on stabilized sand resistance (Stypulkowski, 1981)

Requirements to concrete mixes used to develop concrete surfaces (Polish experience): concrete composition.

- 6% of weight for the concrete exposed to constant or periodical humidity and traffic of low and/or medium intensity.

The selection of ingredients for industrial flooring concrete requires paying attention to the following aspects:

- low shrinkage,
- B25 minimum class,
- water/concrete (w/c) lower than 0.5,
- proper workability.

According to PN-88/B-06250, concrete mix control implies estimation of the concentrated load strength distribution in each batch of concrete.

Cement grades are listed in Table 4 in relation to the concrete class. Table 5 shows the concrete classes and respective guaranteed resistance.

Table 4. Portland cement grade and concrete classes (Rowinski et al., 1980)

Cement grade	Concrete class	
	Structure	
	Monolithic	Prefabricated
250	Up to B10 inclusive	Up to B15 inclusive
350	B10–B15	B15–B35
400 and 450	B15–B35	B25–B40
500	B25	B35

Table 5. Concrete classes and the corresponding strength guaranteed by PN-88/B-06250 (Wolski, 1996)

Concrete class	R_b^c	
B7.5	7.5	11
B10	10	14
B15	15	20
B20	20	25
B25	25	32.5
B30	30	40
B35	35	45
B40	40	50
B50	50	60

Aggregate granulation

Aggregate makes approximately 75% of concrete, which means it influences considerably the concrete quality. Selection of aggregate has a great impact on cement consumption, workability, resistance and durability of concrete. Each specific concrete class requires different type and kind of aggregate. Granulation provides the mix impermeability and consistence. Relations between aggregate and concrete classes are shown in Table 6.

B30 concrete needs to be based on natural aggregate with max. 16 mm granulation (up to 8mm is recommended) compliant with PN-83/B-06712.

Resistant concrete is based on thick aggregate described in Table 7.

Table 6. Aggregate type and its influence on the concrete class

Concrete class	Type and kind of aggregate
Higher than B25	Crushed stones, natural fine aggregate, natural thick aggregate, natural thick aggregate in the volume not exceeding 30% of the general quantity over 2 mm
Lower than B25	Natural thick aggregate, 20 grade gravel, natural fine aggregate
Lower than B15	As above but grade 10
Lower than B10	Sand and gravel mixes, natural fine aggregate

Thick natural aggregate is made of crushed volcanic or metamorphic rocks, compliant with PN-83/B-06712 for crushed fieldstone grade 30 having the following parameters:

- abrasion resistance — min. 120 MPa
- water absorption — below 1%,
- Boehme disc abrasiveness — max. 0.35 cm (corundum B80),
- granulation — according to the Table.

Table 7. Thick aggregate selection criteria to make abrasion-resistant concrete (Potrzebowski, 1998)

no.	Abrasive layer thickness [mm]	Largest approved granulation [mm]	Thick aggregate fraction	
			Fraction [mm]	Content in thick aggregate [%]
1	<10	4	2–4	100
2	10 to 20	8	4–8	100
3	20 to 30	16	4–16	100
4	>30	16	2–4	25
			4–16	75

The granulation given by S. Rolla (1983, 1985) applied to regular types of concrete for concrete undercoat and lean concrete is presented in charts. Aggregate granulation can vary within the curves. The curve contained in this area can be a kinked one indicating the presence of certain intermediate fractions.

Forming conditions: mix workability and consistence

Consistence and workability are the features which define concrete mix properties and ability to fill the molds and keep the shape after the molds are disassembled.

The concrete mix consistence is examined using the Ve-Be or cone slump method. The first one is recommended for plastic and dense mixes, the second one works better with liquid mixes.

Both methods have been standardized and described in PN-88/B-06250.

Recommendations on workability and consistence are given in Table 8.

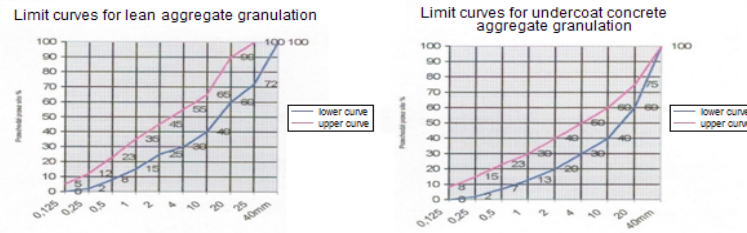


Figure 3. Limit curves for lean and undercoat concrete aggregate granulation

Table 8. Mix consistence recommendations according to PN-88/B-06250 (Rowinski, 1978)

Concrete mix consistence	Consistence symbol	Consistence indicator	
		Ve-Be [s]	Cone slump [cm]
Humid	K-1	Exceeding 30	N/A
Dense/plastic	K-2	16–30	N/A
Plastic	K-3	8–16	2–8
Semi-liquid	K-4	5–8 not recommended	8–12
Liquid	K-5	N/A	Exceeding 12

Table 9. Concrete mix consistence regarding the structure and densification method. PN-88/B-06250 (Rowinski, 1978)

Consistence	Type of construction and method of compacting
Humid	Prefabricates subject to vibration densification at frequency 100 Hz. Prefabricates subject to vibration compaction. Manually applied non-construction concretes
Dense/plastic	Concrete and reinforced concrete, mechanically densified. Concrete and reinforced concrete construction, prefabricated construction, surface vibration densification or with simple vibration probes. Manually densified non-construction concretes
Plastic	Regular concrete and reinforced concrete structures, densified with vibration probes or attached vibrators. Concrete and reinforced concrete structures, densified with vibration probes or attached vibrators and shaped in thin vertical walls
Liquid and semi-liquid	Construction concretes, manually densified, or self-densified.

Concrete consistence provides a great impact on cement consumption, so it needs to be limited by the densest concrete mixes having plasticizers.

Influence of fibers on concrete workability

In terms of workability, introduction of fibers reduces the quality of concrete by one class. Therefore, achieving K3/K4 requires using a plasticizer and achieving K4/K5 requires using a superplasticizer.

K3/K4 consistence is recommended when the fibers are added into the concrete delivered in trucks. This corresponds to the Abrams cone slump of 4–6 cm after the fibers are added; the maximum value of 10 cm can be reached before adding the fibers.

If the concrete is pumped to the work area, it should have consistence of K4/K5 which corresponds to the Abrams cone slump of 8–10 cm after the fibers are added and 12–14 cm before the fibers are introduced.

Cement volume and w/c ratio

Concrete composition involves such basic indicator as cement-water (c/w) which constitutes a cement to water

weight ratio. The lower the water content (above a certain level), the more resistant the concrete is.

The relation between conditions of application and concrete mix is expressed through the smallest acceptable cement volume as shown in PN-88/B-06250. The parameters are listed in Table 10.

Table 10. Minimum cement volume with regard to conditions of application [PN-88/B-06250] (Rowinski, 1978)

Structures and operating conditions	Minimum cement volume kg/m^3 for:	
	Structures	
	Reinforced	Regular
Structures not exposed to weather conditions	0.4z	0.35z
Structures exposed to weather conditions	0.5z	0.45z
Structures exposed to constant water penetration and frost	0.5z	0.50z

The highest cement volume in kg/m³ should not exceed:

550 — for medium compression resistant concretes — higher or equal to 40 MPa,

450 — for other types of concrete.

In road concrete, it should not exceed:

400 — for the surface concrete,

250 — for the undercoat concrete,

150 — for lean undercoat concrete.

Frost resistance

The concrete exposed to humidity and frost should feature the following:

- average resistance: minimum 15 MPa,

- frost resistance expressed with maximum 5% erosion (shown in samples),

- frost resistance defined with compression resistance decrease: max 20 %.

Moreover, the concrete exposed to direct influence of liquids needs to be water-proof with pressure of at least 0.7 MPa in at least four samples.

Conclusion

The article discusses recommendations for selecting processes and materials used depending on the floor category and the application purpose. For the purpose of constructing industrial concrete floors based on the experience of Polish construction companies, recommendations are made for developing substructures under the industrial surface in line with characteristics of seven types of soil, showing the influence of the cement stabilizer on the mechanical properties of sand. Solution examples to make concrete mixes for concrete foundation using the French experience are given. Selection of grading aggregate for concrete depending on the class of concrete is presented on the basis of Polish experience guidelines. General terms of producing and molding concrete mixes to develop industrial concrete floors are discussed.

References

- Czarnecki, L., Rydz, Z. (1995). Rozwój posadzek przemysłowych [Development of industrial flooring]. *Materiały budowlane [Construction Materials]*, 9, pp. 12–13. (in Polish)
- Czarnecki, L., Rydz, Z. (1998). Posadzki przemysłowe betonowe i z żywic syntetycznych [Industrial flooring: concrete and synthetic resin flooring]. *Materiały budowlane [Construction Materials]*, 9, pp. 2–7. (in Polish)
- Jamroz, Z. et al. (1990). *Betony specjalne konstrukcyjne [Special structural concretes]*. Krakow: Krakow Polytechnic University. (in Polish)
- Potrzebowski, J. (1998). Dobór warstw posadzek przemysłowych [Selection of industrial flooring layers]. *Materiały budowlane [Construction Materials]*, 9. (in Polish)
- Rajczyk, J. (2013). Modelling the geometric structure of concrete work item processing. *Applied Mechanics and Materials*, 405–408, pp.638–643. DOI: 10.4028/www.scientific.net/AMM.405-408.638
- Rajczyk, J., Kosin, M., (2011). Methodology of analyzing a new geometry design of a friction plate effect on the engineered surfaces. *IET Conference Publications*, 2, pp. 177–180.
- Rajczyk, J., Rajczyk, M., Kalinowski, J. (2016). Performance parameters of concrete and asphalt-concrete surfaces. In: *Proceedings of the International Conference on Advanced Materials and Engineering Structural Technology (ICAMEST 2015)*, pp. 419–422.
- Rolla, S. (1983). *Nowoczesne nawierzchnie betonowe [Modern types of flooring]*. Warsaw: Transport and Communication Publishers. (in Polish)
- Rolla, S. (1985). *Badania materiałów i nawierzchni drogowych [Testing of materials and road surfaces]*. Warsaw: Transport and Communication Publishers. (in Polish)
- Rowinski, L. (1978). *Zmechanizowane roboty budowlane [Mechanized construction operations]*. Warsaw: Arkady. (in Polish)
- Rowinski, L. et al. (1980). *Technologia monolitycznego budownictwa betonowego [Technology of monolithic construction from concrete]*. Warsaw: Polish Scientific Publishers. (in Polish)
- Stypulkowski, B. (1981). *Materiały w budownictwie [Materials in construction]*. Warsaw: Transport and Communication Publishers. (in Polish)
- Wolski, Z. (1996). *Roboty podłogowe [Flooring construction]*. Warsaw: Arkady. (in Polish)

STUDY OF THE INFLUENCE OF THE ENERGOINFORMATIONAL FIELD ON QUALITY OF THE FUEL APPLIED IN INTERNAL COMBUSTION ENGINES OF ROAD-BUILDING MACHINERY

Ravil Safiullin ¹, Mukhtar Kerimov ², Alexander Afanasyev ³

^{1,2} Saint Petersburg State University of Architecture and Civil Engineering
Vtoraja Krasnoarmejskaja ul. 4, St. Petersburg, Russia

³ Saint Petersburg Mining University
21st Line, 2, St. Petersburg, Russia

¹ safravi@mail.ru

Abstract

Directions for the improvement of the performance of road-building machinery and transportation vehicles, as well as technological properties of fuels are considered. A model for the improvement of road-building machinery performance when using fuels of various physical and chemical composition is developed.

The specified model includes a system of immediate fuel quality assessment. Experimental studies were carried out in order to determine the influence of the energoinformational field produced by the Kozyrev heavy particles generator on fuel performance characteristics.

The obtained results show a decrease in fuel consumption by internal combustion engines of road-building machinery concurrently with changes in the harmful substance concentration in exhaust gases.

Recommendations for calibration of electronic systems of internal combustion engines are elaborated.

Keywords

Technology level, motor fuel, energoinformational field, performance, integrated assessment, road-building machinery.

Introduction

With the development of regional construction and transportation industries, the number of road-building machines and vehicles, being sources of the formation of technical services and main consumers of fuel and energy resources, increases. The transportation work load increases as well. Modern road-building machinery becomes more complex, equipped with various innovative electronic and telematic systems. We face a crucial task to increase the service life of internal combustion engines (ICE) due to a decrease in their calorific intensity. Increasingly strict requirements on the assurance of energy efficiency and environmental safety are imposed upon ICE. As a result, we encounter a problematic situation where the adequate and prompt solution of this problem depends largely on the implemented means and methods. The achievement of the stated objective through

the development of new ICE types during a short period of time seems to be impossible in terms of design and economically impractical (Safiullin, and Kerimov, 2014a, 2014b). Therefore, the rational use of fuel by means of fuel composition optimization concurrently with the improvement of ICE design based on intelligent on-board systems represents a scientific problem of academic and practical interest.

Methods

The fuel quality level is a relative value based on the comparison of values characterizing technological and environmental maturity of complex indicators of the assessed fuel. At the present time, quality is becoming a "control object". In other words, we refer to the development of a quality optimization system, quality planning, control and regulation during operation of road-building

machinery ICE (Safiullin and Kerimov, 2014c, 2014d; Denisov, 1998).

The quality level mostly depends on technological methods affecting fuel, technological intensity and controllability of the implemented process, efficiency of ICE electronic modules and ICE adaptational and organizational level (Figure 1).

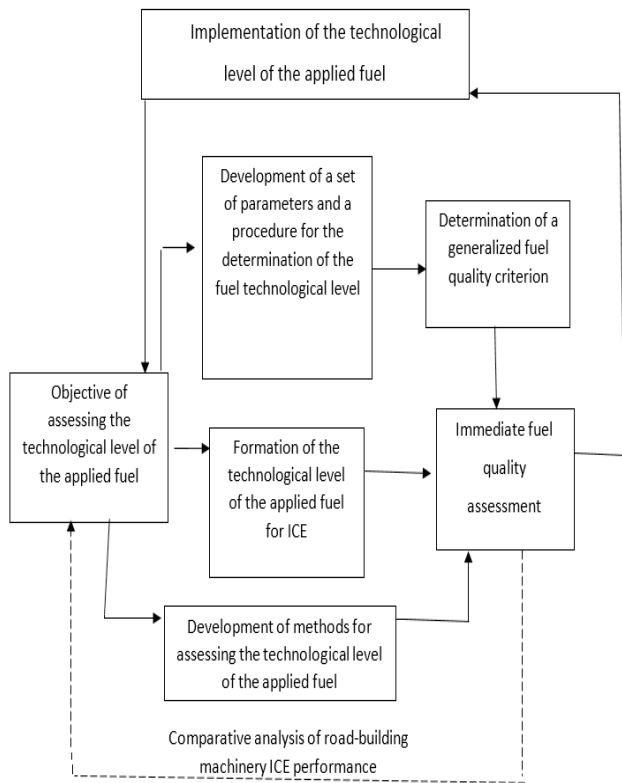


Figure 1. Model of influence of the technological level of the applied fuel on road-building machinery performance

The experimental studies were continued in order to determine the influence of the energoinformational field produced by the Kozyrev heavy particles generator (KHPG) on fuel performance characteristics. A KHPG is a centrifuge and vortex device forming a vertical flux of particles, changing the space structure (Denisov, 1975,

1998). The process of fuel quality formation under the influence of the KHPG is presented in Figure 2.

The experimental studies were carried out in the Transportation Energy laboratory of the Automobile and Road-Building Department of the Saint Petersburg State University of Architecture and Civil Engineering on a test bench equipped with the VAZ-2112 engine with a 5-speed manual transmission. Engine operation control is carried out using an automated system for the control of the data on the transportation vehicle ICE technical condition (Safiullin, 2017) concurrently with the control of the loading device.

The determination of the gasoline fraction composition was carried out using the ARN-LAB-03 device for the distillation of oil products. The recording of changes in fuel performance characteristics was carried out using the ShatoxSX300 device for the determination of the knock characteristic of gasolines, hypergolicity of diesel fuels based on the measurement of their dielectric permittivity and specific volume resistivity. The study procedure provides for the implementation of the following actions.

Table 1. Sequence of studies on the influence of the energoinformational field on performance characteristics of fuels

Experiment	Actions
1	1. Determination of the fraction composition of non-modified gasoline using a device for the determination of the fraction composition of oil products. 2. Recording of the data on performance characteristics of non-modified gasoline using the ShatoxSX300 device.
2	1. Influence of the KHPG on the applied gasoline during 60 minutes. 2. Determination of the fraction composition of modified gasoline using a device for the determination of the fraction composition of oil products. 3. Recording of the data on performance characteristics of modified gasoline using the ShatoxSX300 device.
3	1. Determination of the fraction composition of non-modified diesel fuel using a device for the determination of the fraction composition of oil products. 2. Recording of the data on performance characteristics of non-modified diesel fuel using the ShatoxSX300 device.
4	1. Influence of the KHPG on the applied diesel fuel during 60 minutes. 2. Determination of the fraction composition of modified diesel fuel using a device for the determination of the fraction composition of oil products. 3. Recording of the data on performance characteristics of modified diesel fuel using the ShatoxSX300 device

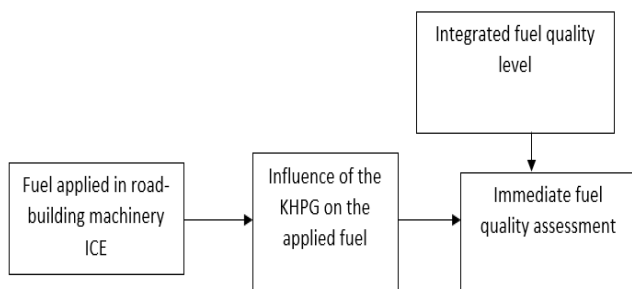


Figure 2. Flow chart of fuel quality formation under the influence of the KHPG

Main body

Due to the fact that the technological system is implemented under the action of random factors, values of all individual indicators of fuel quality are also random. Therefore, the integrated assessment of probabilistic characteristics of these values serves as an indicator of the efficiency of such technological system.

A model for the improvement of road-building machinery performance when using fuels of various physical and chemical composition, including the fuel quality assessment system (FQAS) presented in Figure 3, is developed.

The specified system allows for quick changes in fuel metering, ignition dwell angle and other ICE adjustment parameters in all operation modes. It also allows informing the driver of the improper fuel composition leading to a breakdown. After the combination of physical properties of fuels according to the level of the influence on road-building machinery performance, we will obtain the following three groups:

- indicators characterizing energetic properties;
- indicators characterizing carburetion characteristics;
- indicators characterizing fuel contamination.

An integrated approach to fuel quality level assessment based on the application of a weighted average is taken as the basis for the procedure being developed. For

this purpose, the following equation is used (Safiullin and Kerimov, 2014d):

$$N = A_x B_y C_z \int\int\int_D \alpha_x dx dy dz = \tag{1}$$

$$= \psi_0 \int\int\int_D \alpha_y dx dy dz = \psi_{01} \int\int\int_D \alpha_z dx dy dz$$

where: α_x is a group quality indicator characterizing performance characteristics of fuel; α_y is an integrated quality indicator characterizing performance characteristics of fuel; α_z are individual quality indicators obtained upon fuel testing; A_x is a weight coefficient of an i -th group quality indicator; B_y is a weight coefficient of an i -th integrated quality indicator; C_z is a weight coefficient of an i -th individual quality indicator; ψ_c is a weight coefficient of certain quality indicators; D is a range of values of quality indicators characterizing fuel of a particular type, regulated by standards.

A relationship between fuel characteristics and its electrical and physical parameters, in particular, dielectric permittivity (DP) Ω , is included in the fuel quality assessment system. Figure 3 presents the results of studies on

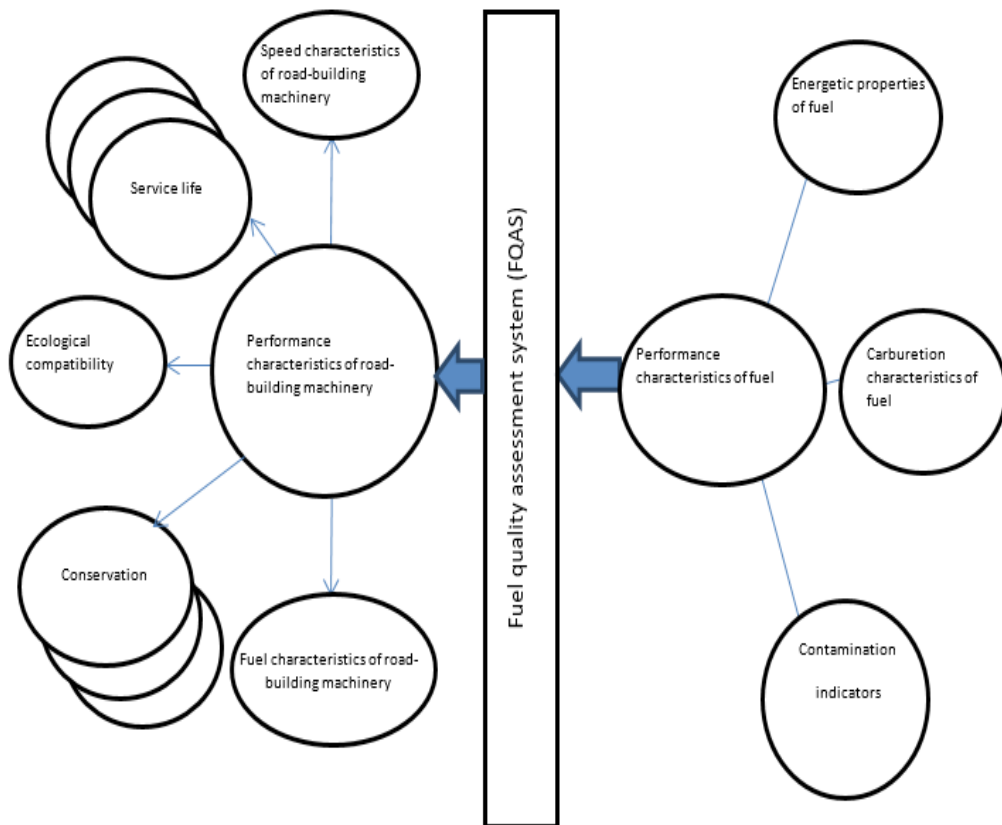


Figure 3. Model for the improvement of road-building machinery performance when using fuels of various physical and chemical composition

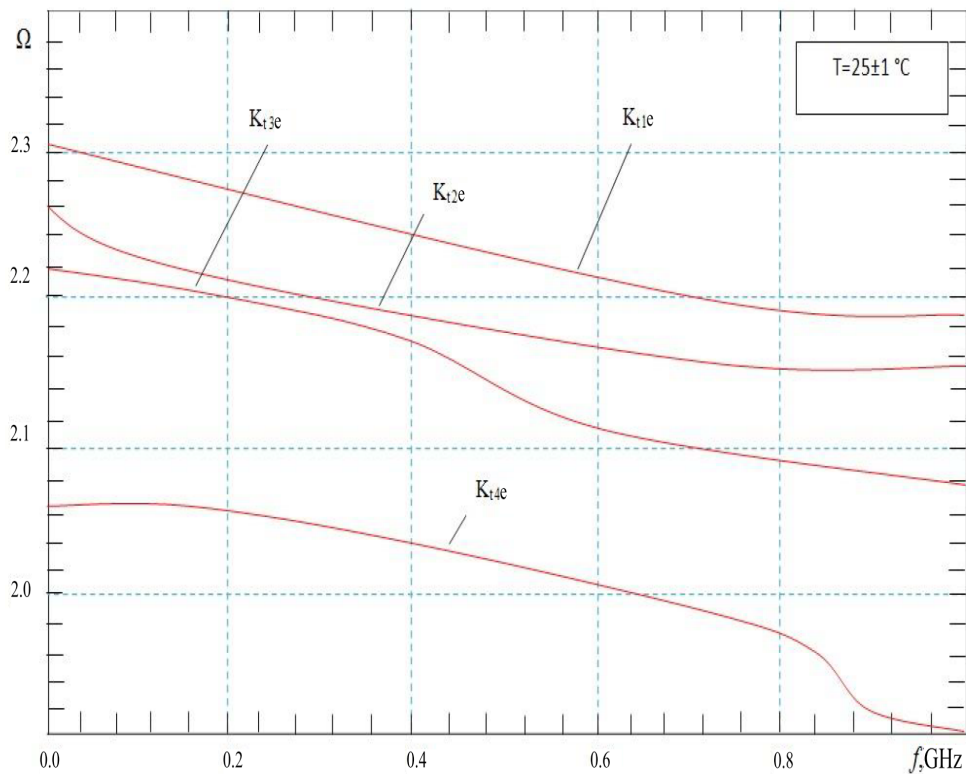


Figure 4. Results of the study on DP real part values for fuels based on WFE and conventional diesel fuel on various frequencies at a constant temperature

DP of fuels from Faeton, Neste, PTK (Saint Petersburg) filling stations on various frequencies at a constant temperature. According to the results, fuels of different quality have different values of dielectric permittivity on different frequencies. Therefore, we can conclude that the set of the data on DP values can be used for the qualitative assessment of fuels (Safiullin and Kerimov, 2014c, 2014d).

Results of the study

According to the results of the study on dielectric permittivity of fuels, the values of characteristics of diesel fuel based on water-fuel emulsion (WFE) are several-fold larger than the same values of conventional fuels. Figure 4 presents diagrams of DP real part values on various frequencies for 4 clusters corresponding to four identified groups of fuels: K_{t4} — fuel L-0,2 GOST 305-82, K_{t3} , K_{t2} , K_{t1} — WFE with water content of 5, 10 and 20% by mass, respectively.

As a result of the processing of the experimental data, regression equations were obtained: the first one corresponds to a group of fuels with a low value of Kt (groups 1 and 2), and the second one corresponds to group 3 (Safiullin and Kerimov, 2014c, 2014d):

$$K_{t1e} = -164.54 + 260.407 \times \Omega - 89.53 \times \Omega^2 + 12.793 \times \Omega^3 - 0.65 \times \Omega^4 \quad (2)$$

$$K_{t2e} = -1230 + 897 \times \Omega - 67.55 \times \Omega^2 + 12.793 \times \Omega^3 \quad (3)$$

$$K_{t3e} = -3561.3 + 3494.64 \times \Omega - 835.55 \times \Omega^2 \quad (4)$$

To assess the technological level of fuel, 3 subsets were composed: the first and the second subsets include samples of diesel fuel with a rather low value of K_{t1} , 2 corresponding to WFE with water content of 5, 10% by mass (curves 1, 2, Figure 5), and the third value of K_{t3} includes fuel based on WFE with water content of 20% by mass (curve 3, Figure 5). The testing of the obtained models, which was carried out using the fuels not included into the sample group, has shown that the error in values of the generalized fuel quality criterion Kt with regard to the samples does not exceed the permissible level. To calculate the fuel quality criterion K_t , the following sequence of operations shall be performed:

- receipt of a polymetric signal;
- primary signal processing in order to reduce the interference effect;
- calculation of parameters in the time domain: delays between pulses, pulse amplitudes, fuel level calculation, determination of DP and fuel utilization coefficient values;
- assessment of fuel affiliation with one of the groups identified during cluster analysis;

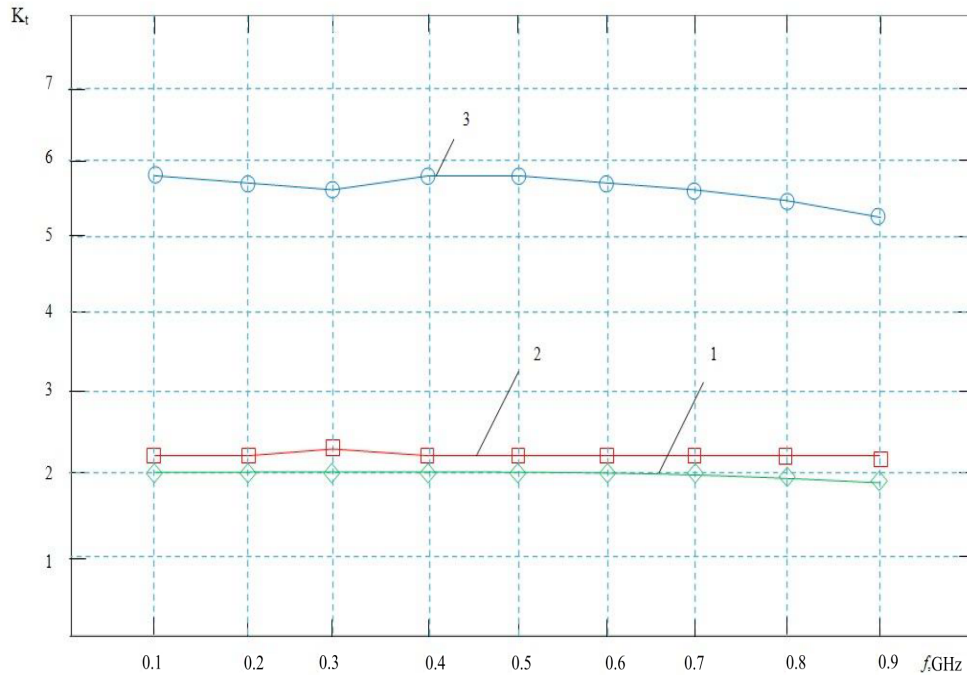


Figure 5. Results of the study on quality of fuels based on WFE with water content of 5, 10 and 20% by mass according to DP on various frequencies and at a constant temperature

- fuel quality assessment according to the value of the fuel utilization coefficient depending on the chosen group.

To improve quality assessment accuracy, it is proposed to identify a class (group) of the studied fuel automatically based on the information on the value of its complex DP on various frequencies. The preliminary division of fuels into groups is performed based on the cluster analysis of the experimental data on fuel utilization coefficient values on various frequencies. It allows applying fuel quality assessment systems upon real-time monitoring of fuel parameters directly in ICE.

The obtained results are presented in Tables 2–6 as well as in Figures 6–8.

Table 2. Fraction composition of non-modified and modified gasoline (experiment 1)

Fraction (%)	t (non-modified)	t (modified)
0	38	42
5	45	51
10	50	56
15	54	57
20	58	57
30	66	62
40	77	69
50	88	81
60	104	104
70	119	120
80	138	138
90	160	154
95	125	168

Table 3. Performance characteristics of the SX300 gasoline (experiment 2)

Parameter	Non-modified	Modified
Oct(ROn)	96.7	96.6
Oct(MON)	87.1	87.0
Tbd	1,601	1,695
Eps(U)	2.2259	2.2152
Eps(P)	3.1885	3.1796
Kw	0.4%	0.3%
Oct+Ad	0.01%	0.00%
ON	3.6	0%
p	6.74*10 ⁻¹⁶	6.49*10 ⁻¹⁶
β	0.733	0.739

Table 4. Performance characteristics of diesel fuel (experiment 4)

Parameter	Modified	Non-modified
Cet	51.1	50.5
t (freezing)	-10.2	-11.4
Eps(U)	2.2159	2.2199
Eps(P)	3.1085	3.1368
Kw	0%	0.4%
p	3.36*10 ⁻¹²	3.38*10 ⁻¹²
β	0.829	0.827

Table 5. Determination of the fraction composition of non-modified and modified diesel fuel (experiment 3)

Fraction (%)	t (non-modified)	t (modified)
0	172	174
5	188	190
10	201	202
15	209	211
20	217	218
30	237	235
40	254	250
50	265	260
60	277	275
70	289	289
80	313	310
90	327	330
95	334	347

Eps (U) — dielectric permittivity (pouring)
Eps (P) — dielectric permittivity (submerging)
Kw — water content, %
p — volume resistivity, Ohm · m
ρ — density, kg/m³

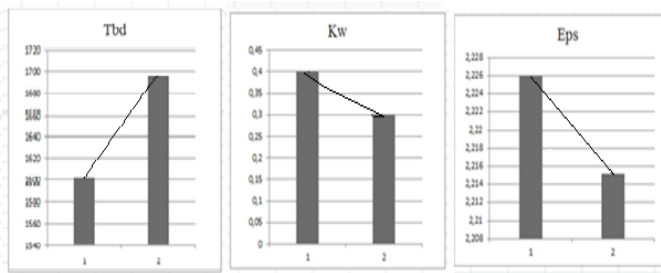


Figure 6. Influence of the KHPG vortex effect on the octane number, water content, induction period of oxidation and dielectric permittivity of gasoline

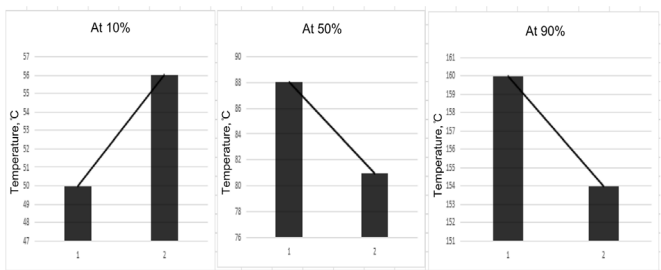


Figure 7. Influence of the KHPG vortex effect on the starting (at 10%), power (at 50%) and tail (at 90%) fractions of gasoline

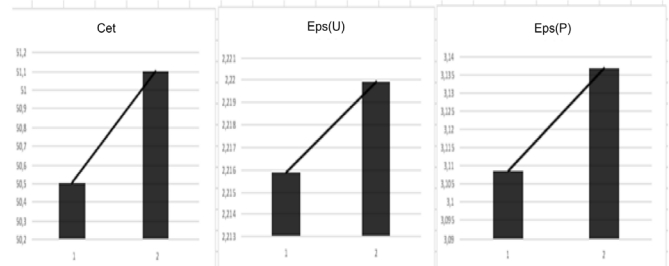


Figure 8. Influence of the KHPG vortex effect on the cetane number and dielectric permittivity of diesel fuel (1 — modified, 2 — non-modified)

According to the performed studies, changes in the parameters characterizing hourly consumption and performance characteristics depending on the KHPG influence on gasoline were established (Figures 5–10).

Under the influence of the KHPG, the temperature of distillation of 50% of gasoline decreases, which has positive effect on engine warm-up intensity, stability of its performance at a low crankshaft speed, as well as acceleration time (Safiullin, 2017; Hilliard, 1988; Makerle, 1987; Safiullin and Kerimov, 2016).

According to the results of the preliminary experimental studies, the temperature of medium gasoline fraction boil-off decreases significantly (by 7–10%), which has positive effect on ICE performance due to smoother entering of the fuel-air mixture of the required composition to the cold engine. The decrease in the temperature of distillation of 90% of gasoline indicates the increase in fuel-air mixture combustion intensity and efficiency as well as engine power.

The results of the KHPG influence on fuel and environmental characteristics of ICE are presented in Table 6.

Accepted designations:

- FREQ — readings of the engine crankshaft rpm sensor, rpm;
- JAIR — air-mass flow, kg/h;
- JGBC — amount of fuel injected into the engine cylinder per 1 stroke, mg/stroke;
- JQT — fuel consumption, kg/h;
- THR — throttle position, %;
- INJ — injection time, ms;
- TWAT — coolant temperature, °C
- CO — CO volume content in exhaust gases, %
- CO₂ — CO₂ volume content in exhaust gases, %
- HC — CH volume content in exhaust gases, %
- O₂ — O₂ volume content in exhaust gases, %
- NOx — NOx volume content in exhaust gases, %

Diagrams showing the KHPG influence on fuel (Figure 9) and environmental characteristics (Figure 10) of ICE performance are constructed based on the obtained data.

Table 6. Results of the KHPG influence on fuel and environmental characteristics of ICE in experimental studies

Parameter	Values									
	Without KHPG	After KHPG action								
FREQ rpm	1,040	1,040	1,800	1,840	2,240	2,200	2,480	2,520	2,880	2,800
JAIR kg/h	18.4	14.6	24.7	21	31.5	24.9	33.1	27.6	40.9	33.9
JGBC mg/stroke	150	123.3	115.3	98.67	116.7	95.33	110.7	94.67	113.3	98.67
JQT kg/h	1.7	1.4	2.2	1.9	2.8	2.2	2.9	2.5	3.5	2.9
THR %	0	3	2	5	3	5	4	6	5	7
INJ ms	3.4	2.85	2.69	2.41	2.81	2.34	2.73	2.41	2.81	2.42
TWAT °C	90	90	95	91	101	91	99	99	99	95
CO, %	0.09	0.03	0.04	0.11	0	0.11	0	0.08	0	0.02
CO ₂ , %	13.8	13.1	14.2	13.8	13.4	13.5	13.5	13.7	13.5	13.8
HC, %	87	88	77	87	49	77	38	65	30	44
O ₂ , %	2.73	1.36	2.59	1.36	2.73	1.36	2.73	1.36	2.73	1.5
NO _x , %	1.13	1.067	1.122	1.061	1.14	1.062	1.139	1.063	1.139	1.073

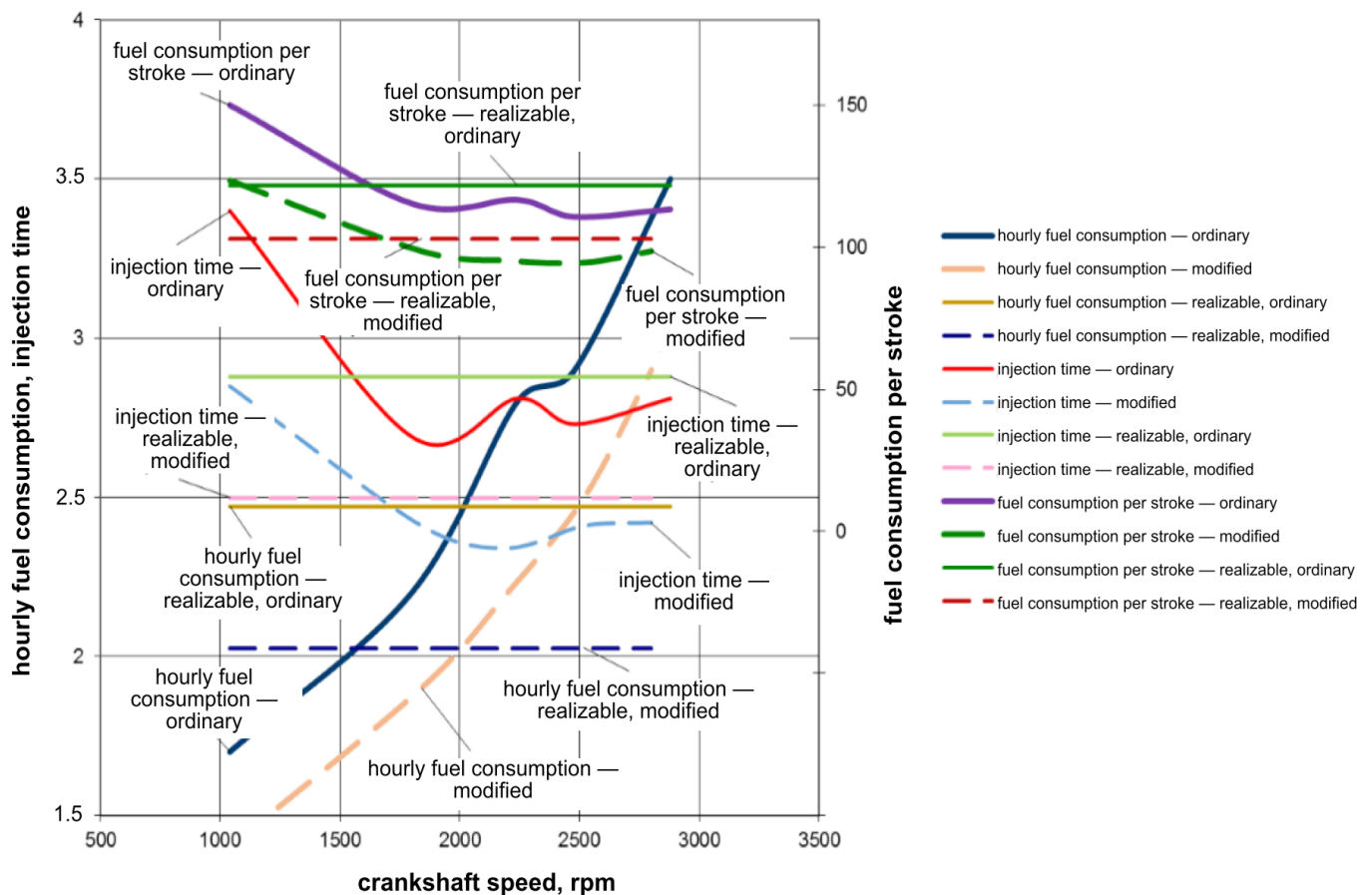


Figure 9. Fuel-efficient characteristics of ICE when using the KHPG

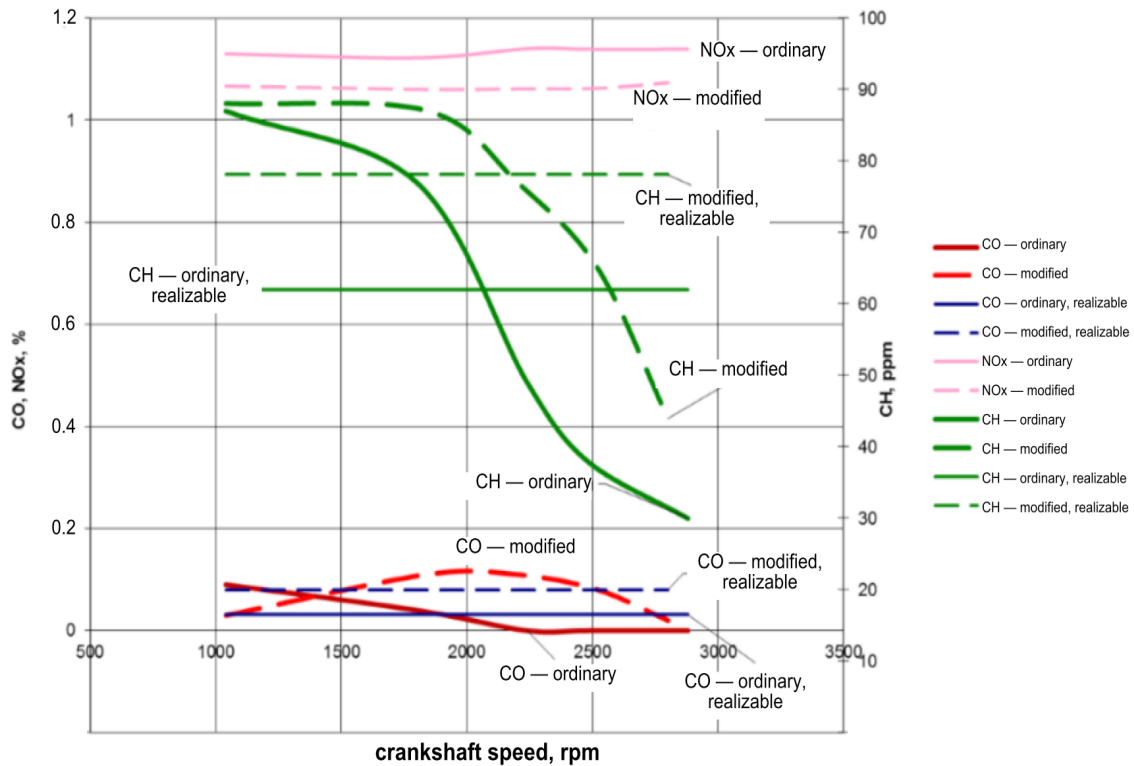


Figure 10. Environmental characteristics of ICE when using the KHPG

Conclusions

A theoretical basis for the formation of the technological level of the applied fuel in road-building machinery ICE are developed based on the carried-out studies. A physical model for studies of the influence of the technological level of the applied fuel on the performance of road-building machinery, transportation vehicles and equipment is proposed.

According to the results of the experimental studies on the KHPG influence on motor fuel, the following preliminary conclusions can be drawn:

1. Changes in the parameters characterizing fuel consumption and performance characteristics depending on the KHPG influence on gasoline were established (Figures 9–10):

- decrease in the ICE temperature at the same loads (up to 20%);
- decrease in fuel consumption (up to 20%);
- decrease in oxygen concentration in exhaust gases (up to 50%);
- decrease in nitrogen oxide concentration in exhaust gases (up to 10%).

Under the influence of the KHPG, the temperature of distillation of 50% of gasoline decreases, which has positive effect on ICE warm-up intensity, stability of its perfor-

mance at low crankshaft speeds, as well as acceleration time.

2. According to the results of the preliminary experimental studies, the temperature of medium gasoline fraction boil-off decreases significantly (7–10%), which has positive effect on ICE performance. The decrease in the fuel distillation temperature indicates the increase in fuel-air mixture combustion intensity and efficiency as well as engine power.

3. Figures 3–4 present the results of DP studies showing that fuels of different quality (K_f) have different values of dielectric permittivity under the KHPG influence with a different period of exposure. The decrease in dielectric permittivity of gasoline indicates the increase in fuel energy capacity.

4. Changes in engine performance parameters after KHPG action can occur both as a result of the integrated influence on fuel and engine systems and as a result of the influence on an individual factor which represents a primary cause of subsequent changes in parameters.

5. The recommendations for calibration of electronic engine control systems were developed. For purposes of full-scale studying of the KHPG influence on performance characteristics of fuels, it is necessary to perform further comprehensive studies.

References

- Denisov, A.A. (1998). *Informacionnoe pole [Information field]*. Saint Petersburg: Omega, p. 64. (in Russian)
- Denisov, A.A. (1975). *Teoreticheskie osnovy kibernetiki [Theoretical bases of cybernetics]*. Leningrad: LPI, p. 40. (in Russian)
- Hilliard, J., Springer, G. (1988). *Toplivnaja jekonomichnost' avtomobilej s benzinovym dvigatelem [Fuel economy in road vehicles powered by spark ignition engines]*. Moscow: Mashinostroyeniye, p. 142. (in Russian)
- Makerle, Ju. (1987). *Sovremenniy ekonomichnyy avtomobil [Modern economy car]*. Moscow: Mashinostroyeniye, p.231. (in Russian)
- Safiullin, R.N., Kerimov, M.A. (2014a). Teoreticheskie osnovy kompleksnoj optimizacii osnovnyh velichin i parametrov DVS ATS pri primenenii topliv razlichnogo kachestva DVS [Theoretic complex optimization basics of the main values and parameters of ICE (internal combustion engine) of AMV (automatic motor vehicles) at applying various quality fuels]. *Vestnik Grazhdanskikh Inzhenerov [Bulletin of Civil Engineers]*, 4 (45), pp. 104–111. (in Russian)
- Safiullin, R.N., Kerimov, M.A. (2014b). Metodika ocenki i realizacii kachestvennyh pokazatelej topliva na osnove issledovanija ego himmotologicheskikh processov i svoystv [A technique of assessment and realization of fuel quality indicators on the basis of researching its chemmotology processes and properties]. *Vestnik Grazhdanskikh Inzhenerov [Bulletin of Civil Engineers]*, 3 (44), pp. 184–188. (in Russian)
- Safiullin, R.N., Kerimov, M.A. (2014c). Razrabotka programmno-adaptivnyh sistem upravlenija po ocenke i realizacii racional'nyh kachestvennyh pokazatelej primenjaemyh topliv DVS [Development of program and adaptive control systems for assessment and realization of rational quality indicators of applied ICE fuels]. *Vestnik Grazhdanskikh Inzhenerov [Bulletin of Civil Engineers]*, 2 (43), pp. 139–146. (in Russian)
- Safiullin, R.N., Kerimov, M.A. (2014d). Optimal'noe upravlenie DVS v diapazone jekspluatacionnyh rezhimov pri ispol'zovanii avtomatizirovannoj sistemy stendovyh ispytanij (ASSI) [Optimum control of ICE in the range of operational modes when using the ASSI]. *Vestnik Grazhdanskikh Inzhenerov [Bulletin of Civil Engineers]*, 1 (42), pp. 121–126. (in Russian)
- Safiullin, R.N. (2017). *Data of the automated control system on the technical condition of the internal combustion engine of the vehicle*. Utility Model Patent No. 174174 dd. 05.10.2017. (in Russian)
- Safiullin, R.N., Kerimov, M.A. (2016). *Sredstva fotovideofiksacii narushenij PDD: normativnoe regulirovanie i praktika primenenija: [Methods of photo-video recording of traffic violations: control and practical application]*. Moscow: Direkt-Media, p.355. (in Russian)

IN MEMORY OF PROFESSOR RAY W. CLOUGH OF THE CALIFORNIA UNIVERSITY AT BERKELEY, WHO DIED ON OCTOBER 8, 2016

Ray W. Clough, Nishkian Professor of Civil Engineering, Emeritus, University of California, Berkeley, Honorary Member of IAEE, and Founding Editor of Earthquake Engineering & Structural Dynamics. Born July 23, 1920, he grew up in Seattle, Washington.



Ray W. Clough

He received his B.S. degree from the University of Washington, Seattle, in 1942, and the Sc.D. degree at M.I.T. in 1949. He chose Civil Engineering as his undergraduate major because of his love of the outdoors. During those years he had trekked extensively and climbed several of the major volcanic peaks—Rainier, Baker, Glacier, and St. Helens — in the states of Washington and Oregon. Professor Ray Clough was a dedicated skier and mountaineer. We climbed together Mt. Olympus in Greece.

Immediately after completion of his doctoral studies, Ray Clough came to Berkeley as an Assistant Professor. Despite receiving numerous offers from other universities, his entire academic career was at Berkeley until he retired from teaching in 1987. Ray's contributions in teaching, research and consulting during 1950–1995 in the fields of finite element analysis, structural dynamics and earthquake engineering have been monumental. On his arrival at Berkeley, Ray Clough was assigned to develop a graduate course on Dynamics of Structures. He, Joseph Penzien, and Vitelmo Bertero developed the teaching program in structural dynamics and earthquake engineering at Berkeley that many considered to be the best in the world. It led to the book Dynamics of Structures (co-authored with Joseph Penzien) published in 1975 and again

in 1993. It was a landmark book in terms of its broad scope, comprehensive coverage, and philosophy. Several generations of students and engineers, in the United States and abroad learned the subject from this very book. It has been translated into Chinese, Greek, French, Japanese, Russian, Bahasa Indonesian etc. Perhaps his most important research contribution in structural engineering was as a co-developer in the "Finite Element Method" beginning with a classic paper in 1956. With the advent of digital computers the finite element method forever revolutionized the field of structural analysis and design. The method has been extended to many fields of engineering and makes it possible to analyze complex systems of many different kinds, including those encountered in design and safety evaluation of structures, and in aircraft, automobile, nuclear and oil industries. Because of the fundamental nature of the finite element concept, researchers in diverse fields of applied science and engineering recognized its potential in solving problems in their respective fields.

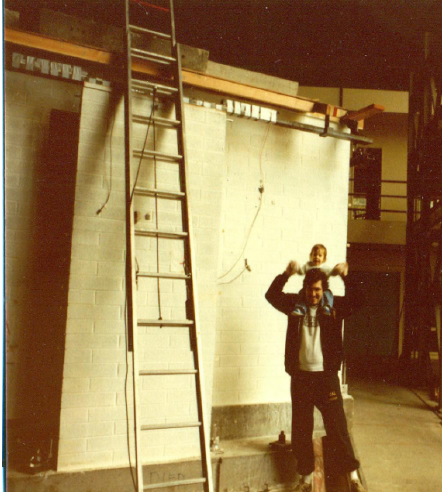
Although Ray Clough was a leader in the development of analytical methods to predict the effects of earthquakes on structures, he had been cognizant of the limitations of these methods.



Elephant foot bulge during the May 1983 Coalinga Earthquake

Recognizing that analytical capabilities have advanced beyond the experimental results on which they should be based, during the 1970s and 1980s he directed his research activities toward the experimental side of this dual development. His experiments on concrete, steel, and masonry buildings and liquid-storage tanks using the Berkeley shaking table received world-wide attention and the findings of these experiments have influenced design

practice. Similarly, a series of papers that appeared in the 1960s and 1970s presented new and accurate methods utilizing the finite element concept for earthquake analysis of concrete dams. He served as a consultant for many of these projects for the U.S. Bureau of Reclamation, U.S. Army Corps of Engineers, the World Bank, and many private companies.



A Single-Story Masonry House on the EERC earthquake simulator facility

This was the reason for my first meeting with Professor Ray Clough at the University of South Wales at Swansea in 1975 during a international Congress on the Numerical Analysis of Dams under the presidency of Professor Oleg Zienkiewicz. Professor Clough remained active for a

long time in his research on the dynamic and earthquake response of large dams. He established international co-operation on this subject and he was active in performing many in-situ tests. The following are research areas that I had the privilege to cooperating with Professor Clough:

Research on Liquid Storage Tanks Full-scale experiments conducted at the EERC Earthquake Simulator Facility. Relevant publications: - The measured and predicted shaking table response of a broad tank model, GC Manos, RW Clough Am. Soc. Mech. Eng., Pressure Vessels Piping Div.,(Tech. Rep.) PVP. - Tank Damage during the May 1983 Coalinga Earthquake, Manos G.C. and Clough R.W. Int. J. Earth. Eng. Str. Dyn., Vol. 13, pp. 449-466, (1985). - Manos G.C. Earthquake Tank Wall Stability of Unanchored Tanks, ASCE Journal of Str. Eng. ASCE, Vol. 112, No 8, pp. 1863-1880 (1986).

Research on Masonry Houses for the Department of Housing and Urban Development USA (1975-1984). Full-scale experiments conducted at the EERC Earthquake Simulator Facility. Relevant publications: - Shaking Table Study of Single-Story Masonry Houses GC Manos, RW Clough, RL Mayes, EERC 83 (11) - Gulkan P., Clough R.W., Manos G.C. and Mayes R.L. "Seismic Testing of Single-story Masonry Houses : Part 1", Journal of Str. Eng. ASCE, Vol. 116, No 1, January 1990, pp. 235-256. - Gulkan P., Clough R.W., Manos G.C. and Mayes R.L. "Seismic Testing of Single-story Masonry Houses : Part 2", Journal of Str. Eng. ASCE, Vol. 116, No 1, January 1990, pp. 257-274.

Dr. George C. Manos, December 2017